Hypernuclear spectroscopy at Jefferson Lab

F. Garibaldi – Saclay workshop – 19-01-2016

- Hypernuclei: A quick introduction

- Electroproduction of hypernuclei with e.m. probes
  and Experimental challenges

- Hypernuclear Spectroscopy at Jefferson Lab
  - Overview of the Hall C Setup and Results
  - Overview of the Hall A Setup and Results

- Perspectives
  - New proposal at Jlab PAC
    - Few body
    - Medium mass
    - Pb

Summary and Conclusions

Proposal: PR-93-015

Spokespersons: S. Frullani, F. Garibaldi

Title: High Resolution 1*p* Shell Hypernuclear Spectroscopy

Letter to the spokespersons of the Multi-Particle Spectrometer (MPS) proposals

The PAC reviewed three proposals and two letters of intent for a program of measurements which would be carried out using the Multi-Particle Spectrometer (MPS) in Hall A. Since this spectrometer is not yet funded, the PAC did not feel it appropriate to approve any of these experiments at this time. However, the committee wishes to point out that CEBAF has a unique opportunity to study hypernuclear physics. We very strongly encourage the Laboratory and the interested scientists (who include these proponents and others who have approved time in Hall C) to pursue the funding for a high resolution kaon spectrometer.

Of the several physics topics proposed, the PAC believes that only the hypernuclear studies require the high-resolution capabilities of the MPS. For the other topics (kaon electroproduction, deuteron form factor) the MPS would be a valuable device, and could be used if it existed, but the committee believes that these physics topics can be addressed with equipment already existing at CEBAF or with less sophisticated spectrometers. However, as stated above, we believe that the high resolution hypernuclear spectroscopy is of sufficient scientific importance to justify the construction of such a device in either Hall A or C, if the technical issues discussed below can be addressed.

The study of hypernuclear states with high resolution is one of the topics which provided the original justification for the construction of CEBAF ten years ago. Today, much still remains to be learned and CEBAF is in a unique position to advance the field. Proposals 93-005 and 93-015 discuss several interesting initial possibilities for a hypernuclear program using a dedicated kaon spectrometer such as the MPS. The possibility of measuring unnatural parity states and deducing the spin-orbit splitting for the Λ-nucleon system is particularly interesting. The tentative identification of narrow Σ-hypernuclear states is also tantalizing and should be verified at CEBAF if possible.

Measurement and Feasibility:

At present, the cross sections for electroproduction of hypernuclear states are unknown. Furthermore, the kinematics require that the measurements be made at extreme forward angles for both the electron and kaon spectrometers where the background singles rates are very high and particle identification will be difficult. The feasibility of the proposed measurements is tied crucially to the magnitude of these cross sections.

Two experiments have been approved in Hall C (PR-89-009, PR-91-016) which will provide information on the production cross-sections and background rates. The PAC believes that the results from these two experiments will be crucial for the development of the scientific and technical case for a dedicated spectrometer of the kind discussed here. The PAC encourages collaboration between the proponents of this experiment and the Hall C experiments.

HYPERNUCLEAR PHYSICS

- Hypernuclei are bound states of nucleons with a strange baryon (Λ)

- Extension of physics on N-N interaction to system with S#0

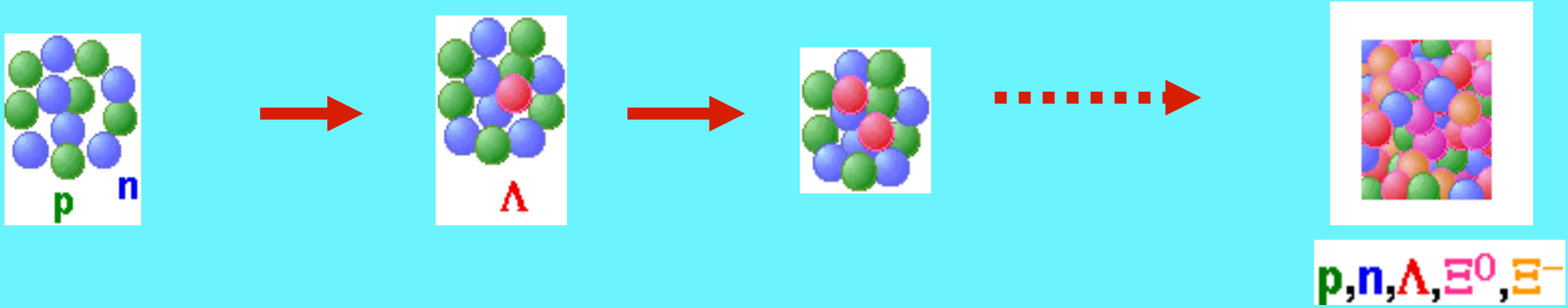

- Internal nuclear shell are not Pauli-blocked for hyperons

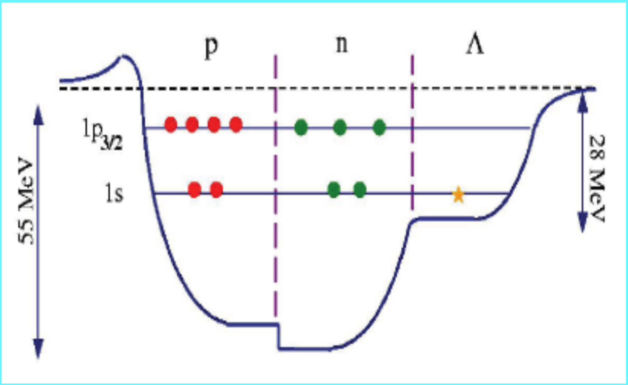

- Spectroscopy

a "laboratory" to study

↓

Λ - N interaction

Unique aspects of strangeness many body problems

Links with astrophysics (NS) ("hyperon puzzle")

Hypernuclear investigation

- Few-body aspects and YN, YY interaction
  - Short range characteritics ofBB interaction
  - Short range nature of the ΛN interaction, no pion exchange: meson picture or quark picture ?
  - Spin dependent interactions
  - Spin-orbit interaction, …….
  - ΛΣ mixing or the three-body interaction

- Mean field aspects of nuclear matter
  - A baryon deep inside a nucleus distinguishable as a baryon ?
  - Single particle potential
  - Medium effect ?
  - Tensor interaction in normal nuclei and hypernuclei
  - Probe quark de-confinement with strangeness probe

- Astrophysical aspect
  - Role of strangeness in compact stars
  - Hyperon-matter, SU(3) quark-matter, …
  - YN, YY interaction information

What do learn from hypernuclear spectroscopy: the Λ−N interaction

Spectroscopy of Hypernuclei

hypernuclear data well described by weak coupling model

Λ (s-shell) + J_{A-1} --------> $J = J_{A-1} \pm 1/2$
(Λ hyperon) (parent nucleus) (create *doublet* state
(J state)

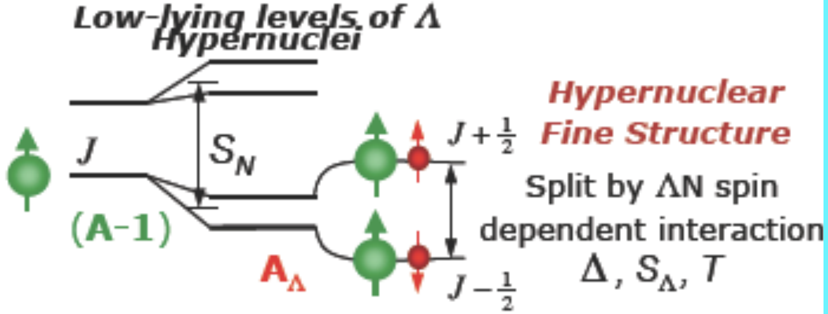

Hypernuclear Fine Structure

Split by ΛN spin dependent interaction
Δ, S_Λ, T

ΛN interaction

$V_{\Lambda N} = V_0(r)$ central

Δ
S_Λ
S_N
T

$+ V_\sigma(r) \bullet \sigma_N \cdot \sigma_\Lambda$ Δ (spin-spin)
$+ V_{\sigma 0}(r) \bullet \lambda_{\Lambda N} \cdot \sigma_\Lambda$ σ_Λ (spin-orbit)
$+ V_{\sigma 0}(r) \bullet \lambda_{\Lambda N} \cdot \sigma_N$ σ_N (spin-orbit)
$+ V_T(r) \bullet S_{12}$ T (tensor)

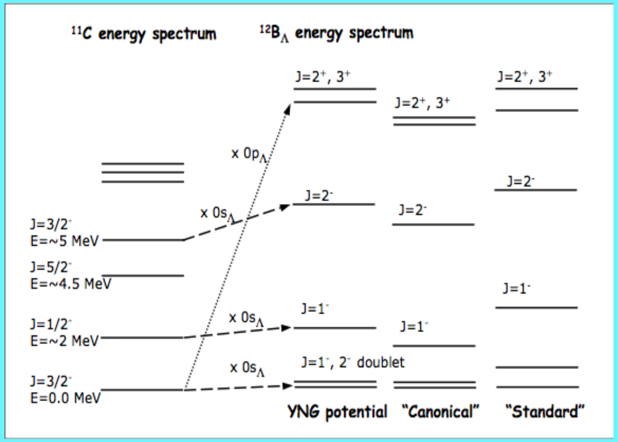

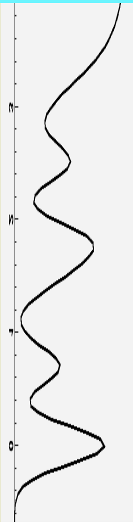

Each of the 5 radial integral (V, Δ, S_Λ, S_N, T) can be phenomenologically determined from the low lying level structure of p-shell hypernuclei

- ✔ most of information is carried out by the spin dependent part
- ✔ doublet splitting determined by Δ, σ_Λ, T

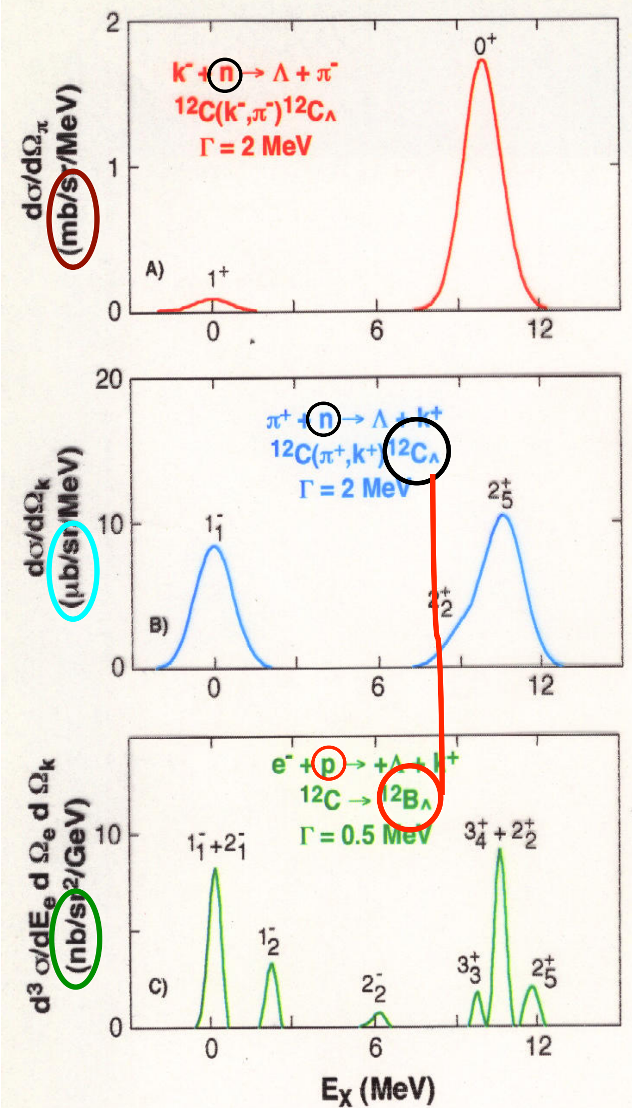

q ≈ 100 MeV/c --> $\Delta\ell = 0$
---> substitutional states
$\Delta s = 0$ --> no spin flip
---> natural parity
($J = 0^+$)
absorption

q ≈ 300 MeV/c --> $\Delta\ell = 1,2$
spin flip (weak for $\Theta_K < 10°$)
$\Delta s = 0$ ---> natural parity
($J = 1^-$, $J = 2^+$)
absorption

q ≈ 300 MeV/c --> $\Delta\ell = 1,2$
--> non substitutional statesd
$\Delta s = 0,1$ (spin flip)
---> unnatural parity
($J = 2^-$, $J = 3^+$)
no absorption

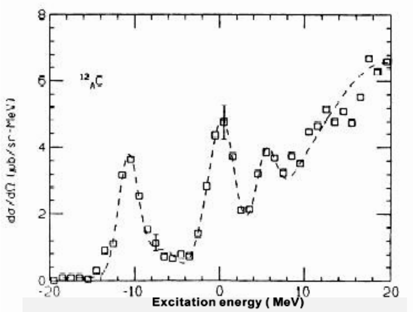

BNL 3 MeV

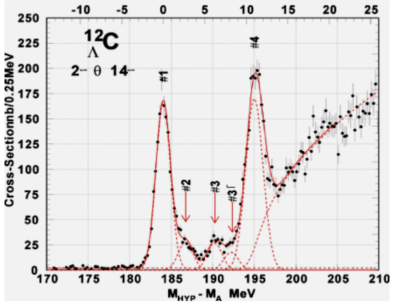

KEK336 2 MeV

Improving energy resolution

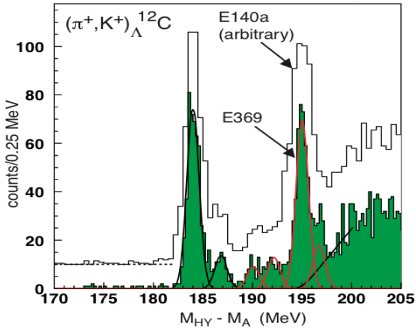

~ 1.5 MeV

and

using electromagneti probe

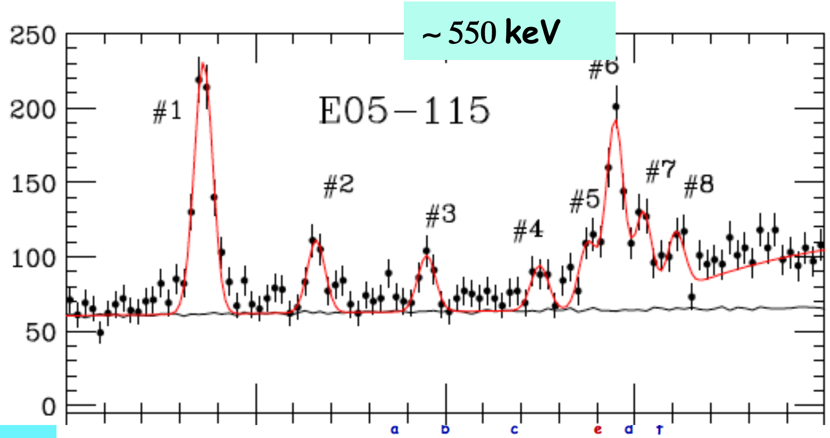

~ 550 keV

High resolutic high yield, ar systematic stu is essential

production of mirror hypernuclei

energy resolution ~ 500 KeV

Absolute energy calibratio with Λ and Σ_0 masses

The CEBAF Accelerator

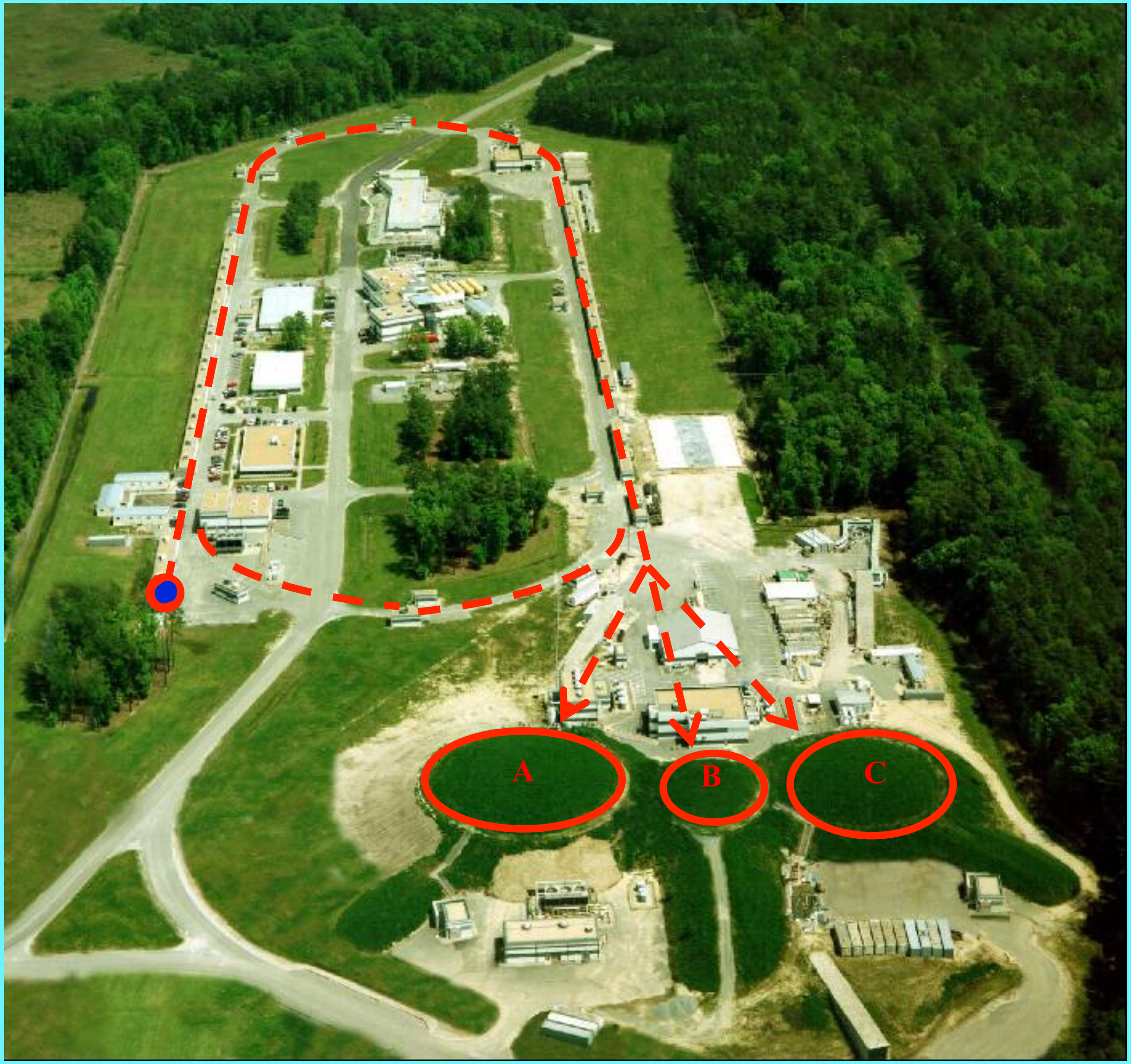

Continuous **E**lectron
Beam
Accelerator
Facility

- Energy 0.8 – 5.7 GeV
- 200 μA, polarization 75-85%
- 1499 MHz operation
- Simultaneous delivery to 3 halls

Hall C: The First Pioneer Experiment
Jlab E89-009 - The HNSS setup

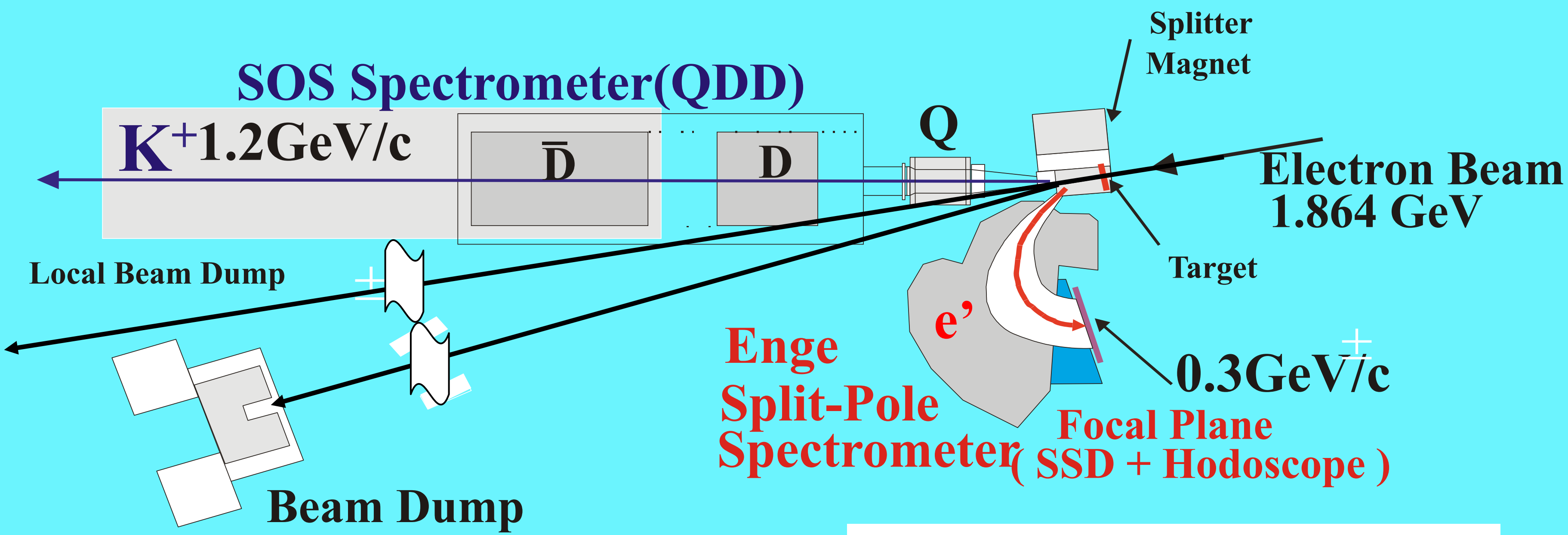

Splitter Magnet

SOS Spectrometer(QDD)

K^+1.2GeV/c

$\bar{D}$

D

Q

Electron Beam 1.864 GeV

Local Beam Dump

Target

e’

Enge Split-Pole Spectrometer

0.3GeV/c

Focal Plane (SSD + Hodoscope)

Beam Dump

Year 2000: The first generation experiment (E89-009, HNSS) on Carbon Target proved that (e,e'K+) hypernuclear study is possible with high quality electron beam at JLab.

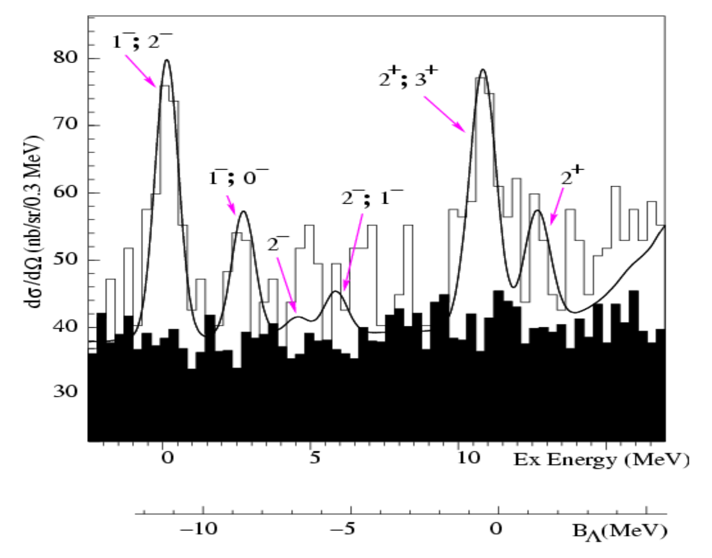

Second Generation E01-011 setup

K^+ 1.2 GeV/c

E 1.8 GeV

E' 0.3 GeV/c

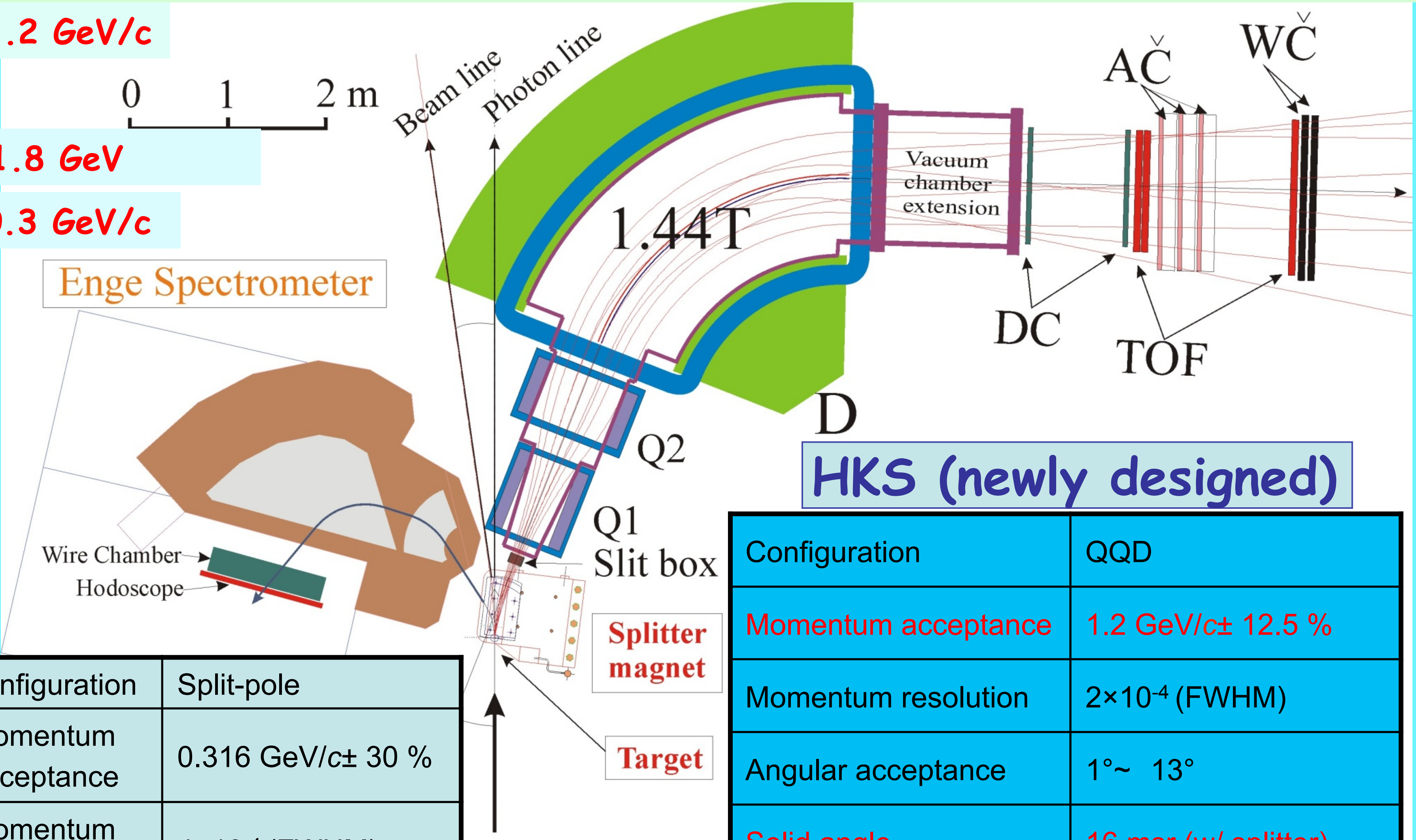

configuration	Split-pole
Momentum acceptance	0.316 GeV/*c*± 30 %
Momentum resolution	4×10^{-4} (FWHM)

HKS (newly designed)

Configuration	QQD
Momentum acceptance	1.2 GeV/*c*± 12.5 %
Momentum resolution	2×10^{-4} (FWHM)
Angular acceptance	1°~ 13°
Solid angle	16 msr (w/ splitter)

2004.2.23.

Tilt method

Background electrons

- Bremsstrahlung

  very forward peaked
- Møller scattering

  scattering angle and momentum are correlated

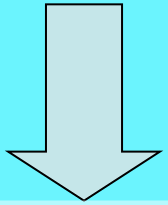

to avoid them

Tilt Enge spectrometer by 8 degree (optimization of e' detection angle)

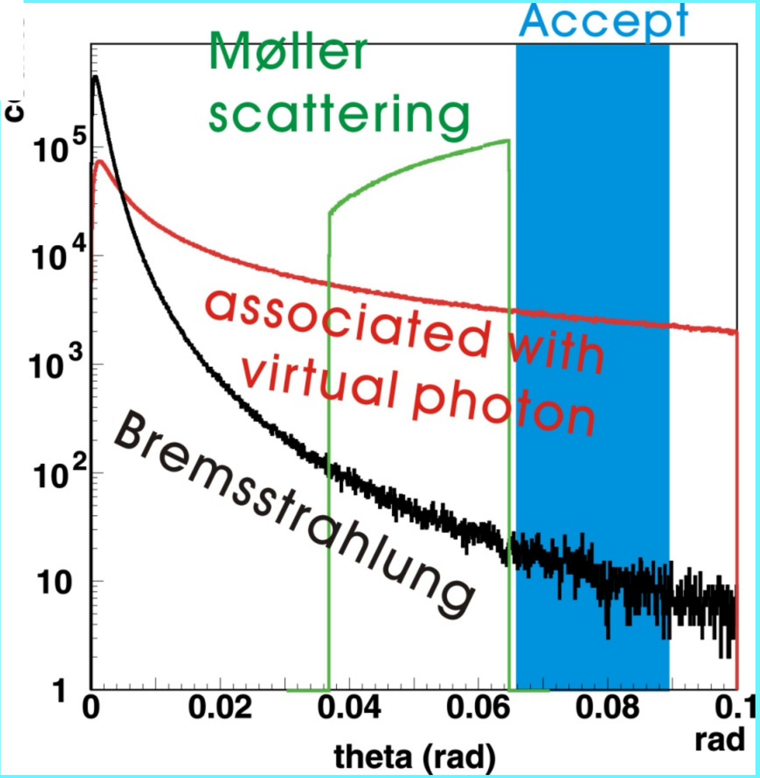

Hall C Second Generation

2005 E01-011

First step to medium heavy hypernuclei (^{28}Si, ^{12}C, ^{7}Li)

Two Major Improvements

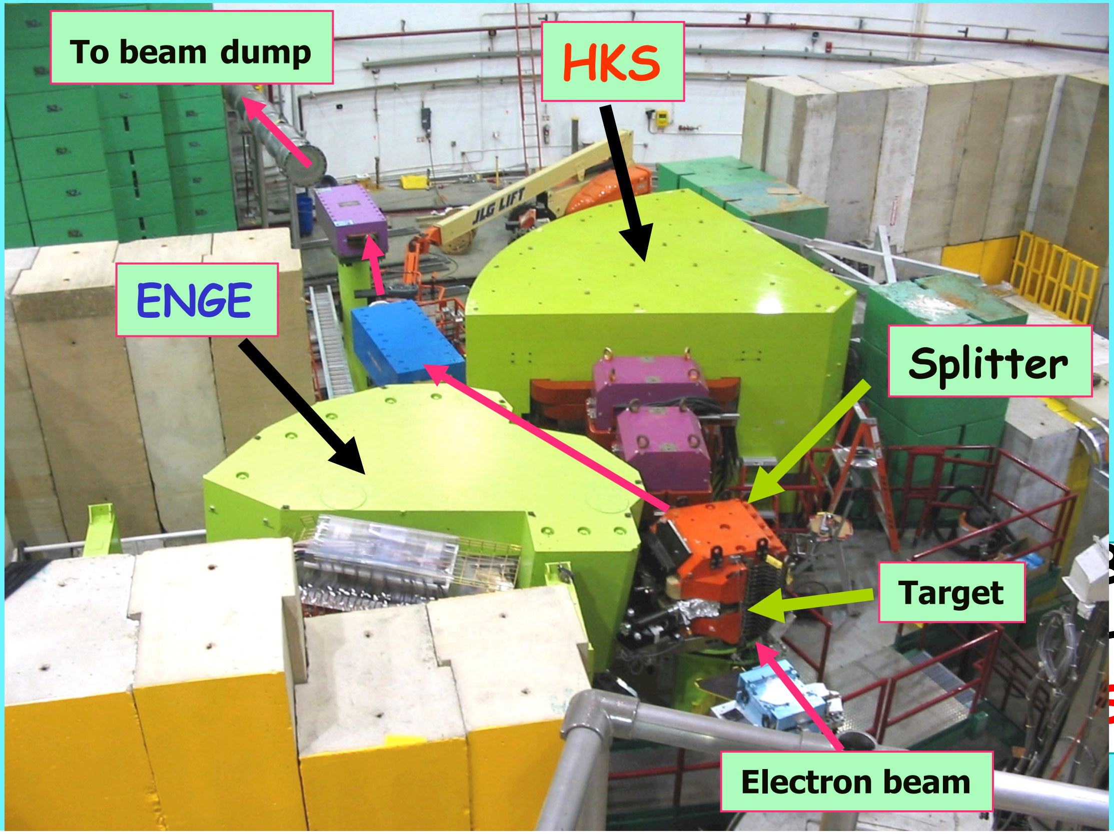

New HKS

Tilt Method

$0^{o} - 4.5^{\circ}$

Beam: 30 μA, 1.8GeV

HKS: $\Delta p/p = 2 \times 10^{-4}$ [FWHM]

Solid angle 16msr(w/splitter)

JLab E05-115 (Hall-C) setup

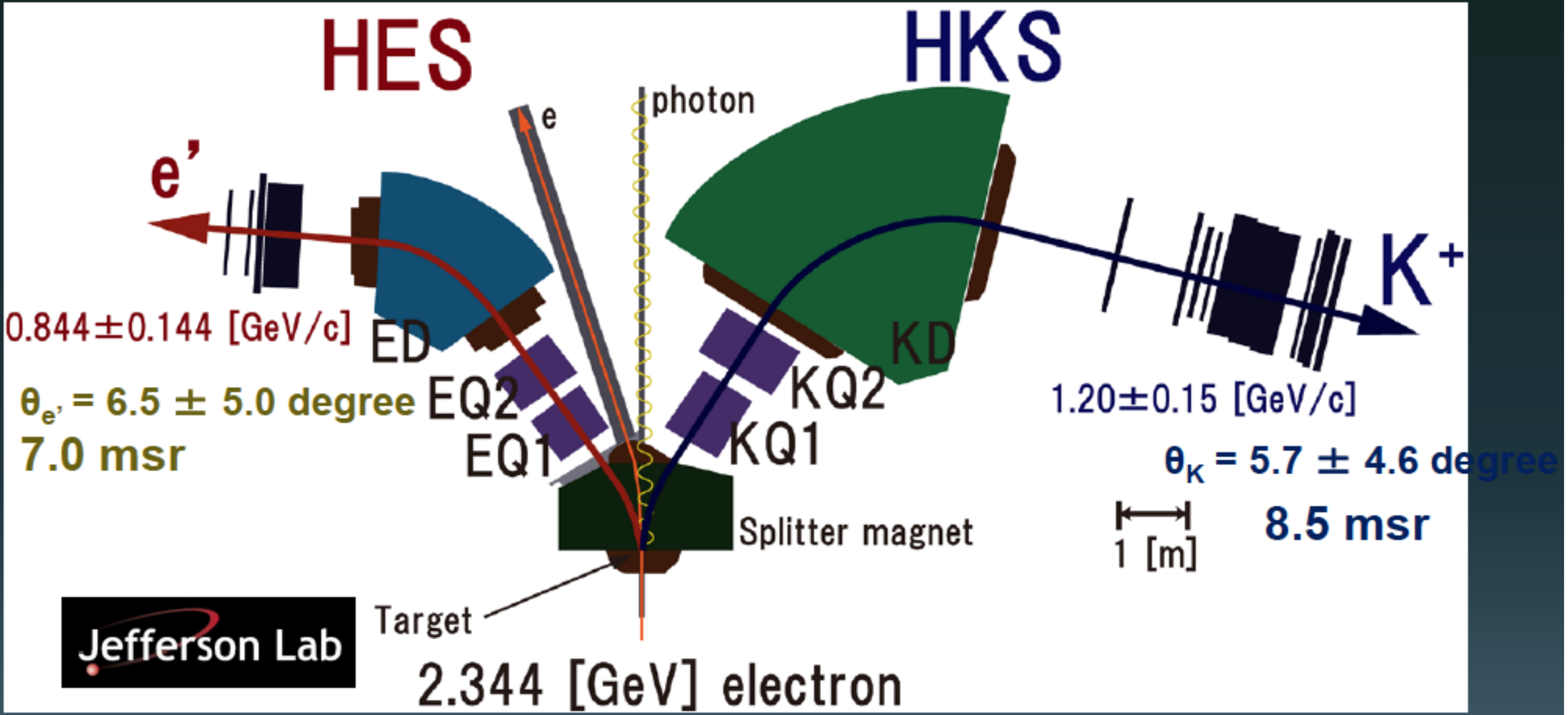

$\Delta p/p \sim 2 \times 10^{-4}$

JLAB Hall A Standard Experimental setup

The two High Resolution Spectrometer (HRS) in Hall A @ JLab

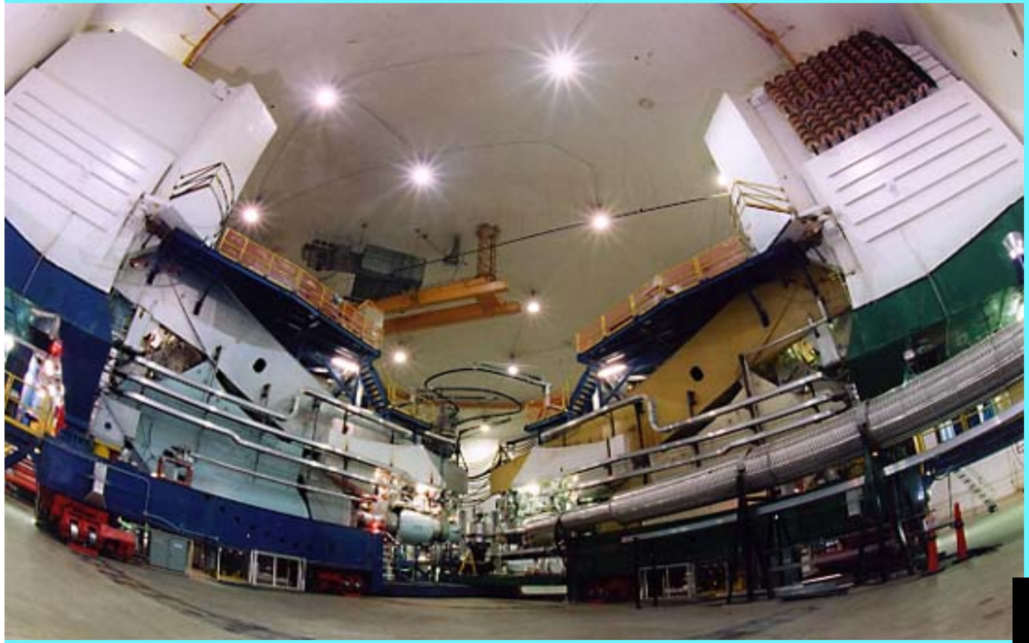

HRS – QDQ main characteristics:
Momentum range: 0.3, 4.0 GeV/c
$\Delta p/p$ (FWHM): 10^{-4}
Momentum accept.: ± 5 %
Solid angle: 5 – 6 msr
Minimum Angle : 12.5°

Improvements are needed for hyperuclear spectroscopy experiments

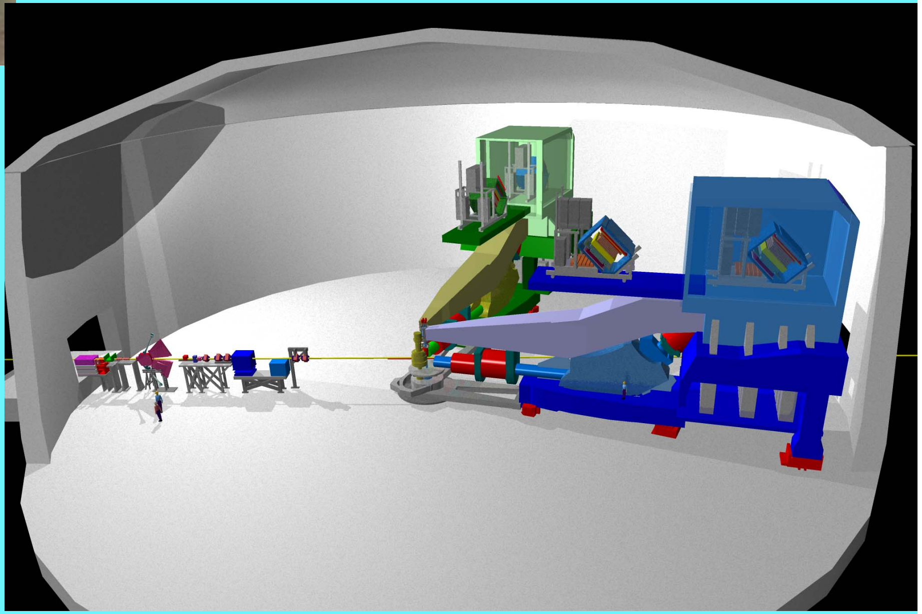

$^{A}Z(e,e'K)^{A}(Z-1)_{\Lambda}$

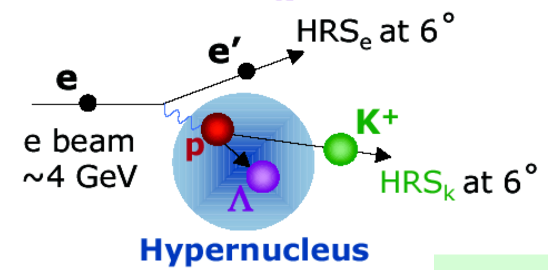

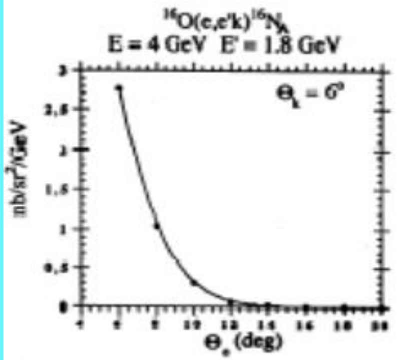

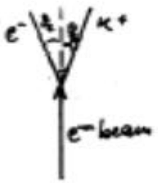

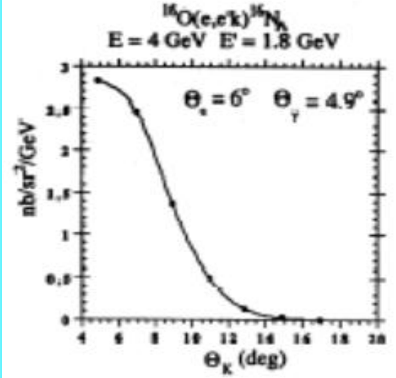

1. $\Delta E_{beam}/E$: 2.5×10^{-5}
2. $\Delta P/P$: ~ 10^{-4}
3. Straggling, energy loss…

~ 670 keV

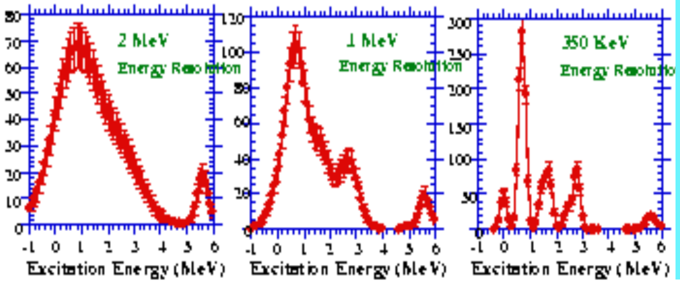

reasonable counting rates

forward angle

septum magnets

good energy resolution

do not degrade HRS

minimize beam energy instability

"background free" spectrum

unambiguous K identification

High P_k/high E_{in} (Kaon survival)

RICH detector

Hall A deector setup

aerogel first generation

aerogel, cherenkov

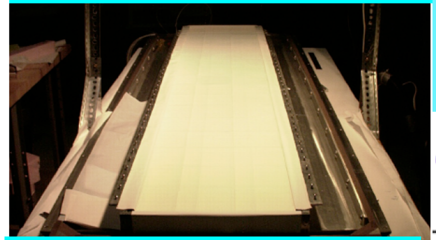

aerogel second generation

hadron arm

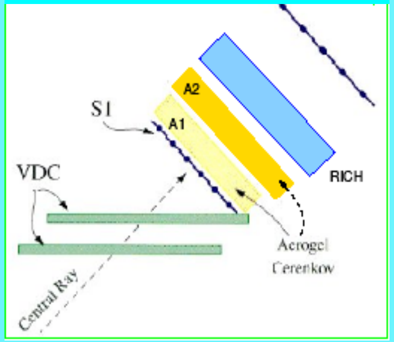

RICH Detector

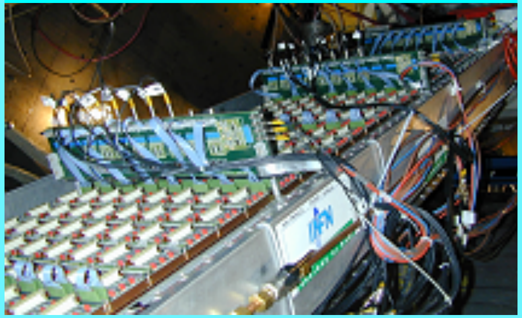

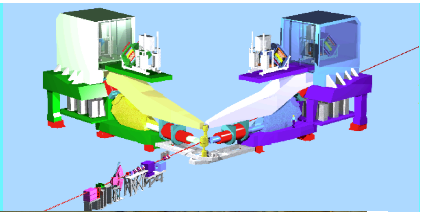

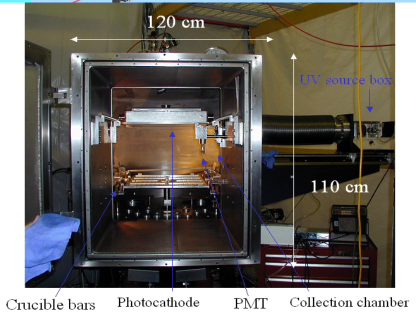

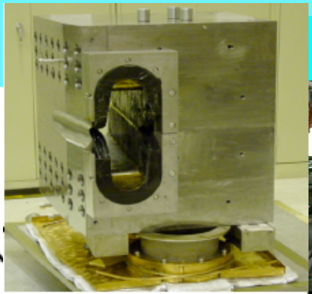

septum magnets

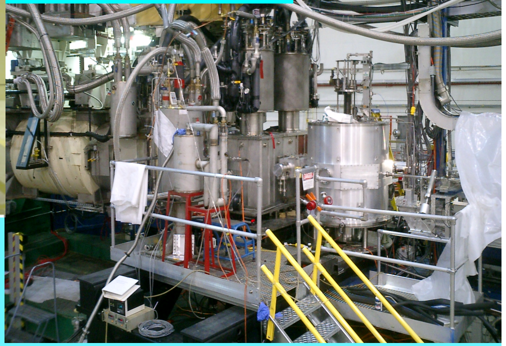

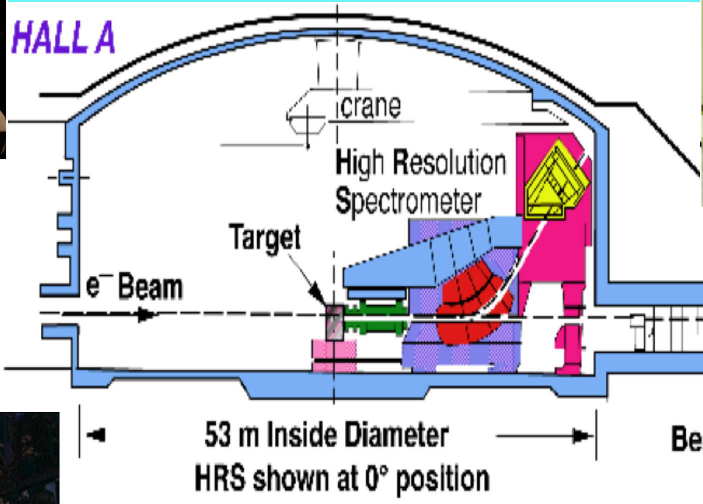

waterfall

gas cherenkov

electron arm

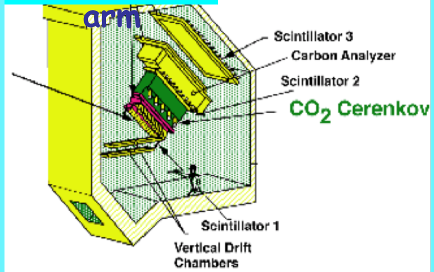

To be added to do the experiment

Kaon collaboration

FLORIDA INTERNATIONAL UNIVERSITY

JLAB Hall A Experiment E94-107

E94107 COLLABORATION

A.Acha, H.Breuer, C.C.Chang, E.Cisbani, F.Cusanno, C.J.DeJager, R. De Leo, R.Feuerbach, S.Frullani, F.Garibaldi*, D.Higinbotham, M.Iodice, L.Lagamba, J.LeRose, P.Markowitz, S.Marrone, R.Michaels, Y.Qiang, B.Reitz, G.M.Urciuoli, B.Wojtsekhowski, and the Hall A Collaboration
and Theorists: Petr Bydzovsky, John Millener, Miloslav Sotona

→ ${}^{16}O(e,e'K^+)^{16}{}_{\Lambda}N$

→ ${}^{12}C(e,e'K^+)^{12}{}_{\Lambda}B$

→ ${}^{9}Be(e,e'K^+)^{9}{}_{\Lambda}Li$

→ $H(e,e'K^+)\Lambda,\Sigma^0$

E_{beam} = 4.016, 3.777, 3.656 GeV

P_e= 1.80, 1.57, 1.44 GeV/c P_k= 1.96 GeV/c

$\theta_e = \theta_K = 6°$

$W \sim 2.2$ GeV $Q^2 \sim 0.07\ (GeV/c)^2$

Beam current : <100 μA Target thickness : ~100 mg/cm²

Counting Rates ~ 0.1 – 10 counts/peak/hour

E-98-108. Electroproduction of Kaons up to Q2=3(GeV/c)2 (P. Markowitz, M. Iodice, S. Frullani, G. Chang spokespersons)

~~E-07-012. The angular dependence of ${}^{16}O(e,e'K^+)^{16}N$ and $H(e,e'K^+)\Lambda$ (F. Garibaldi, M.Iodice, J. LeRose, P. Markowitz spokespersons) (run : April-May 2012)~~

UNIVERSITY OF MARYLAND

HAMPTON UNIVERSITY

Jefferson Lab
Exploring the Nature of Matter

The PID Challenge

Very forward angle ---> high background of π and p

-TOF and 2 aerogel in not sufficient for unambiguous K identification !

Kaon Identification through Aerogels

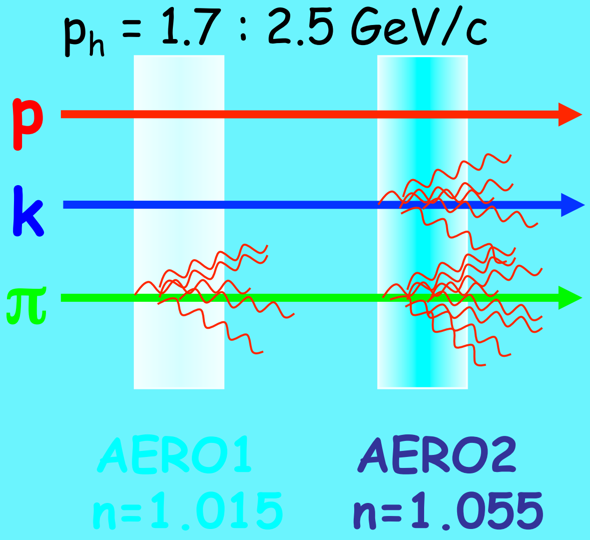

Pions = A1•A2

Kaons = $\overline{A1}\bullet A2$

Protons = $\overline{A1}\bullet\overline{A2}$

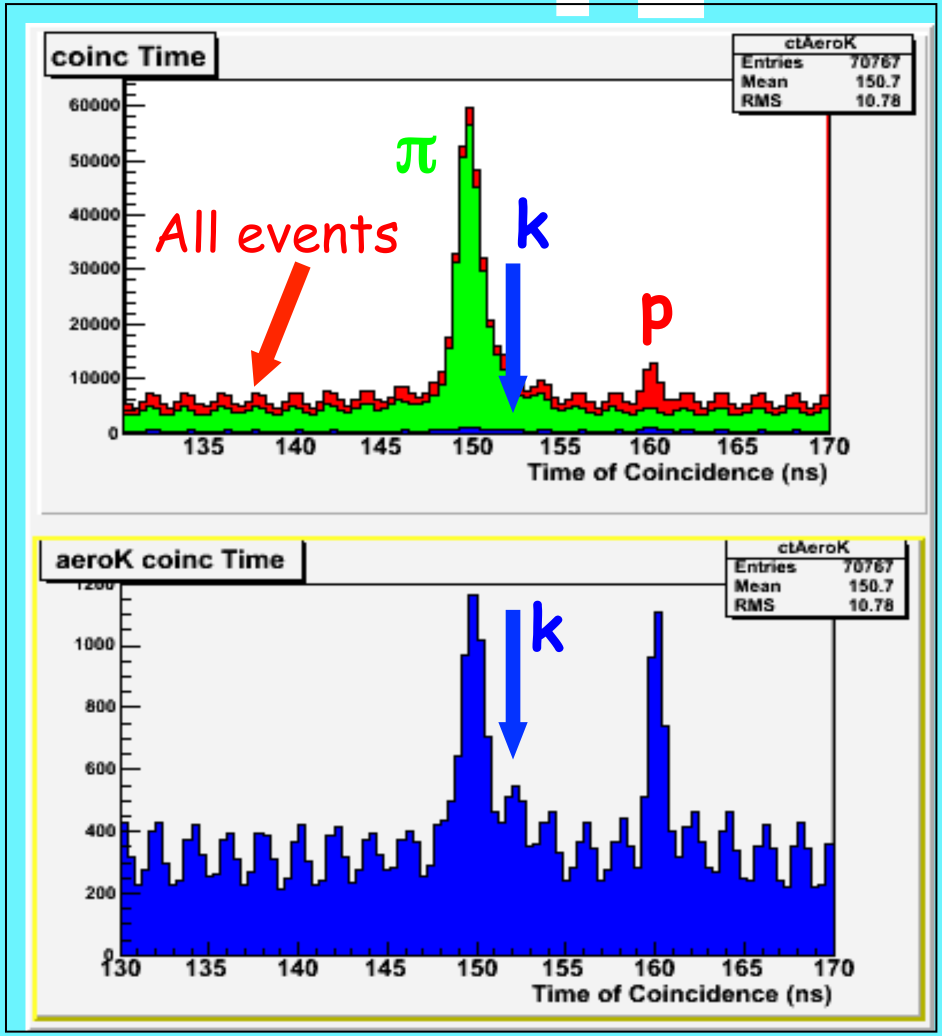

1 7 '00

1 5 '96

Ring Imaging Cherenkov (RICH) detector –C_6F_{14}/CsI proximity focusing RICH

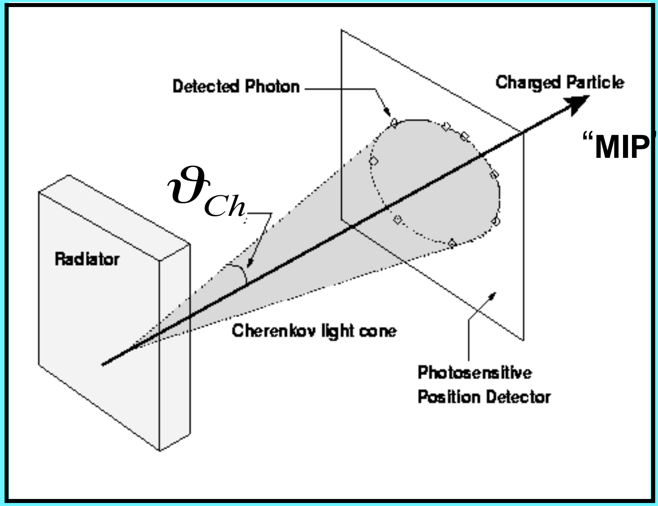

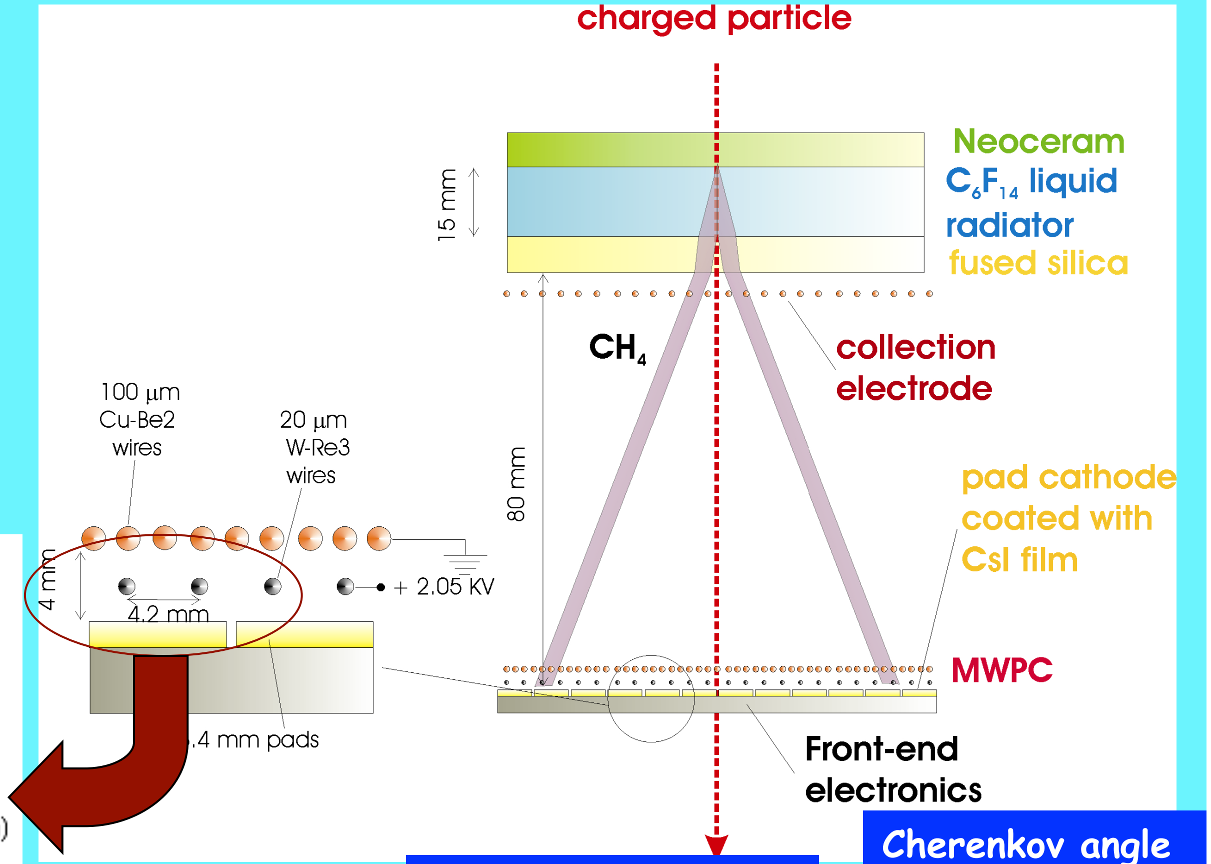

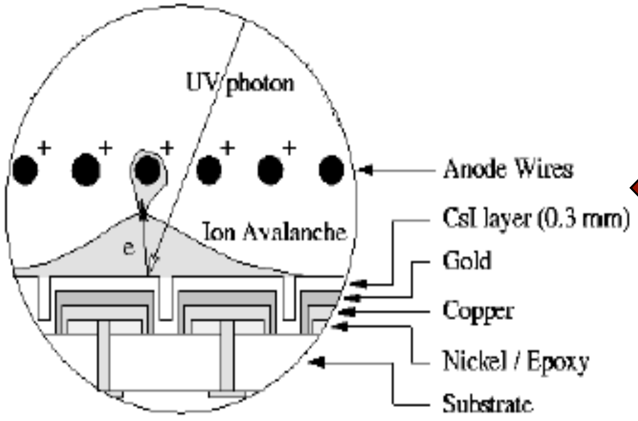

Separation Power

$$\vartheta_2 - \vartheta_1 = n_\sigma \sigma_{\vartheta_c}$$

Cherenkov angle resolution

$$\sigma_{\vartheta_c} = \frac{\sigma_\vartheta^{p.e.}}{\sqrt{N_{p.e}}}$$

N. of detected photoelectrons

$$N_{p.e.} = 370 L \sin^2 \overline{\vartheta}_c \prod_i \varepsilon_i \Delta E \approx 20-50$$

Performances

- $N_{p.e.}$ # of detected photons(p.e.) ← maximize
- and σ_θ (angular resolution) ← minimize

N. of detected photoelectrons

$$N_{p.e.} = 370 L \sin^2 \overline{\vartheta}_c \prod_i \varepsilon_i \Delta E \approx 20 - 50$$

Separation power

$$\vartheta_2 - \vartheta_1 = \mathrm{n}_\sigma \sigma_{\vartheta_c}$$

Particle mass m_1 **Particle mass m_2**

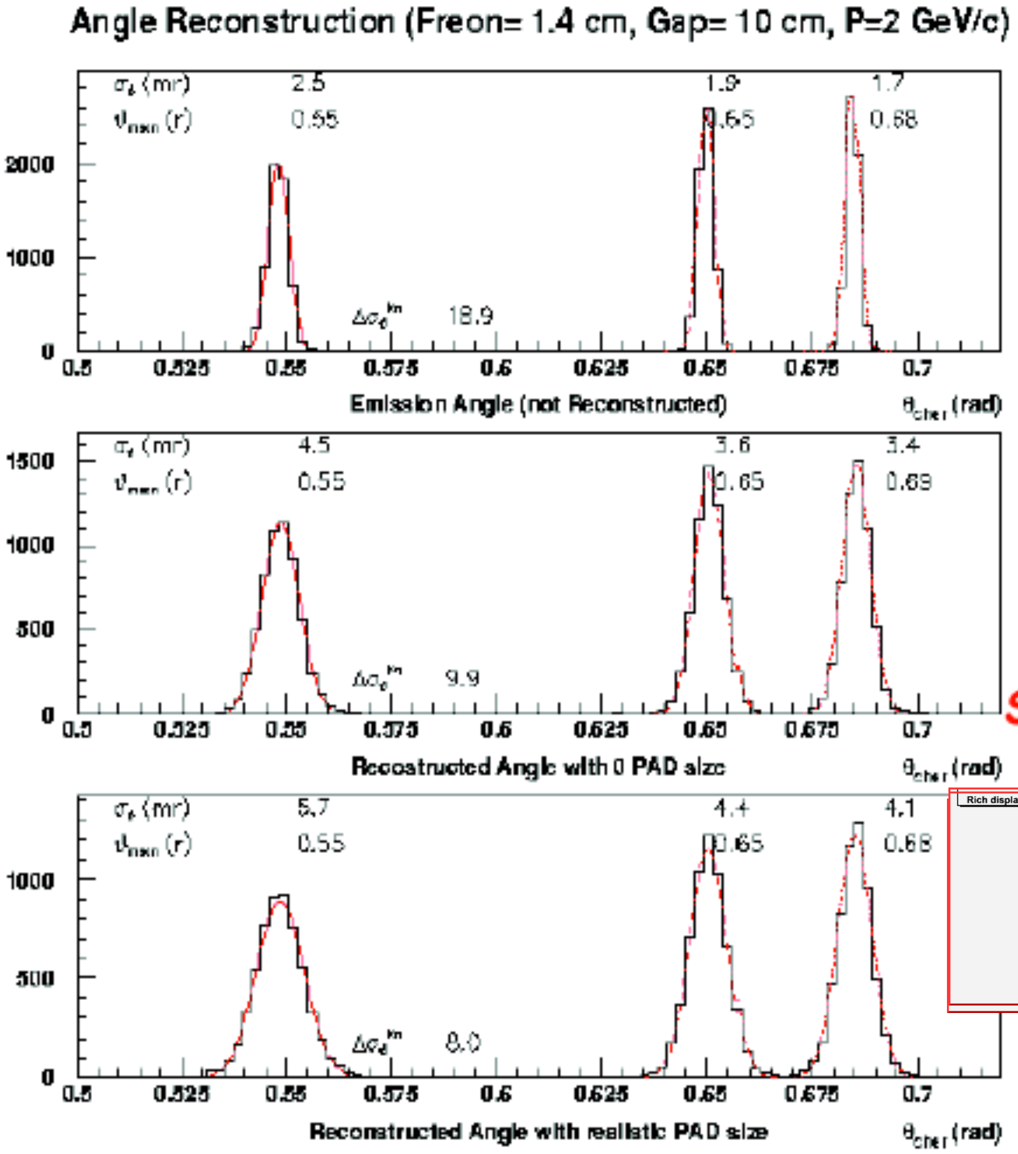

Cherenkov angle resolution

$$\sigma_{\vartheta_c} = \frac{\sigma_\vartheta^{p.e.}}{\sqrt{N_{p.e.}}}$$

Minimize

Maximize

π, K separated by 30 mrad

with 3 mrad: 10 σ

Simulation (spectra) done with 5 σ

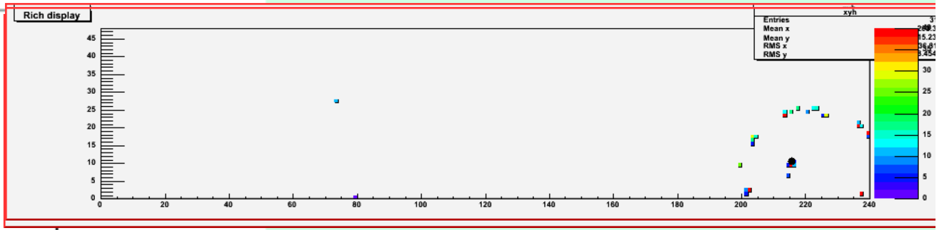

2–axes movement system

3 band filters (160, 185, 220

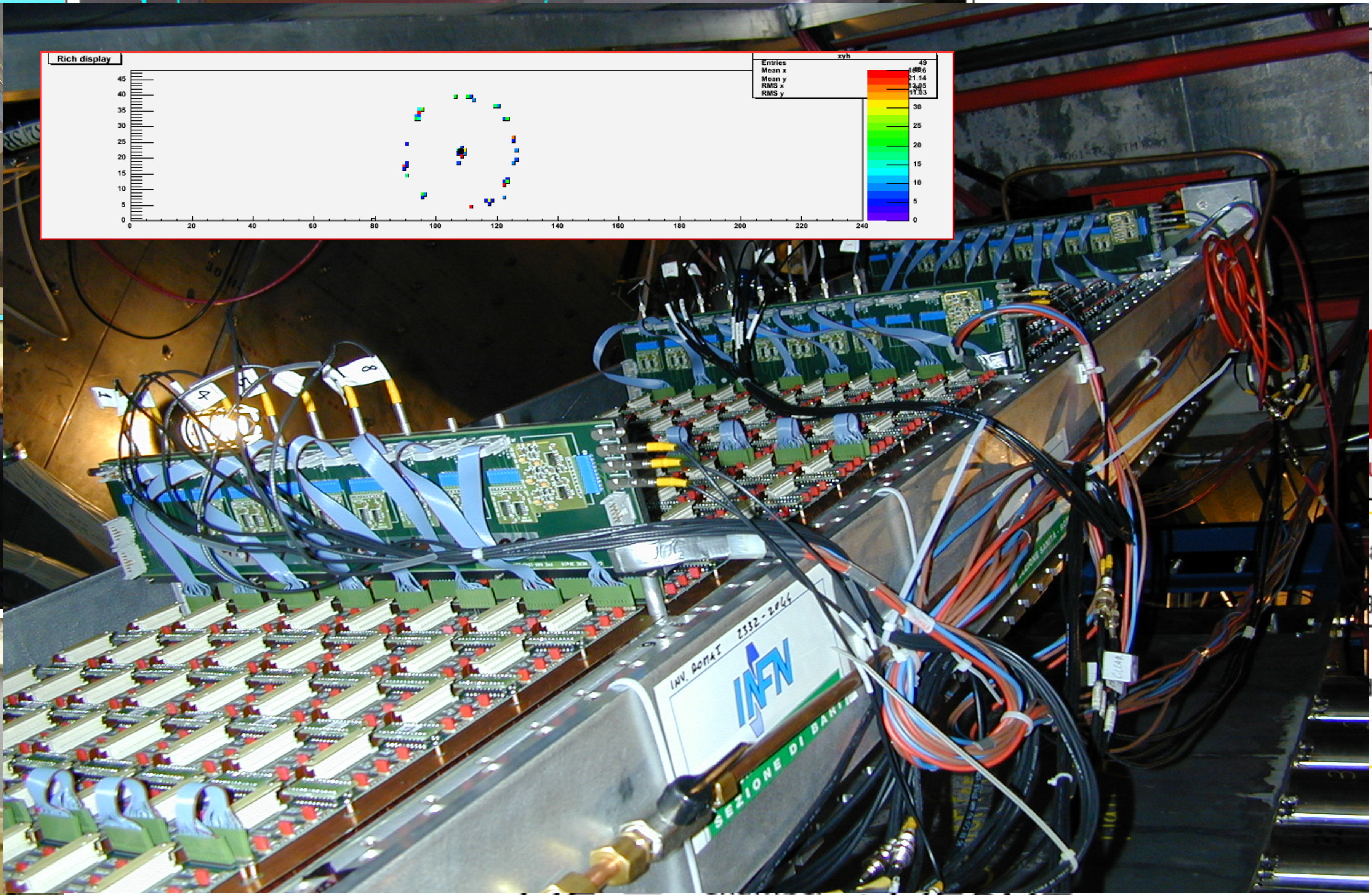

n Dio

um L

ad

80 V)

l (0 V

$$QE = \frac{\quad}{I_{PMT}} \cdot QE_{PMT}$$

RICH - PID - Effect of ‘Kaon selection

Coincidence Time selecting kaons on Aerogels and on RICH

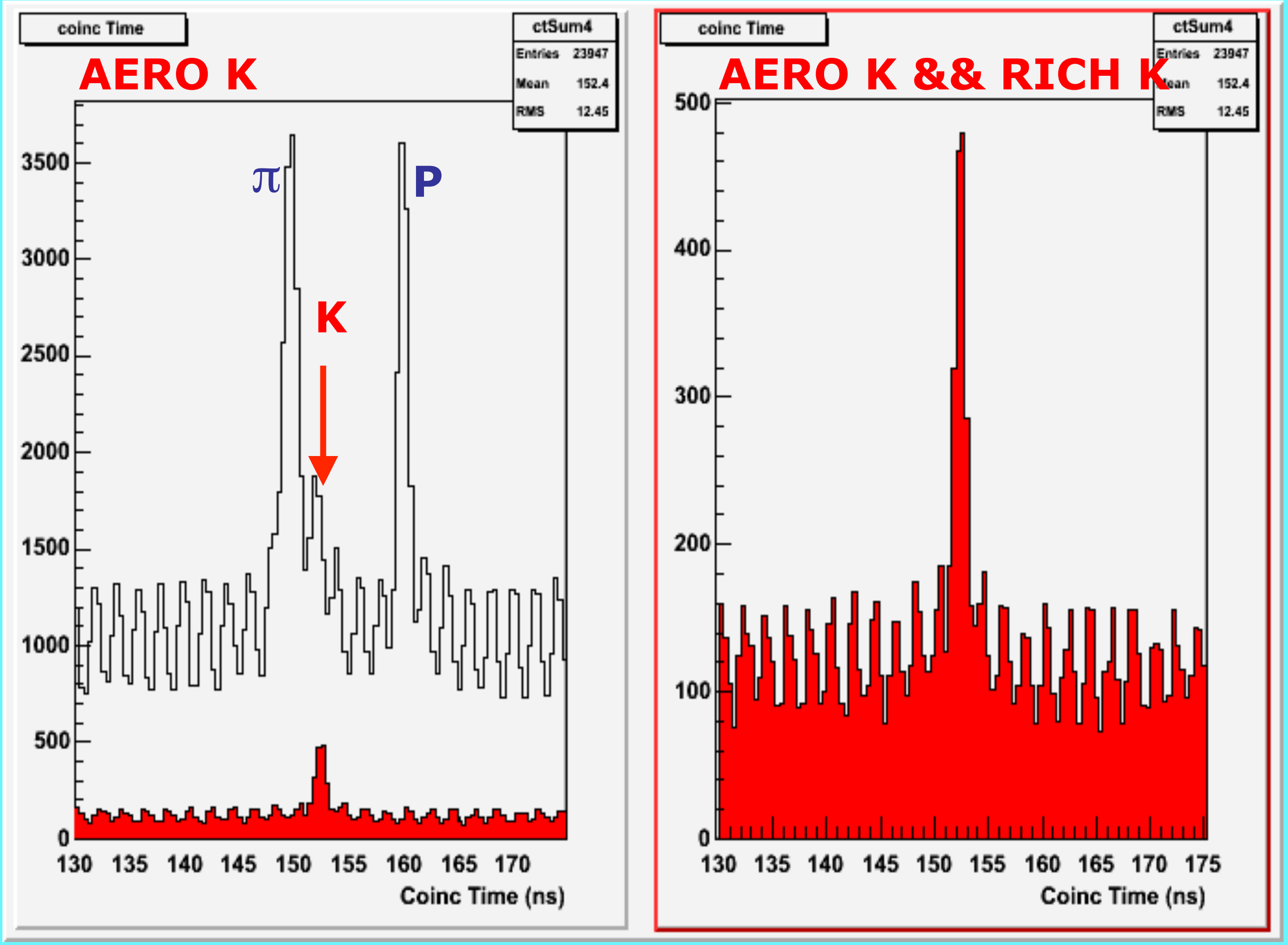

Pion rejection factor ~ 1000

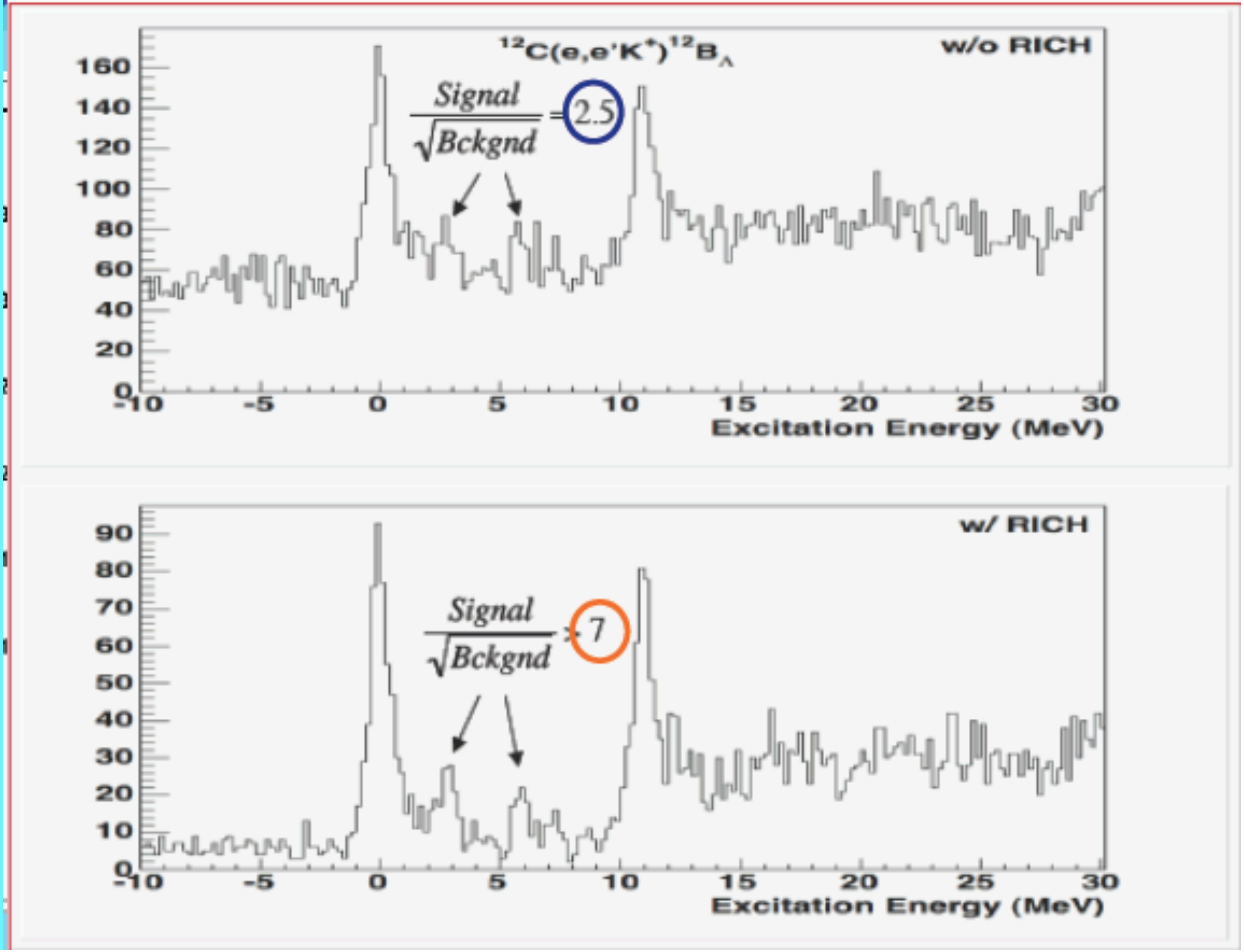
$^{12}C(e,e'K^+)^{12}B_\Lambda$
w/o RICH
$\frac{Signal}{\sqrt{Bckgnd}} = 2.5$
160
140
120
100
80
60
40
20
0
-10
-5
0
5
10
15
20
25
30
Excitation Energy (MeV)
w/ RICH
$\frac{Signal}{\sqrt{Bckgnd}} \approx 7$
90
80
70
60
50
40
30
20
10
0
-10
-5
0
5
10
15
20
25
30
Excitation Energy (MeV)

$^{9}Be(e,e'K^{+})\ ^{9}{}_{\Lambda}Li$

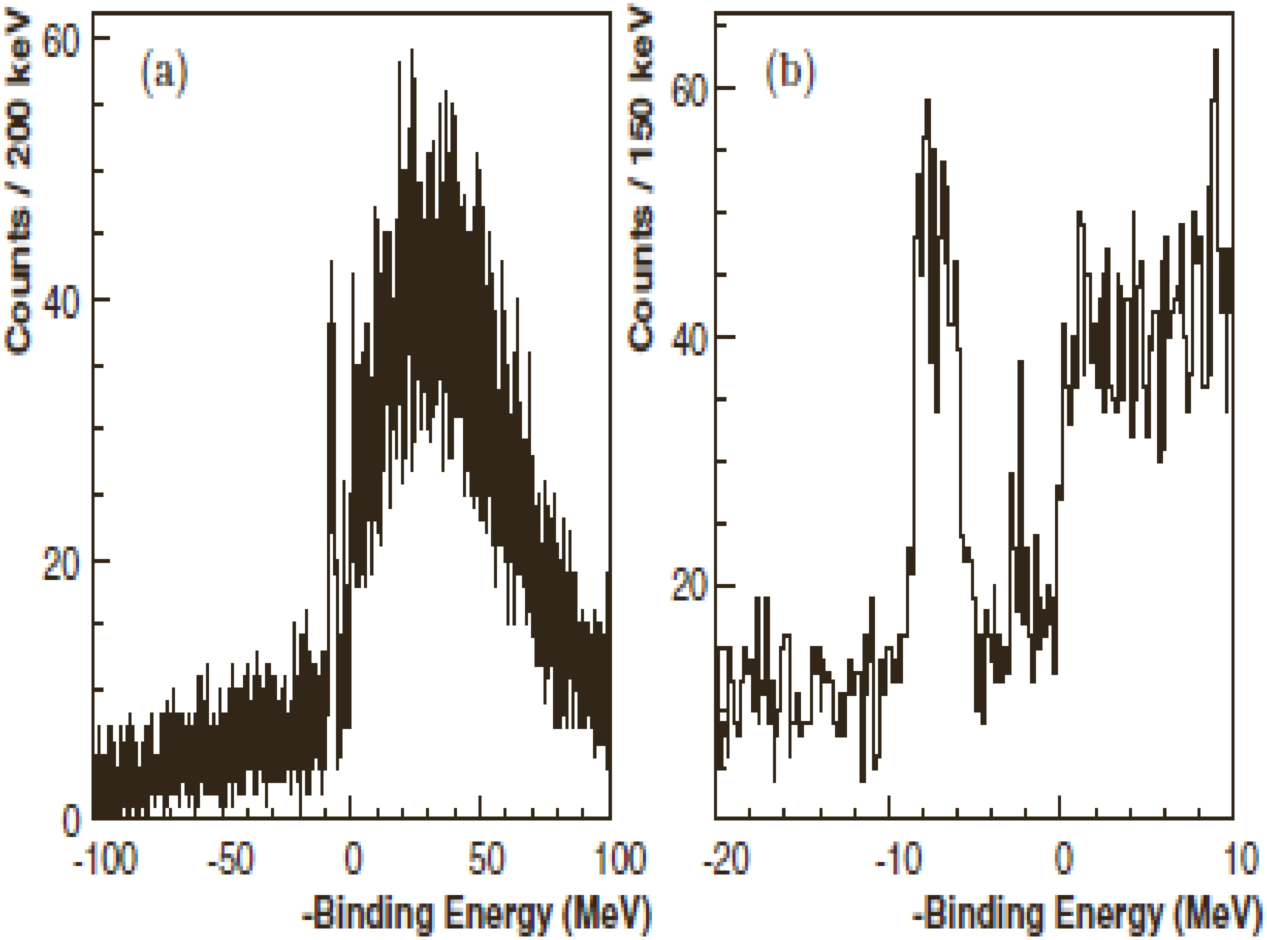

The binding energy spectrum of the hypernucleus $^{9}{}_{\Lambda}Li$ obtained through the reaction $^{9}Be(e,e'K^{+})\ ^{9}{}_{\Lambda}Li$ after kaon selection with aerogel detectors and RICH in a) the whole energy range and b) restricted to the region of interest.

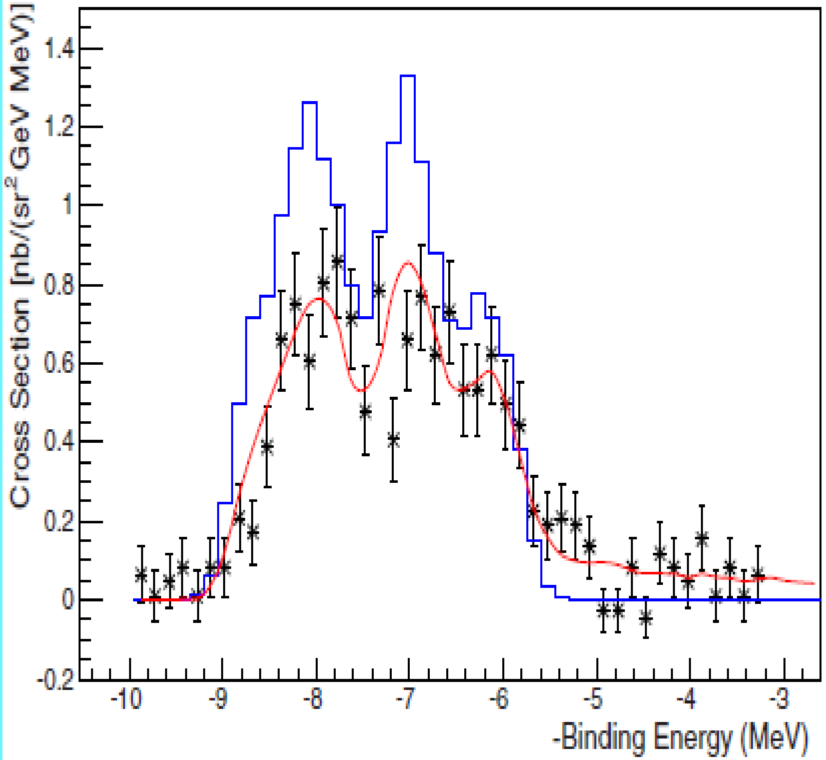

Experimental excitation energy vs Monte Carlo Data (red curve) and vs Monte Carlo data with radiative effects "turned off" (blue curve)

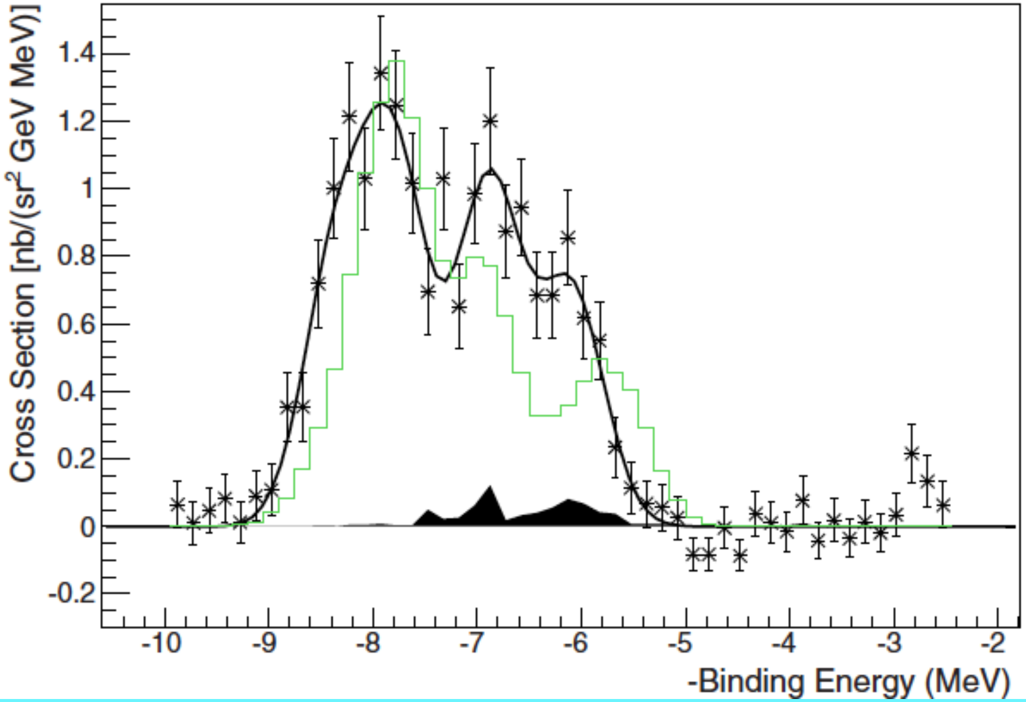

The radiatively unfolded experimental spectrum compared to a theoretical prediction (thin green line). Thesolid black line represents a fit to the data with four Gaussians of a common width.

Radiative corrections not depend on the hypohesis on the peak structure producing the experimental data

Excitation energies, widths and cross sections obtained by fitting the ^{9}Be(e,e'K^{+}) $^{9}_{\Lambda}$Li spectrum (first three columns) compared with theoretical precitions (last four columns)

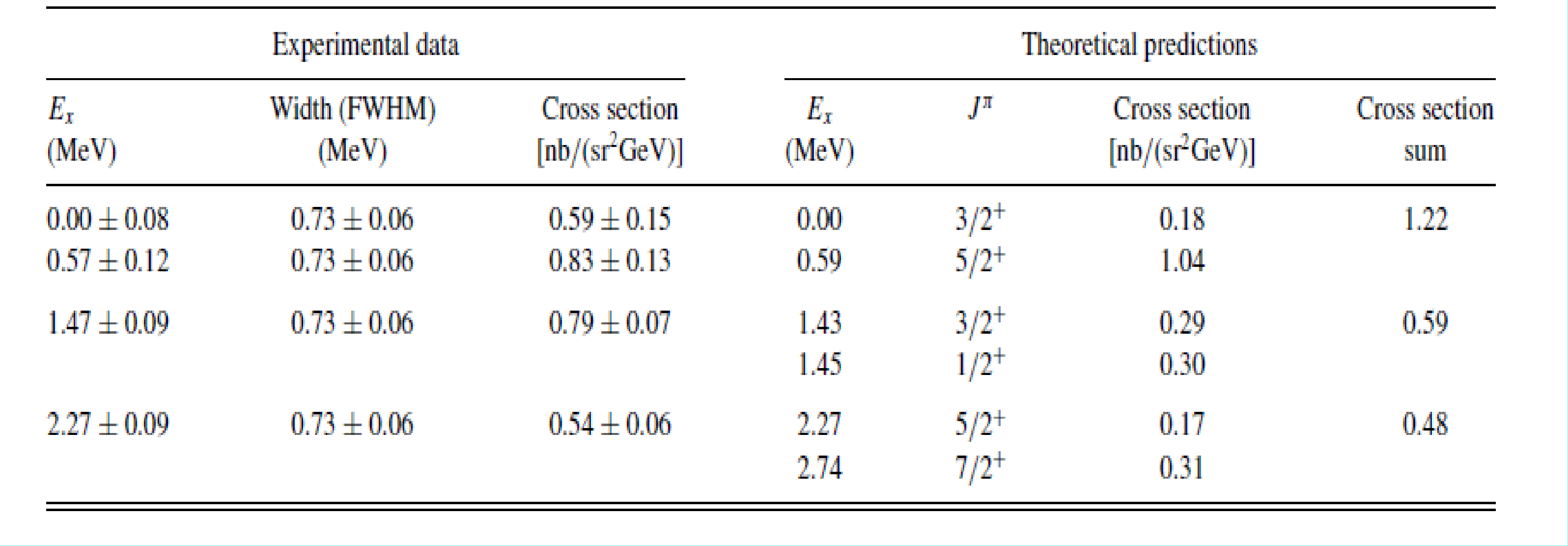

Experimental data			Theoretical predictions			
E_x (MeV)	Width (FWHM) (MeV)	Cross section [nb/(sr^{2}GeV)]	E_x (MeV)	J^π	Cross section [nb/(sr^{2}GeV)]	Cross section sum
0.00 ± 0.08	0.73 ± 0.06	0.59 ± 0.15	0.00	$3/2^+$	0.18	1.22
0.57 ± 0.12	0.73 ± 0.06	0.83 ± 0.13	0.59	$5/2^+$	1.04	
1.47 ± 0.09	0.73 ± 0.06	0.79 ± 0.07	1.43	$3/2^+$	0.29	0.59
			1.45	$1/2^+$	0.30	
2.27 ± 0.09	0.73 ± 0.06	0.54 ± 0.06	2.27	$5/2^+$	0.17	0.48
			2.74	$7/2^+$	0.31	

The experimental peak postions agree quite well with the theoretical predictions

The splitting of the two peaks making up the first doublet (570 ± 120 keV) corresponds very well to the theoretical value of 590 keV

On the other hand, in the first multiplet, the $5/2^{+}$ dos not dominate as theoretically predicted and the third multiplet is observed as a single peak against a theoretically predicted splitting of 470 keV

An elementary model for the (e,e'K^{+}) reaction with a different balance of spin-flip and non-spin-flip amplitudes with respect to what so far assumed might help to resolve this disagreement

A separation energy B_Λ of 8.36 ± 0.08 (stat) ± 0.08 (sys) was measured, quite in agreement with the value of 8.50 ± 0.12 MeV from emulsion data

Results on ^{12}C target
Hypernuclear Spectrum of $^{12}B_\Lambda$

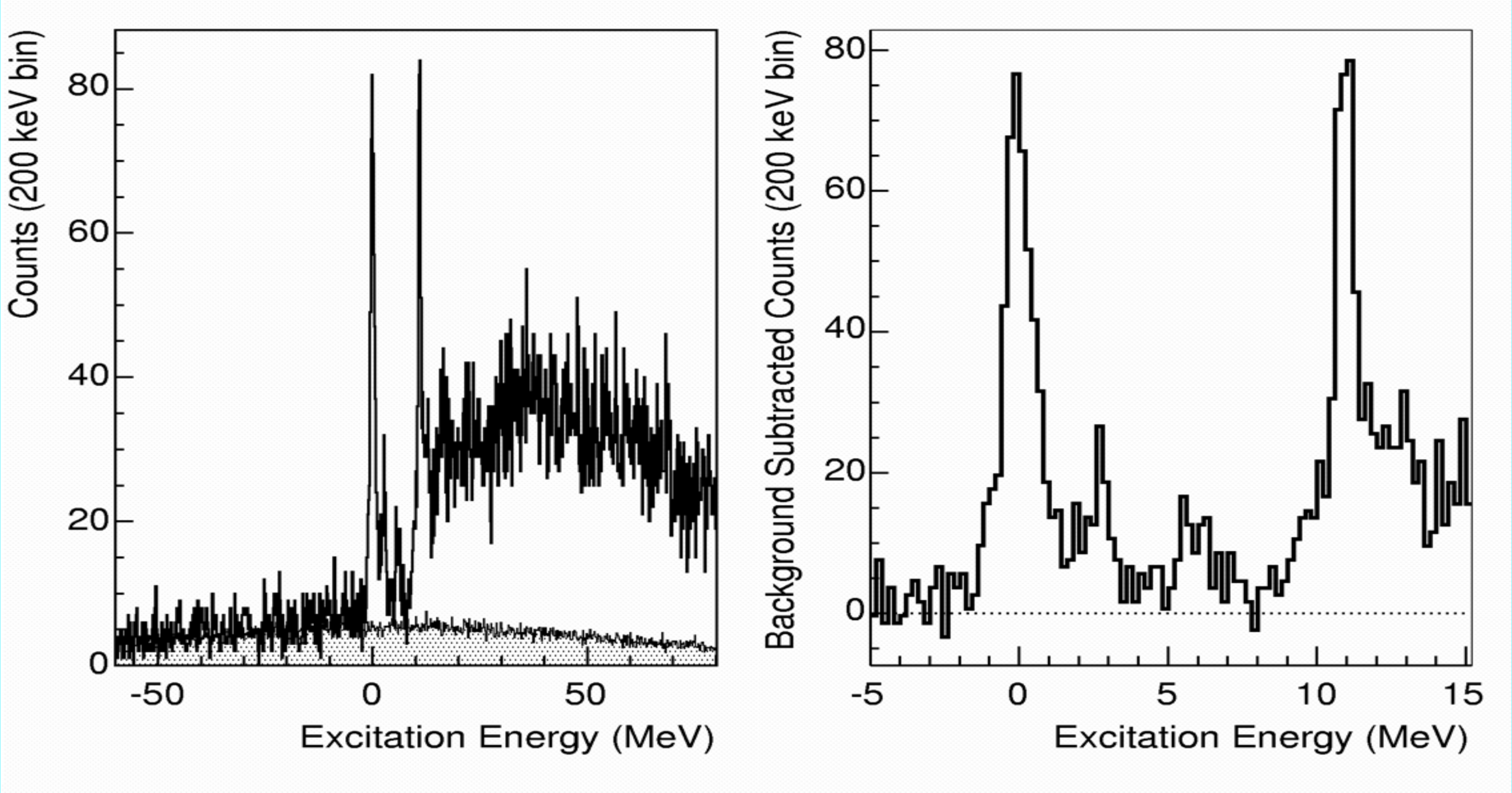

- BACKGROUND level is very low ⇒ Signal/Noise Ratio is very high
- Clear evidence of core excited peak levels between the ground state and the strongly populated p-Lambda peak at 11 MeV
- Quasi free K-Lambda production dominate the spectrum above 13 MeV

Results on ^{12}C target – Hypernuclear Spectrum of $^{12}B_{\Lambda}$

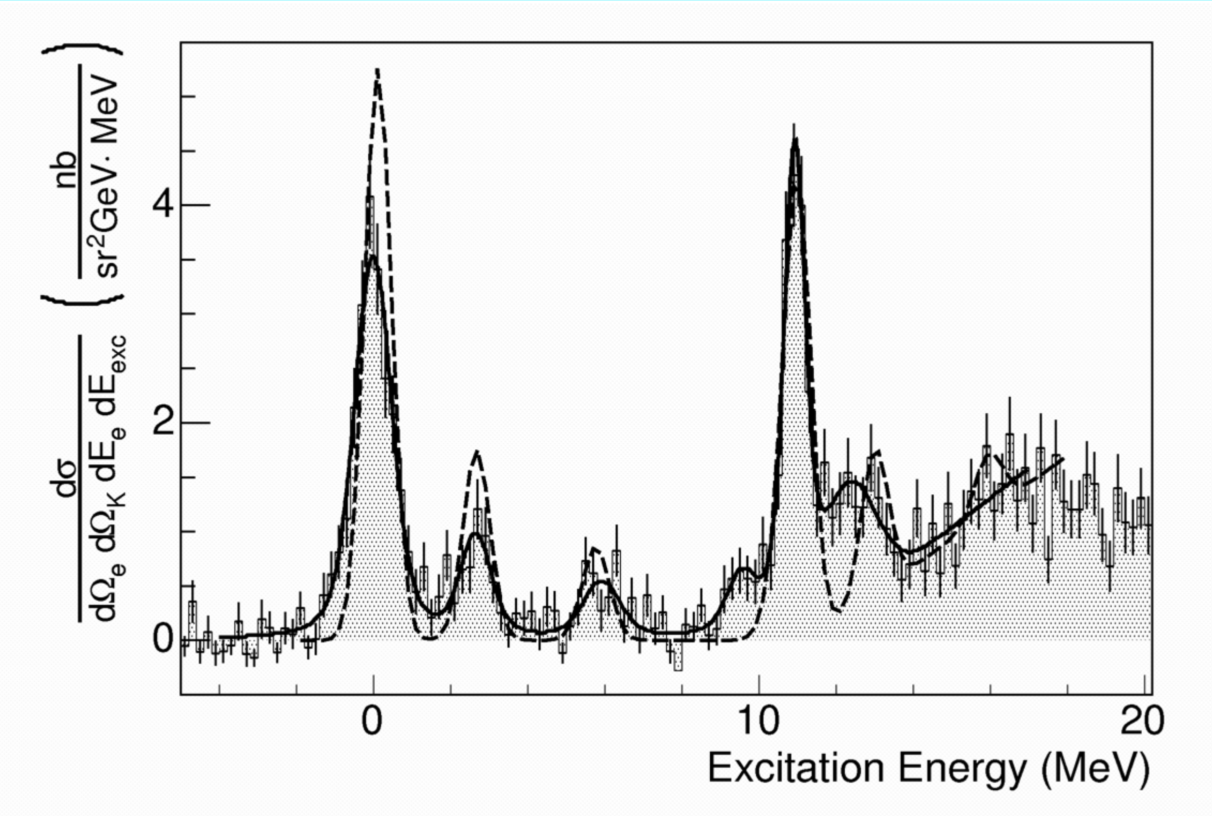

- Peak Search :
Identified 6 regions with excess counts above background

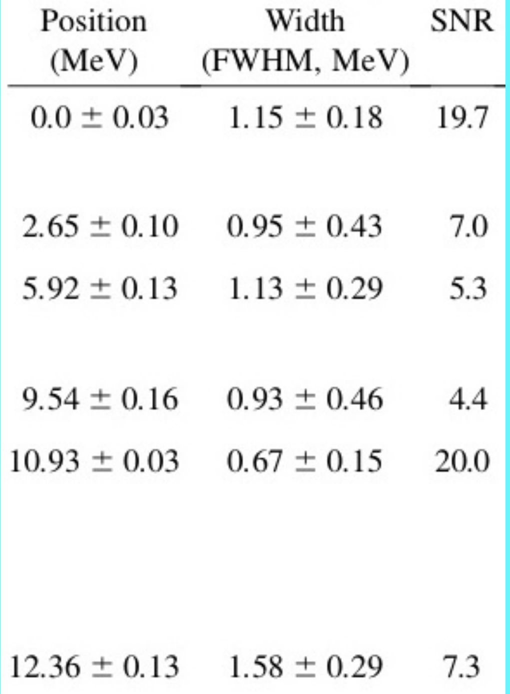

Position (MeV)	Width (FWHM, MeV)	SNR
0.0 ± 0.03	1.15 ± 0.18	19.7
2.65 ± 0.10	0.95 ± 0.43	7.0
5.92 ± 0.13	1.13 ± 0.29	5.3
9.54 ± 0.16	0.93 ± 0.46	4.4
10.93 ± 0.03	0.67 ± 0.15	20.0
12.36 ± 0.13	1.58 ± 0.29	7.3

- **Fit to the data: Fit 6 regions with 6 Voigt functions (convolution of Gaussian and Lorentzian) χ^2/ndf = 1.16**
- **Theoretical model superimposed curve based on :**
  - **Saclay-Lyon-A p(e,e'K+)Λ (elementary process)**
  - **ΛN interaction from $^{7}{}_{\Lambda}$Li γ-ray spectra**

Results on ^{12}C target – Hypernuclear Spectrum of $^{12}B_{\Lambda}$

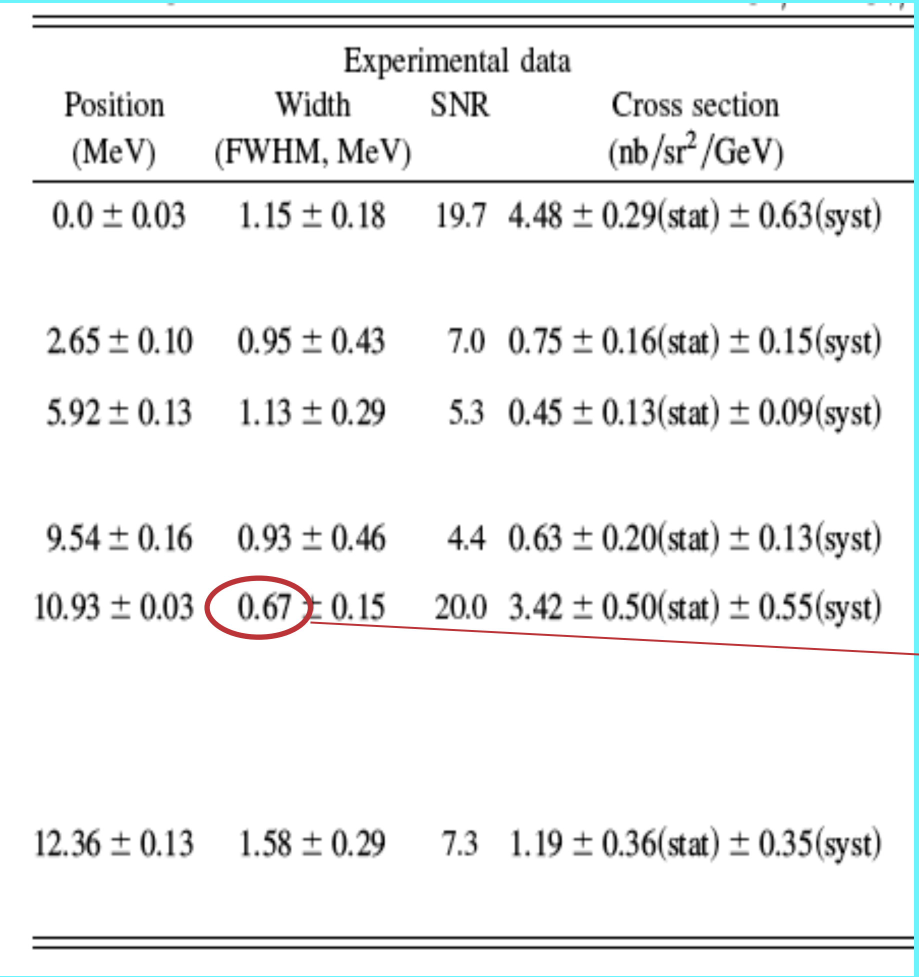

Experimental data			
Position (MeV)	Width (FWHM, MeV)	SNR	Cross section ($nb/sr^2/GeV$)
0.0 ± 0.03	1.15 ± 0.18	19.7	$4.48 \pm 0.29(stat) \pm 0.63(syst)$
2.65 ± 0.10	0.95 ± 0.43	7.0	$0.75 \pm 0.16(stat) \pm 0.15(syst)$
5.92 ± 0.13	1.13 ± 0.29	5.3	$0.45 \pm 0.13(stat) \pm 0.09(syst)$
9.54 ± 0.16	0.93 ± 0.46	4.4	$0.63 \pm 0.20(stat) \pm 0.13(syst)$
10.93 ± 0.03	0.67 ± 0.15	20.0	$3.42 \pm 0.50(stat) \pm 0.55(syst)$
12.36 ± 0.13	1.58 ± 0.29	7.3	$1.19 \pm 0.36(stat) \pm 0.35(syst)$

- Measured cross sections in good agreement with theory
- Energy resolution ~670 keV
- First clear evidence of core excited states with high statistical significance
- Hint for a peak at 9.54 MeV (admixture states)

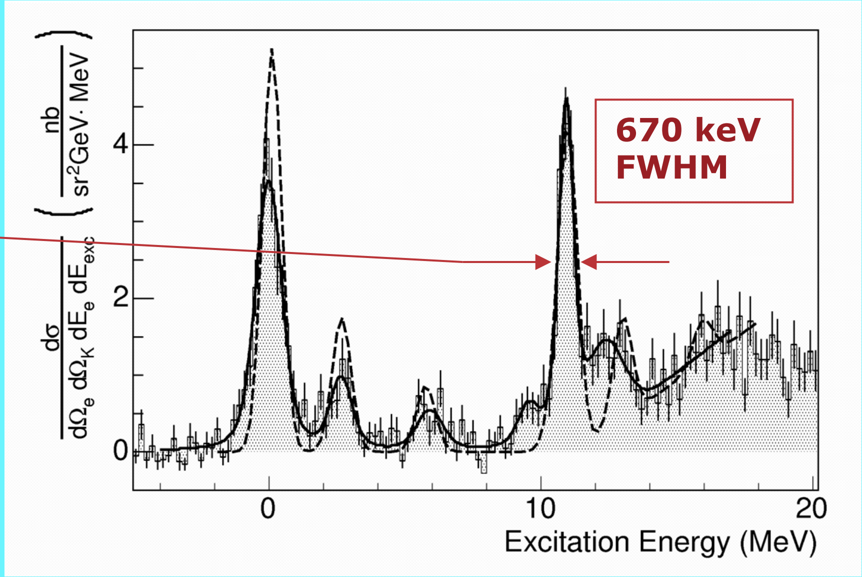

670 keV FWHM

Results on ^{12}C target – Hypernuclear Spectrum of $^{12}B_{\Lambda}$

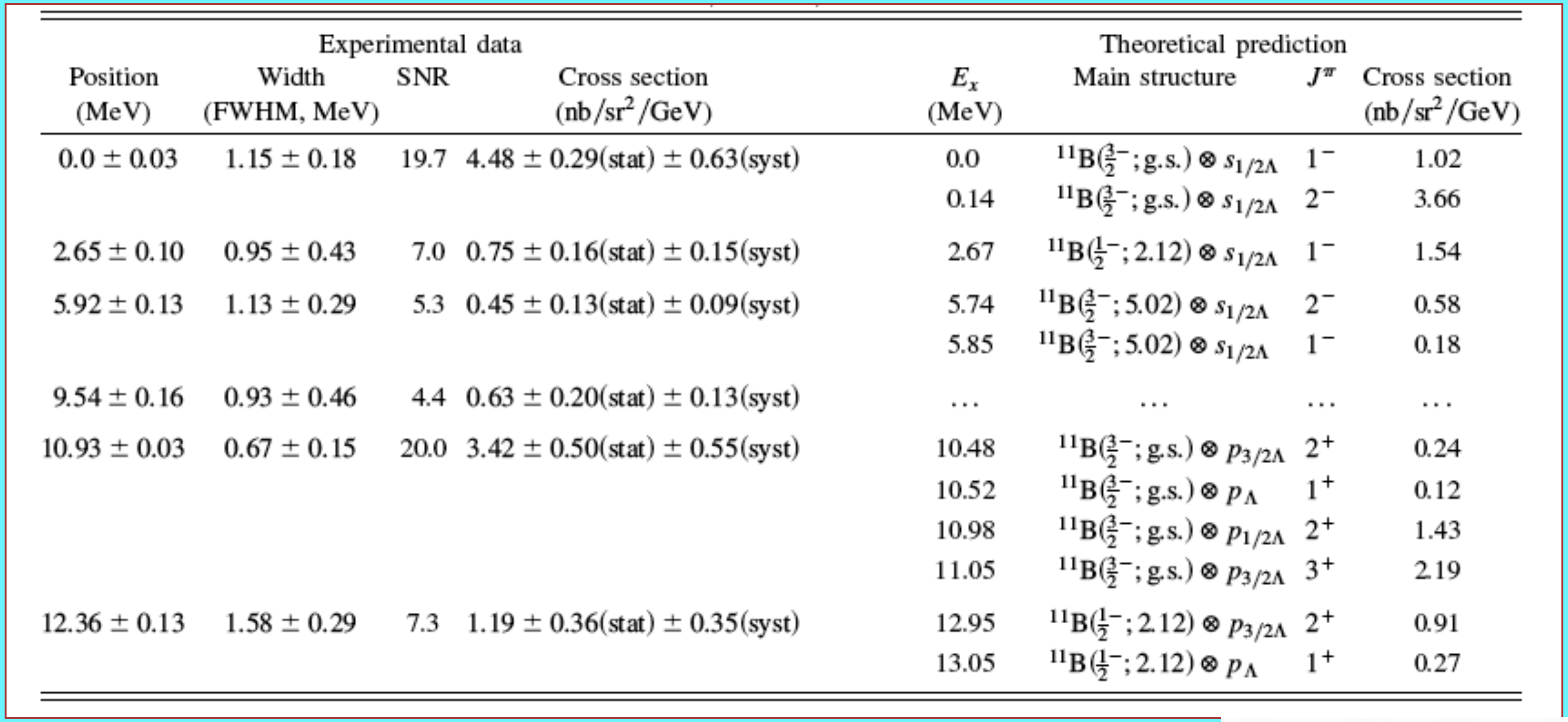

Experimental data				Theoretical prediction			
Position (MeV)	Width (FWHM, MeV)	SNR	Cross section (nb/sr^2/GeV)	E_x (MeV)	Main structure	J^π	Cross section (nb/sr^2/GeV)
0.0 ± 0.03	1.15 ± 0.18	19.7	4.48 ± 0.29(stat) ± 0.63(syst)	0.0	$^{11}\mathrm{B}(\frac{3}{2}^-; \mathrm{g.s.}) \otimes s_{1/2\Lambda}$	1^-	1.02
				0.14	$^{11}\mathrm{B}(\frac{3}{2}^-; \mathrm{g.s.}) \otimes s_{1/2\Lambda}$	2^-	3.66
2.65 ± 0.10	0.95 ± 0.43	7.0	0.75 ± 0.16(stat) ± 0.15(syst)	2.67	$^{11}\mathrm{B}(\frac{1}{2}^-; 2.12) \otimes s_{1/2\Lambda}$	1^-	1.54
5.92 ± 0.13	1.13 ± 0.29	5.3	0.45 ± 0.13(stat) ± 0.09(syst)	5.74	$^{11}\mathrm{B}(\frac{3}{2}^-; 5.02) \otimes s_{1/2\Lambda}$	2^-	0.58
				5.85	$^{11}\mathrm{B}(\frac{3}{2}^-; 5.02) \otimes s_{1/2\Lambda}$	1^-	0.18
9.54 ± 0.16	0.93 ± 0.46	4.4	0.63 ± 0.20(stat) ± 0.13(syst)	...	...	...	...
10.93 ± 0.03	0.67 ± 0.15	20.0	3.42 ± 0.50(stat) ± 0.55(syst)	10.48	$^{11}\mathrm{B}(\frac{3}{2}^-; \mathrm{g.s.}) \otimes p_{3/2\Lambda}$	2^+	0.24
				10.52	$^{11}\mathrm{B}(\frac{3}{2}^-; \mathrm{g.s.}) \otimes p_{\Lambda}$	1^+	0.12
				10.98	$^{11}\mathrm{B}(\frac{3}{2}^-; \mathrm{g.s.}) \otimes p_{1/2\Lambda}$	2^+	1.43
				11.05	$^{11}\mathrm{B}(\frac{3}{2}^-; \mathrm{g.s.}) \otimes p_{3/2\Lambda}$	3^+	2.19
12.36 ± 0.13	1.58 ± 0.29	7.3	1.19 ± 0.36(stat) ± 0.35(syst)	12.95	$^{11}\mathrm{B}(\frac{1}{2}^-; 2.12) \otimes p_{3/2\Lambda}$	2^+	0.91
				13.05	$^{11}\mathrm{B}(\frac{1}{2}^-; 2.12) \otimes p_{\Lambda}$	1^+	0.27

Measured cross sections in good agreement with theory

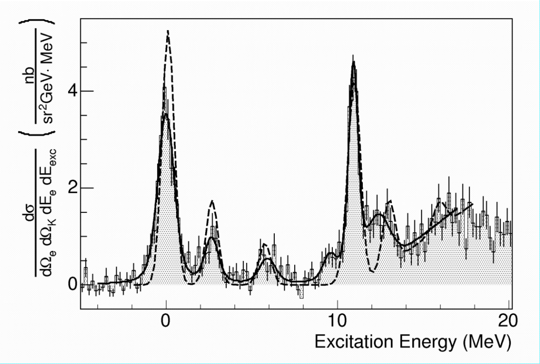

s_Λ states

The energies of the 1/2- and 3/2- levels of the core are raised primarily by the S_N term because the interaction l_N. S_N changes the spacing of the core levels (the magnitude can be changed by changing S_N or changing the p-shell w.f. of the core)

p_Λ states

The overall excitation energy of these states depends on energy separation of the p_Λ and s_Λ single particle states.

Essentially degenerate 2_1^+ and 3_1^+ dominate in the main p-shell peak (~ 11 MeV)1.9 MeV higher is 1/2-$\otimes\Lambda p_{3/2}$ -> 2_2^+

The good resolution of the (e,e'K) reaction may enable a limit to be put on the spacing of 2_1^+ and 3_1^+

The "sixt" peak should be due, in the simplest model, to states based on core states with positive-parity and the lambda in an s state that mix with negative-parity core states coupled to p_Λ.

The **WATERFALL** target: reactions on ^{16}O and ^{1}H nuclei

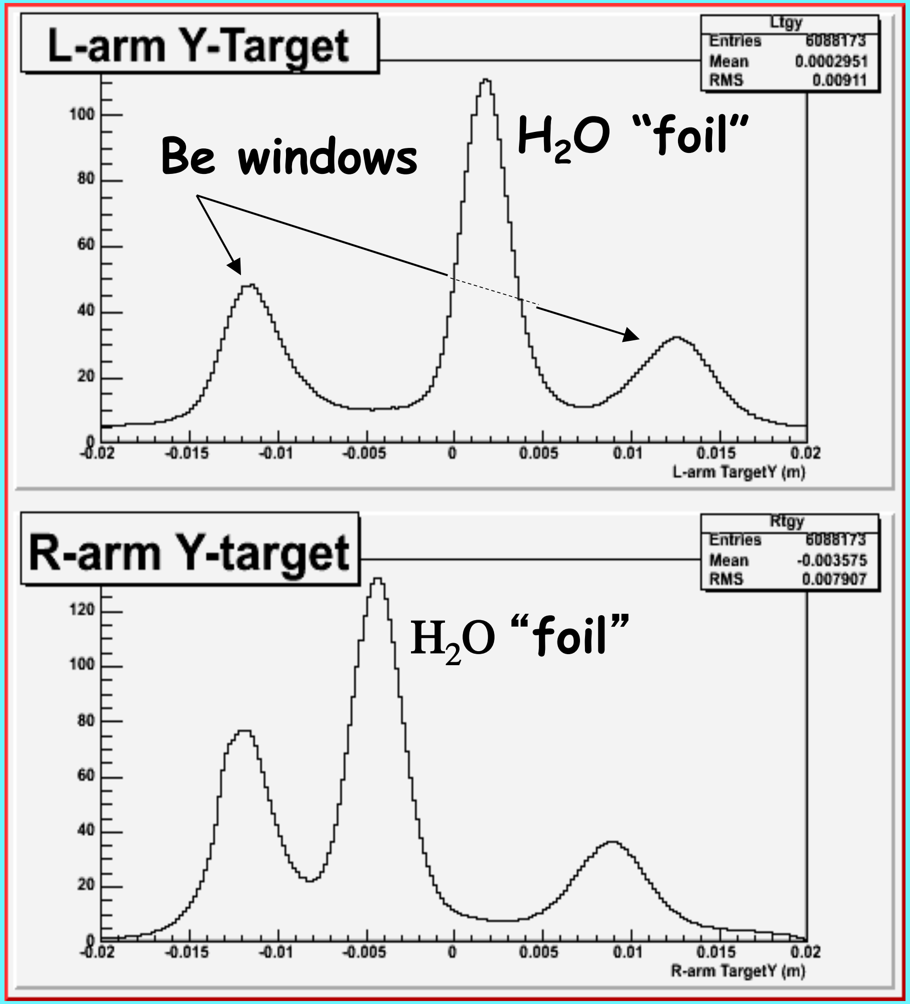

Results on the WATERFALL target - ^{16}O and ^{1}H

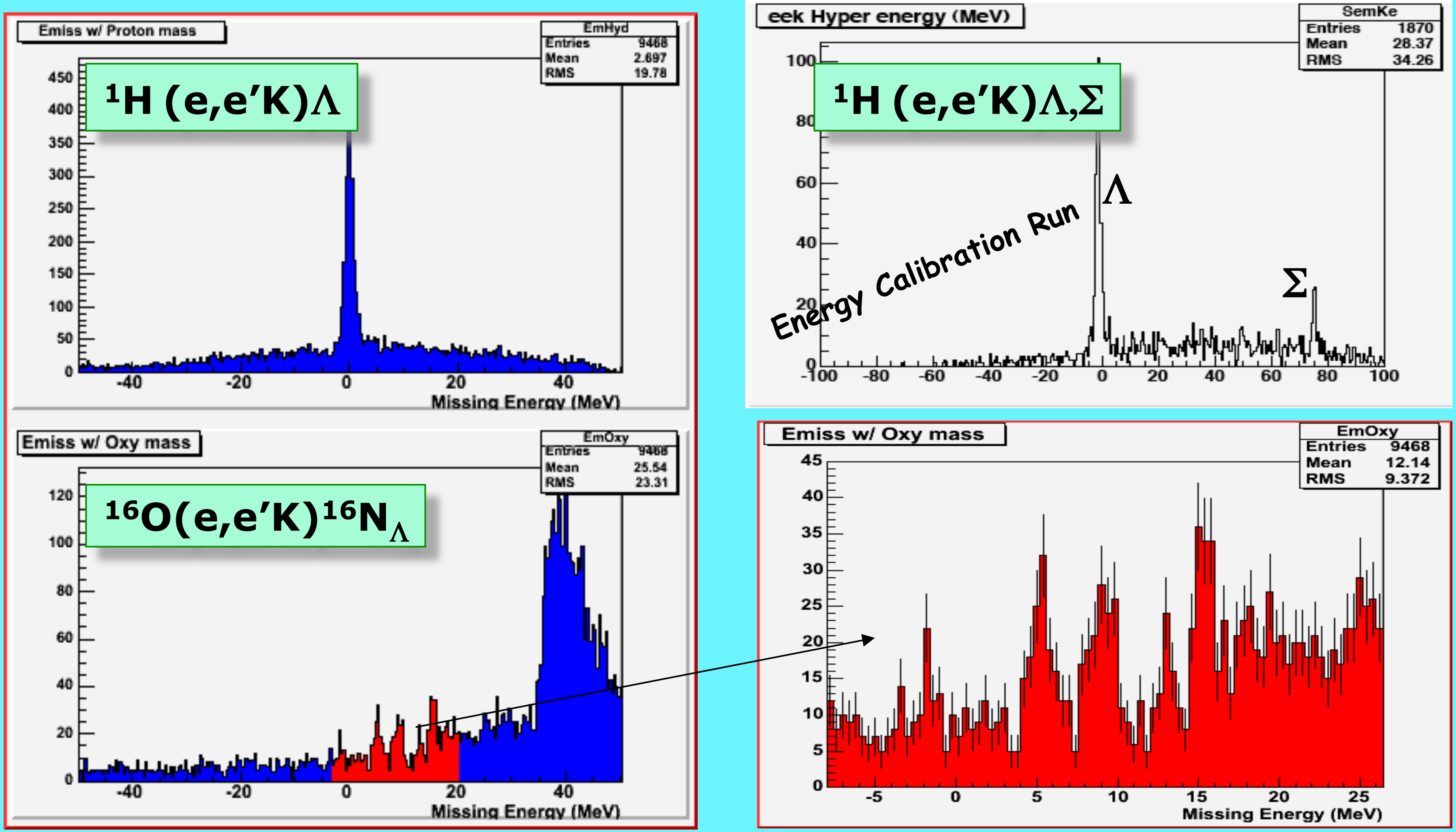

- Water thickness from elastic cross section on H
- Precise determination of the particle momenta and beam energy using the Lambda and Sigma peak reconstruction (energy scale calibration)

Results on ^{16}O target – Hypernuclear Spectrum of $^{16}\mathrm{N}_{\Lambda}$

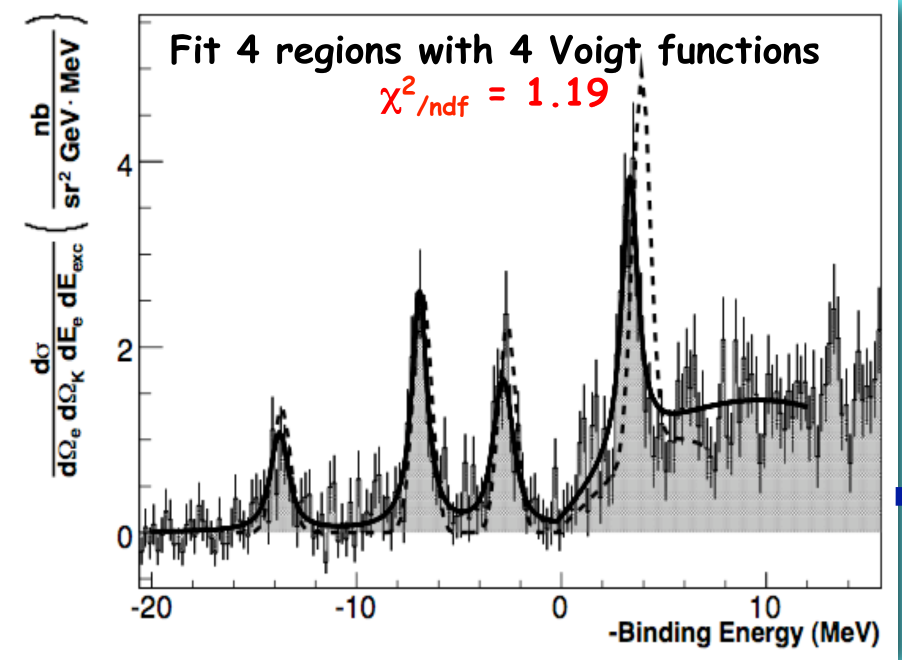

Theoretical model based on :
SLA p(e,e'K$^+$)Λ (elementary process)
ΛN interaction fixed parameters from
KEK and BNL $^{16}{}_{\Lambda}$O spectra

- Four peaks reproduced by theory
- The fourth peak (Λ in p state) position disagrees with theory.

This might be an indication of a large spin-orbit term S_{Λ}

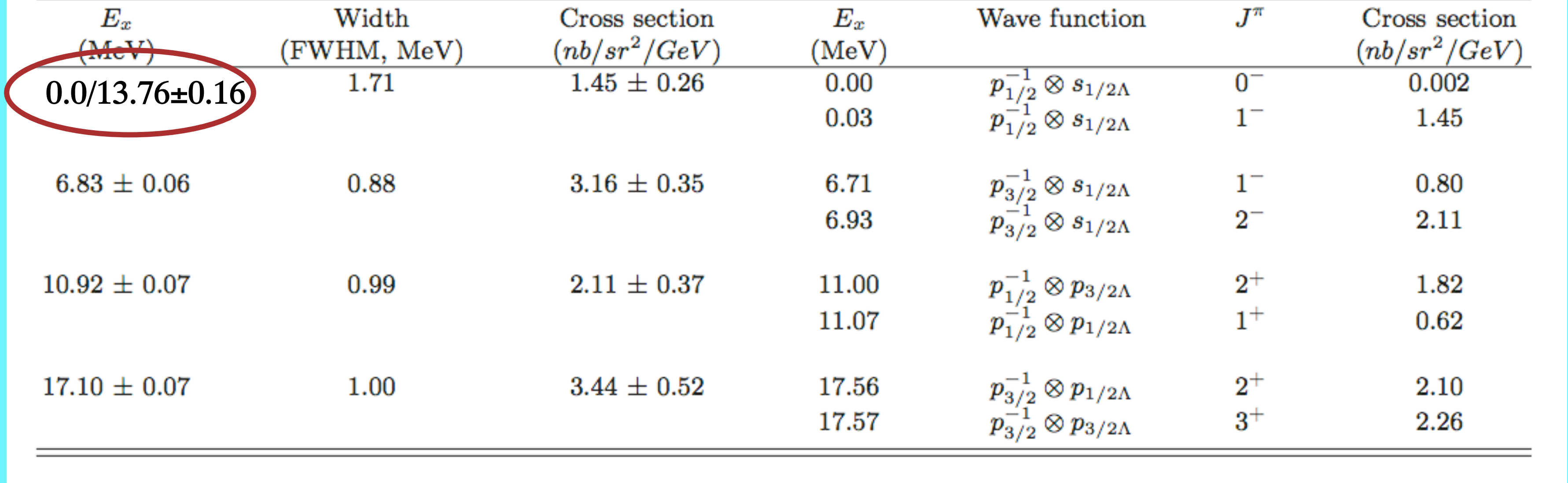

E_x (MeV)	Width (FWHM, MeV)	Cross section ($nb/sr^2/GeV$)	E_x (MeV)	Wave function	J^π	Cross section ($nb/sr^2/GeV$)
0.0/13.76±0.16	1.71	1.45 ± 0.26	0.00	$p_{1/2}^{-1} \otimes s_{1/2\Lambda}$	0^-	0.002
			0.03	$p_{1/2}^{-1} \otimes s_{1/2\Lambda}$	1^-	1.45
6.83 ± 0.06	0.88	3.16 ± 0.35	6.71	$p_{3/2}^{-1} \otimes s_{1/2\Lambda}$	1^-	0.80
			6.93	$p_{3/2}^{-1} \otimes s_{1/2\Lambda}$	2^-	2.11
10.92 ± 0.07	0.99	2.11 ± 0.37	11.00	$p_{1/2}^{-1} \otimes p_{3/2\Lambda}$	2^+	1.82
			11.07	$p_{1/2}^{-1} \otimes p_{1/2\Lambda}$	1^+	0.62
17.10 ± 0.07	1.00	3.44 ± 0.52	17.56	$p_{3/2}^{-1} \otimes p_{1/2\Lambda}$	2^+	2.10
			17.57	$p_{3/2}^{-1} \otimes p_{3/2\Lambda}$	3^+	2.26

Results on ^{16}O target – Hypernuclear Spectrum of $^{16}N_{\Lambda}$

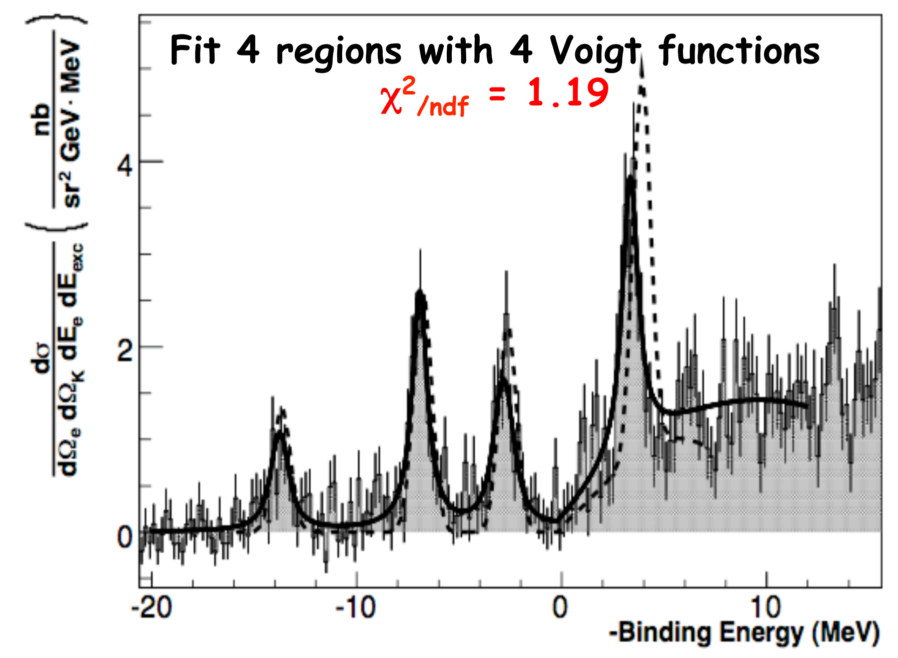

Binding Energy B_L=13.76±0.16 MeV Measured for the first time with this level of accuracy (ambiguous interpretation from emulsion data; interaction involving Λ production on *n* more difficult to normalize)

Within errors, the binding energy and the excited levels of the mirror hypernuclei $^{16}O_{\Lambda}$ and $^{16}N_{\Lambda}$ (this experiment) are in agreement, giving no strong evidence of charge-dependent effects

E_x (MeV)	Width (FWHM, MeV)	Cross section ($nb/sr^2/GeV$)	E_x (MeV)	Wave function	J^{π}	Cross section ($nb/sr^2/GeV$)
0.0/13.76±0.16	1.71	1.45 ± 0.26	0.00	$p^{-1}_{1/2} \otimes s_{1/2\Lambda}$	0^-	0.002
			0.03	$p^{-1}_{1/2} \otimes s_{1/2\Lambda}$	1^-	1.45
6.83 ± 0.06	0.88	3.16 ± 0.35	6.71	$p^{-1}_{3/2} \otimes s_{1/2\Lambda}$	1^-	0.80
			6.93	$p^{-1}_{3/2} \otimes s_{1/2\Lambda}$	2^-	2.11
10.92 ± 0.07	0.99	2.11 ± 0.37	11.00	$p^{-1}_{1/2} \otimes p_{3/2\Lambda}$	2^+	1.82
			11.07	$p^{-1}_{1/2} \otimes p_{1/2\Lambda}$	1^+	0.62
17.10 ± 0.07	1.00	3.44 ± 0.52	17.56	$p^{-1}_{3/2} \otimes p_{1/2\Lambda}$	2^+	2.10
			17.57	$p^{-1}_{3/2} \otimes p_{3/2\Lambda}$	3^+	2.26

Elementary production of Λ in $^{1}H(e,e'K+)\Lambda$

-Calculations of the cross section for the electroproduction of hypernuclei use the elementary amplitudes and a nuclear and hypernuclear wavefunction.

$$\left\langle \psi_H \left| \sum_{i=1}^{Z} \chi_\gamma \chi_K^* \boxed{J^\mu(i)} \right| \psi_A \right\rangle$$

-The cross sections are sensitive only to the elementary amplitude for very small kaon angles.

-Measure the elementary production cross section as input for the hypernuclear calculations and determine its small-angle behavior

-Dynamics of the elementary reaction itself is also interesting in this unexplored kinematics region.

- By measuring the ratio of hypernuclear/elementary reaction makes the interpretation the hypernuclear structure simpler

Results on H target – The p(e,e'K)Λ Cross Section

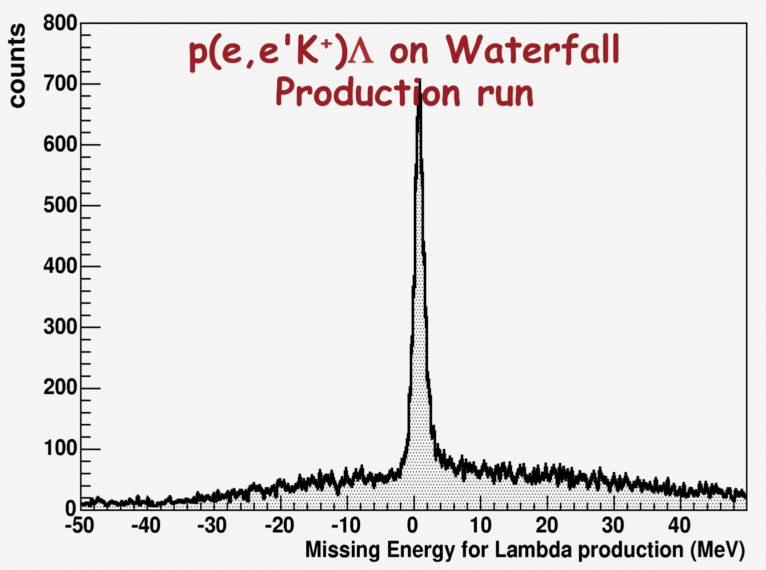

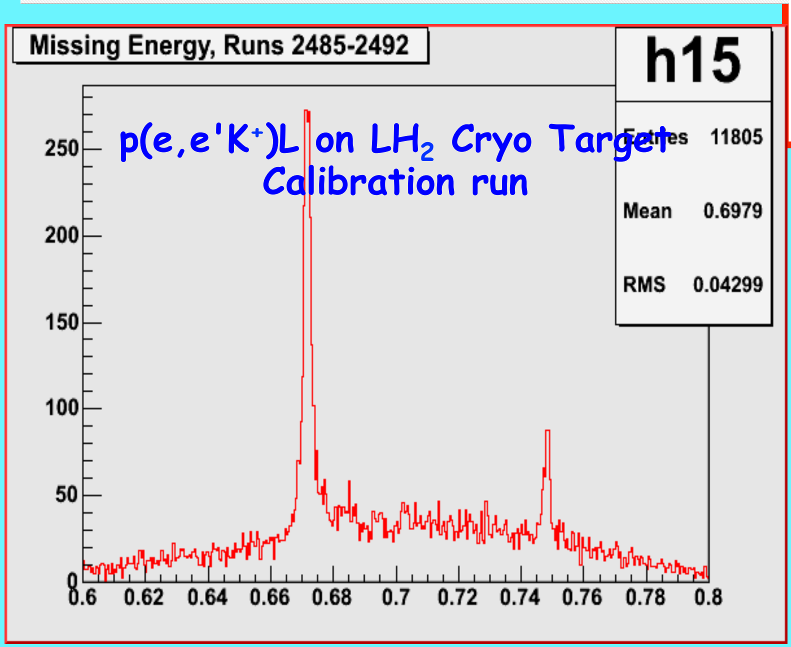

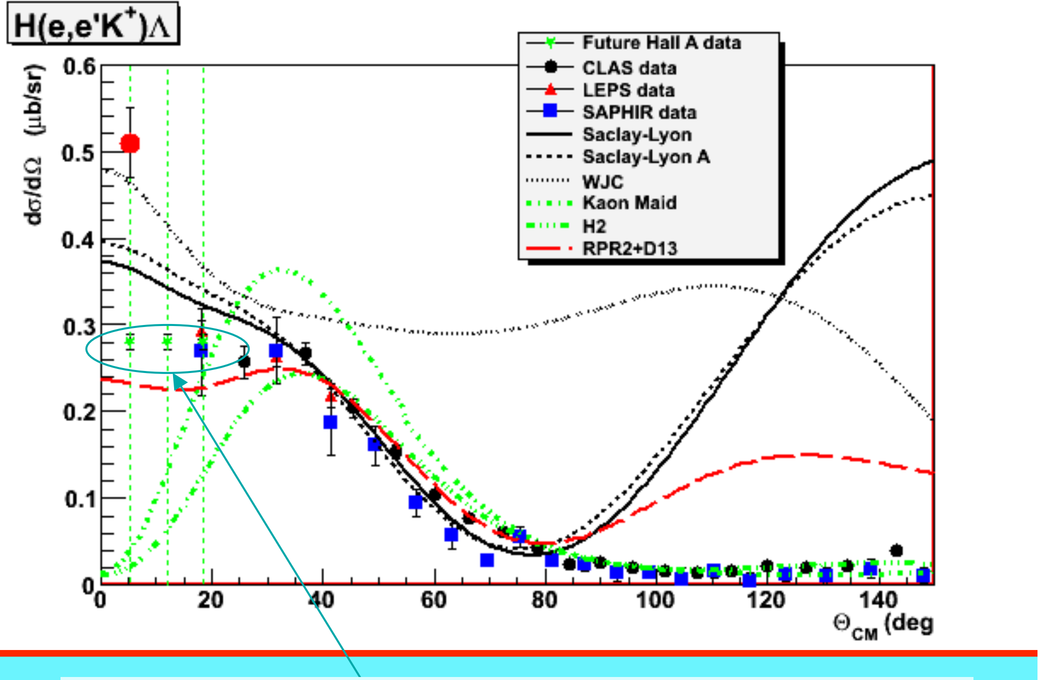

Expected data from E07-012, study the angular dependence of p(e,e'K)Λ and ^{16}O(e,e'K)^{16}N$_{\Lambda}$ at low Q^2

- None of the models is able to describe the data over the entire range
- New data is electroproduction – could longitudinal amplitudes dominate?

Results on H target – The p(e,e'K)Λ Cross Section

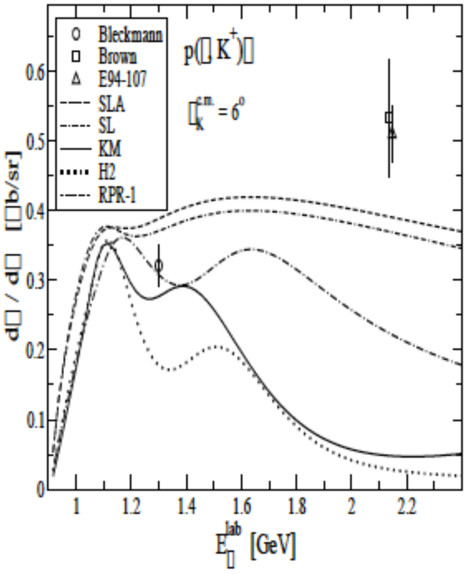

Fig. 1-2: Predictions of isobar (Saclay-Lyon: SL and SLA; Kaon-MAID: KM; and H2 [BYD03]) and Regge-plus-resonance (RPR-1 [BYD12]) models for the photoproduction cross section at kaon c.m. angle 6°. The data point 'Bleckmann' is for photoproduction and the points 'Brown' and 'E94-107' are for electroproduction with very small Q^2.

The small angle behavior of the cross section is poorly known (results from E94-107 running at higher *W*). CLAS, SAPHIR and LEPS have difficulty reaching angles smaller than ~20°.

This experiment will cover the range $\theta_{\gamma K}$ ~ 0 and allow for several bins.

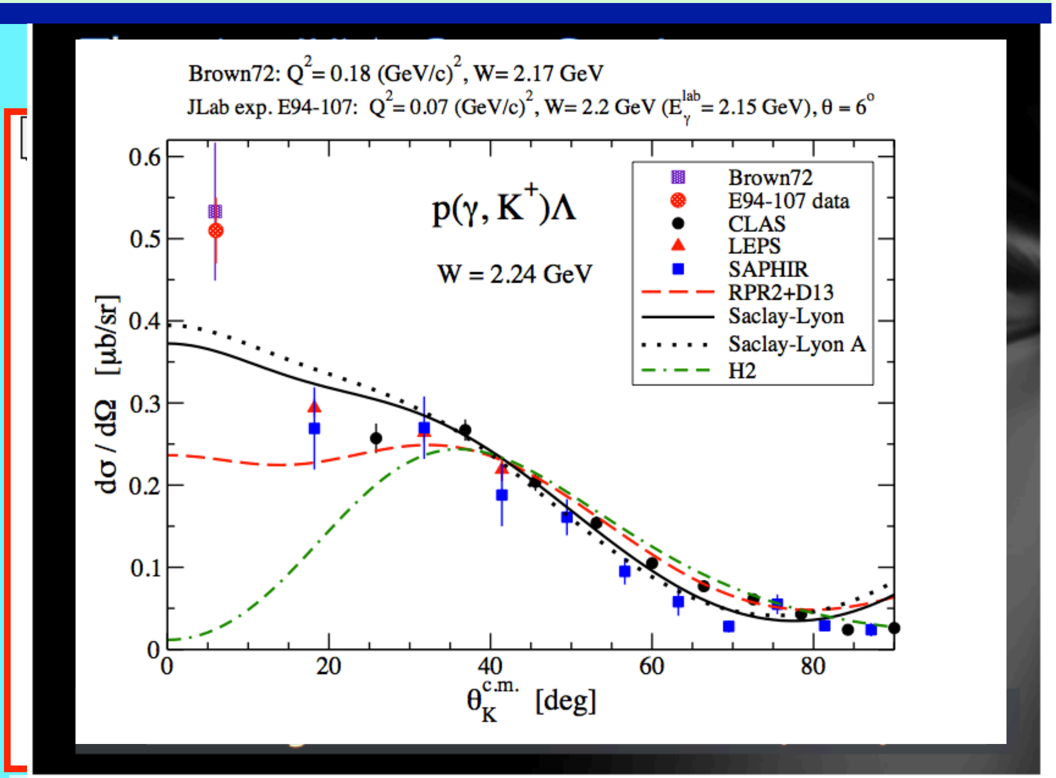

study the angular dependence of $p(e,e'K)\Lambda$ and $^{16}O(e,e'K)^{16}N_\Lambda$

at small kaon angles and at low Q^2

➔ None of the models is able to describe the data over the entire range

➔ New data in electroproduction allows studying dynamics of the models – hadronic form factors, longitudinal couplings…..

JLab E05-115 (Hall-C) setup

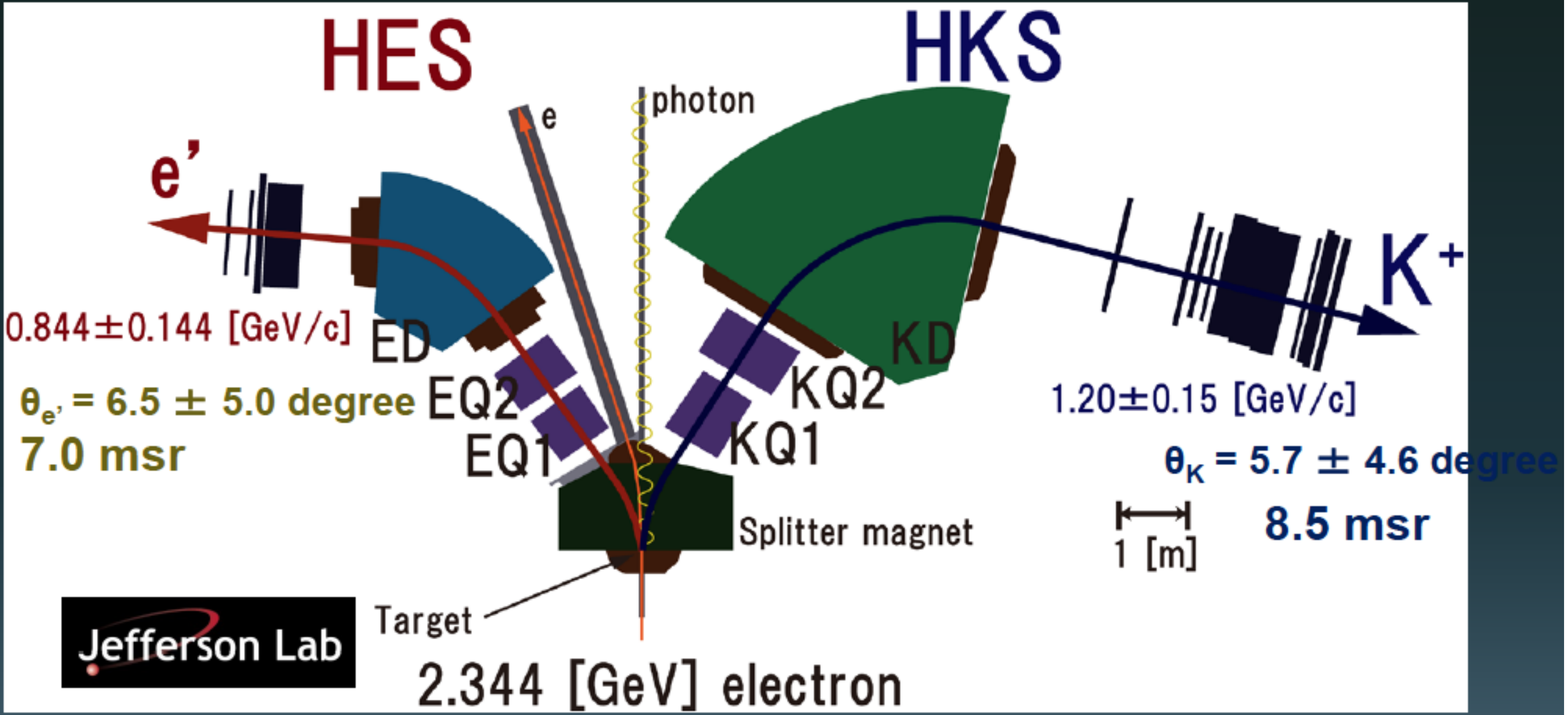

$\Delta p/p \sim 2 \times 10^{-4}$

$^{12}C(e,e'K^{+})^{12}{}_{\Lambda}B$

0.5 MeV (FWHM)

Absolute MM calibration

0.7 MeV (FWHM)

$^{12}C(\pi^{+},K^{+})^{12}{}_{\Lambda}C$

1.45 MeV (FWHM)

$^{12}{}_{\Lambda}C_{gs}$ energy from emulsion

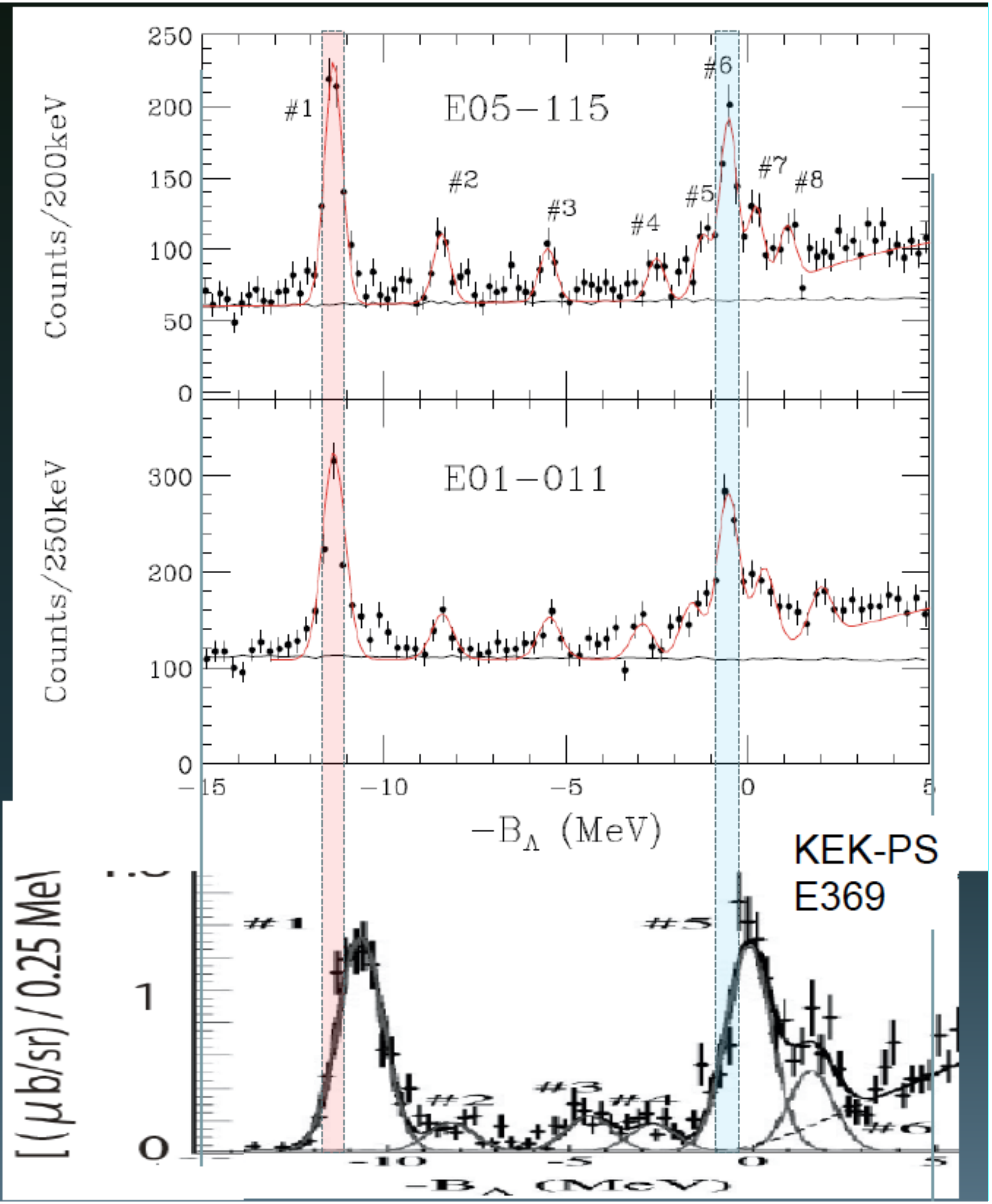

Hall A

Hall C

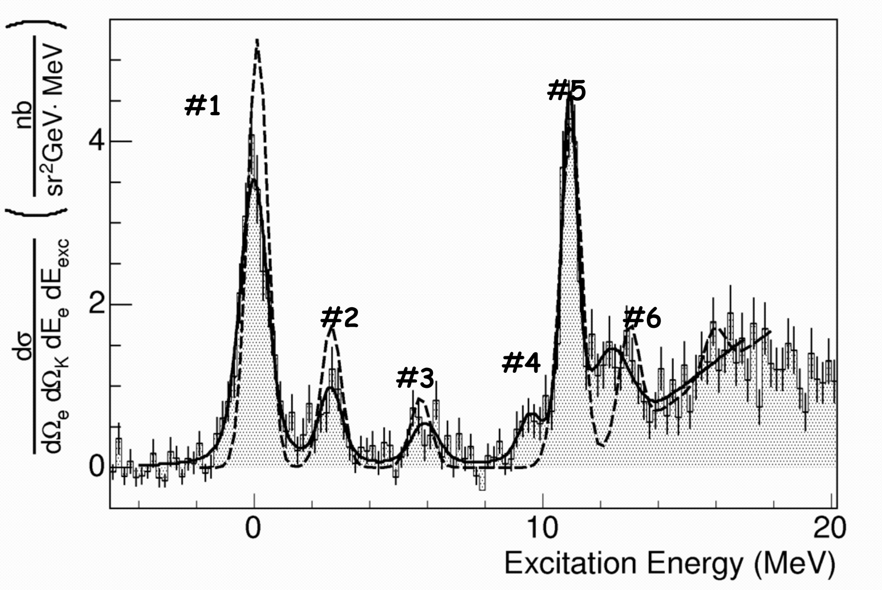

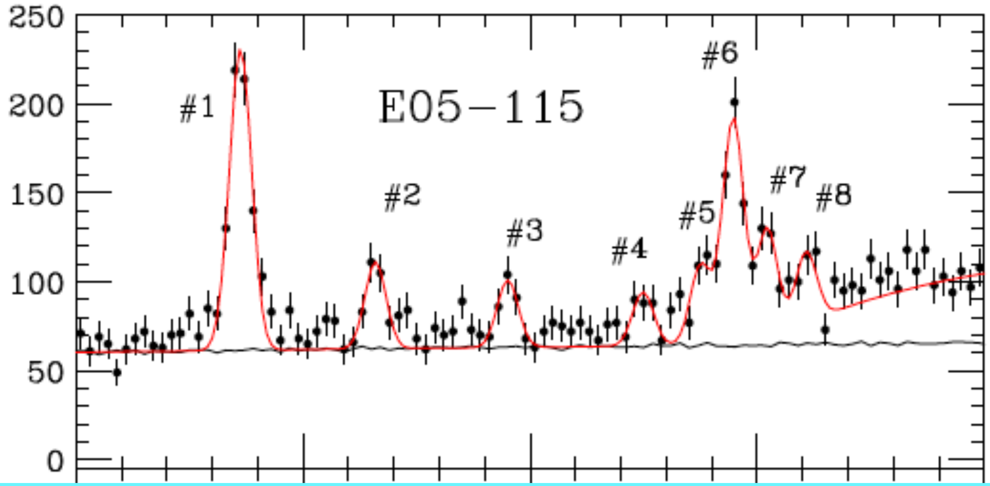

#4 and 5 corresponds to # 4 Hall A (first pair of P_Λ states $(2^+_1, 1^+_1)$

preliminary

6 corresponds to the second pair of P_Λ states $(2^+_2, 3^+_1)$

8 corresponds the third pair of P_Λ states $(2^+_2, 1^+_2)$

This p_Λ configuration infer strong mixing of $p_{3/2\ \Lambda}$ and $p_{1/2\ \Lambda}$

7, 'extra' peak not predicted by $0\hbar\omega$ based calculations using a p-shell core

4 and 7 not predicted, may indicate states with a configuration of s_Λ coupled tothe 3/2+ and 5/2+ + sd-shell ^{11}B core states

Theoretical investigation with full $1\hbar\omega$ based calculations are needed

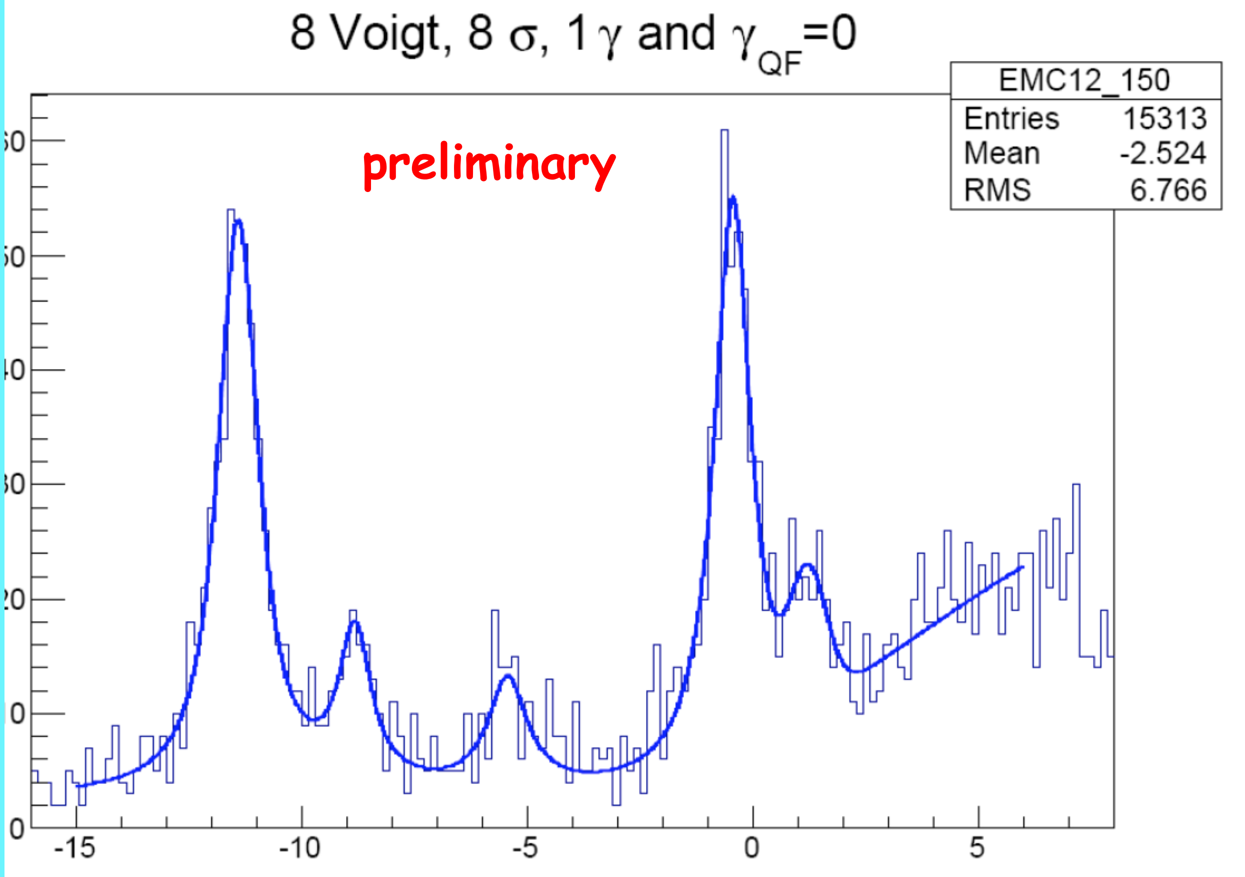
8 Voigt, 8 σ, 1 γ and γ_QF=0
EMC12_150
Entries 15313
Mean -2.524
RMS 6.766
preliminary
0
-15
-10
-5
0
5

$^{7}_{\Lambda}\mathrm{He} = {}^{6}\mathrm{He} + \Lambda$

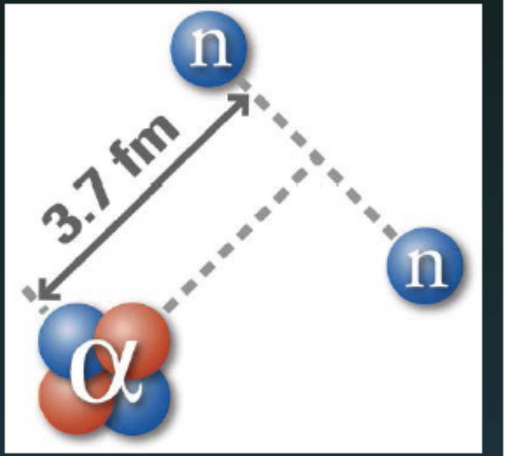

^{6}He : 2n halo

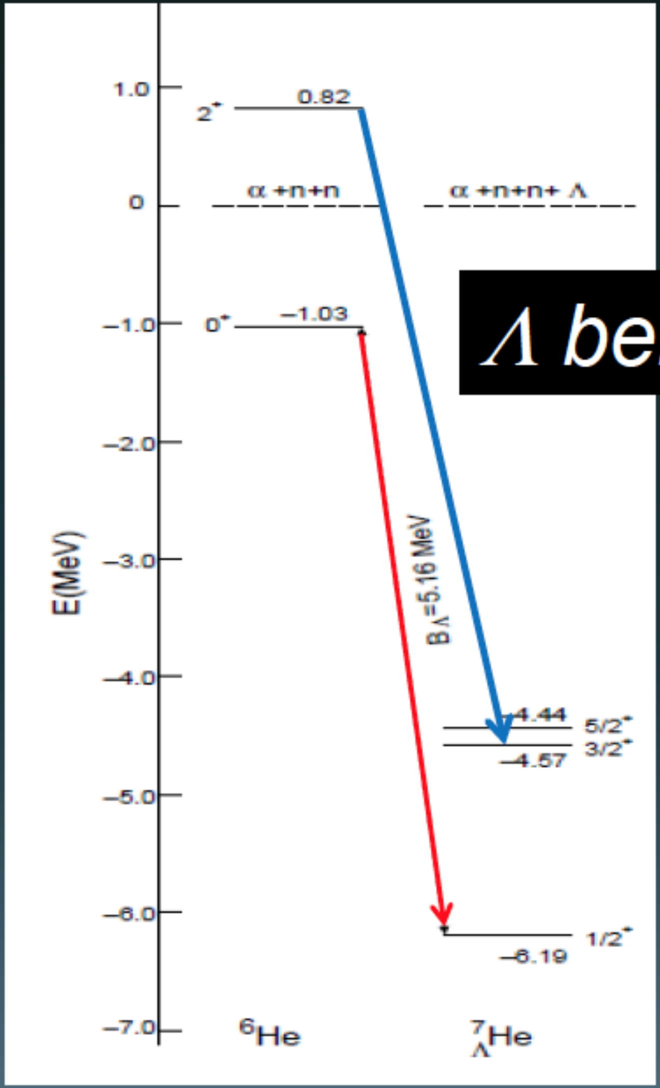

Λ behaves like glue

E.Hiyama et al. PRC 80, 054321 (2009)

${}^{7}_{\Lambda}$He spectrum of E01-01

SNN et al., PRL 110, 012502 (2013)

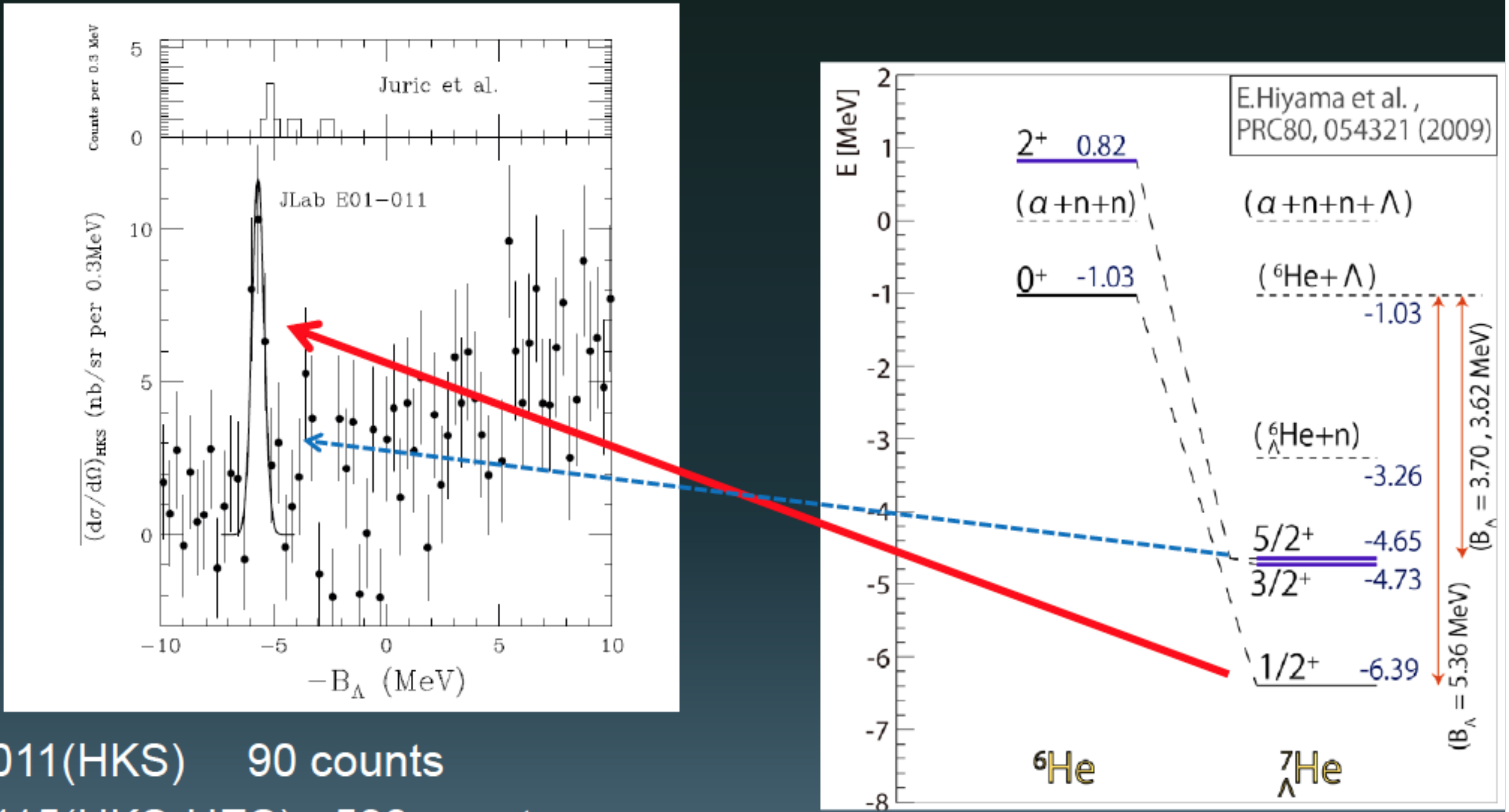

E01-011(HKS) 90 counts

E05-115(HKS-HES) >500 counts

unbound ⁶He excited state + Λ = bound ${}^{7}_{\Lambda}$He excited state

$^{7}{}_{\Lambda}$He spectrum of E05-115

T.Gogami, Doctor Thesis (2014) Tohoku Univ.

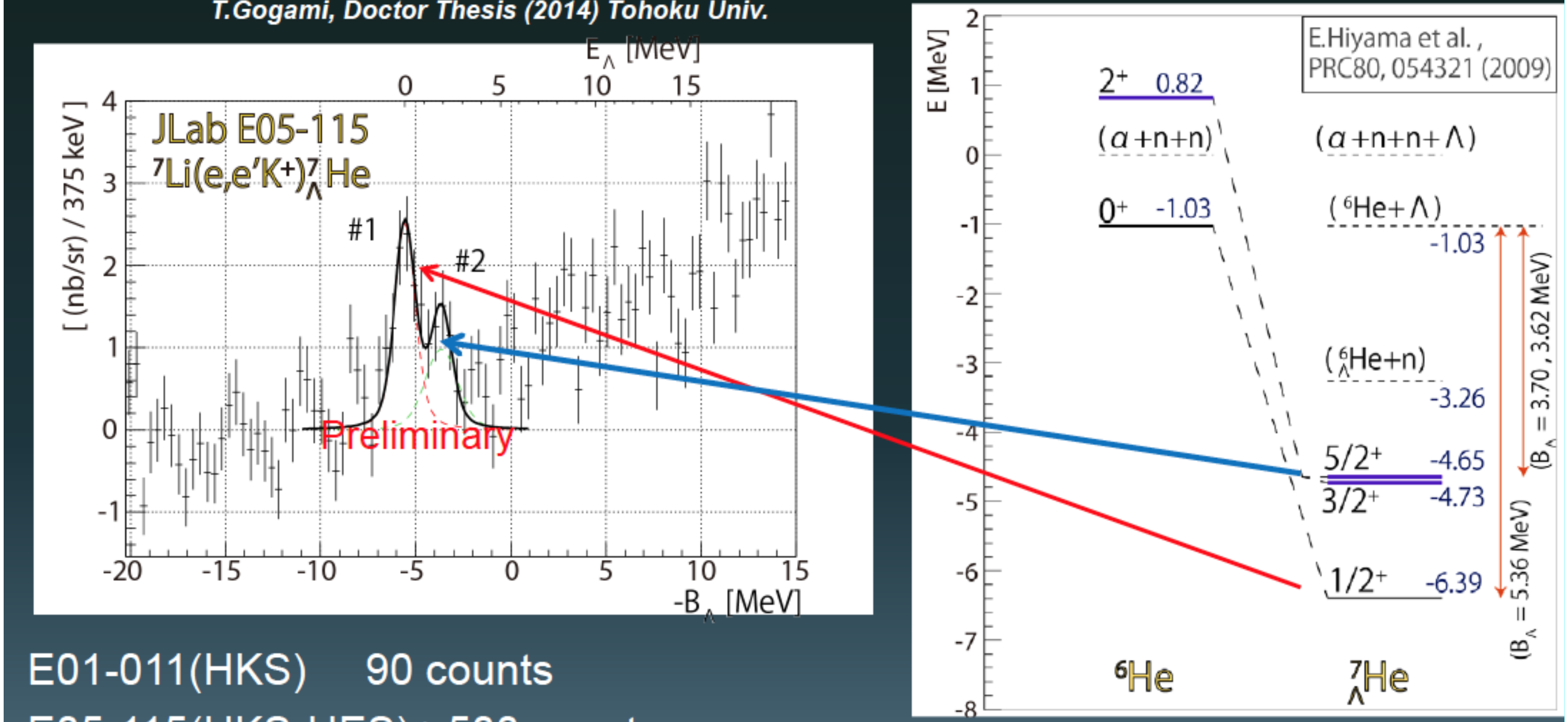

E01-011(HKS) 90 counts

E05-115(HKS-HES) >500 counts

unbound ^{6}He excited state + Λ = bound $^7{}_\Lambda$He excited state

CSB interaction test in A=7 iso-triplet comparison

SNN et al., PRL 110, 012502 (2013)

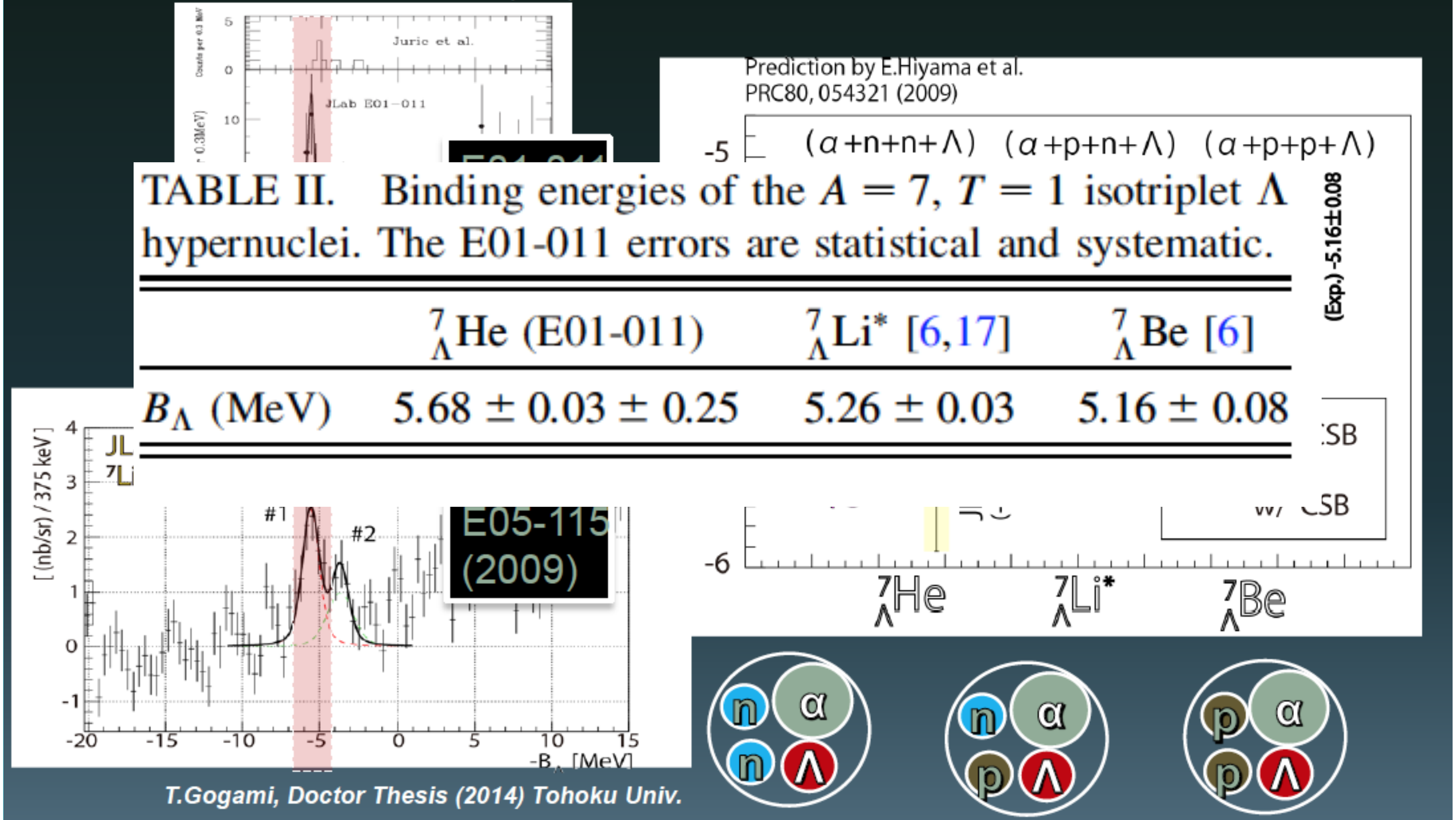

Prediction by E.Hiyama et al.
PRC80, 054321 (2009)

TABLE II. Binding energies of the $A = 7$, $T = 1$ isotriplet Λ hypernuclei. The E01-011 errors are statistical and systematic.

	$^{7}_{\Lambda}$He (E01-011)	$^{7}_{\Lambda}$Li* [6,17]	$^{7}_{\Lambda}$Be [6]
B_Λ (MeV)	5.68 ± 0.03 ± 0.25	5.26 ± 0.03	5.16 ± 0.08

T.Gogami, Doctor Thesis (2014) Tohoku Univ.

$^{10}B(e,e'K^+)^{10}_{\Lambda}Be$

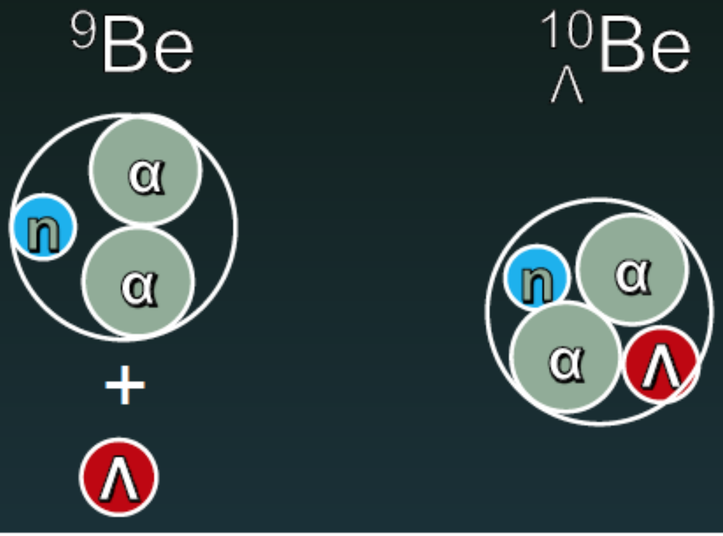

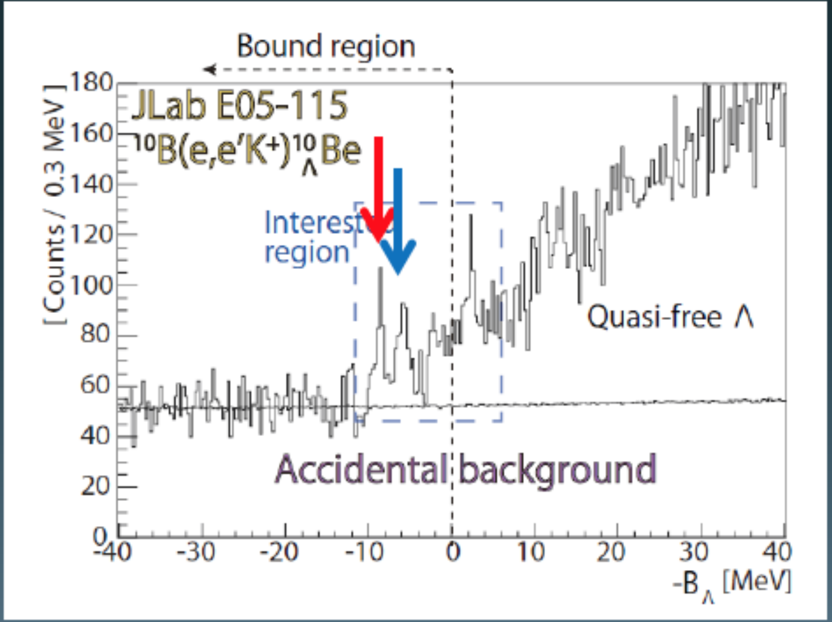

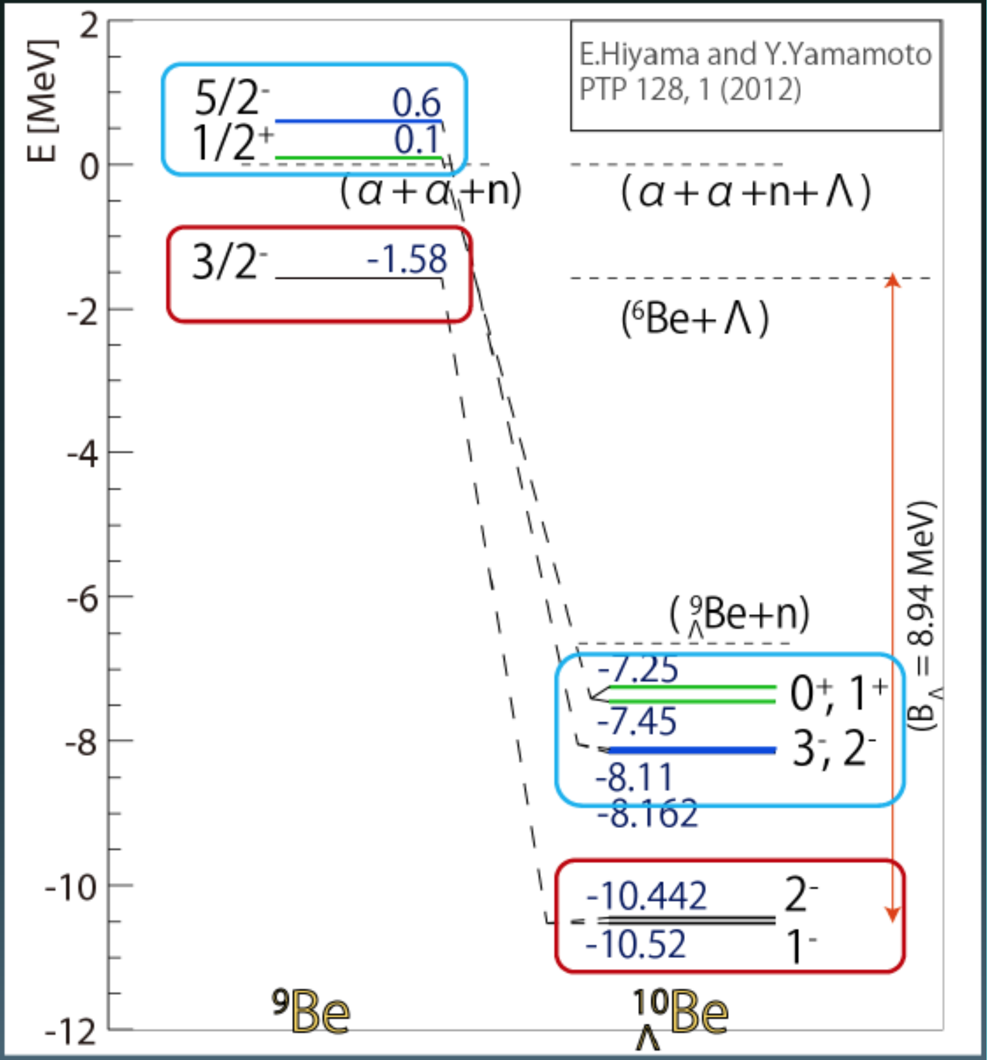

$^{10}{}_{\Lambda}$B and $^{10}{}_{\Lambda}$Be

$^{10}_{\Lambda}$B

$^{10}_{\Lambda}$Be

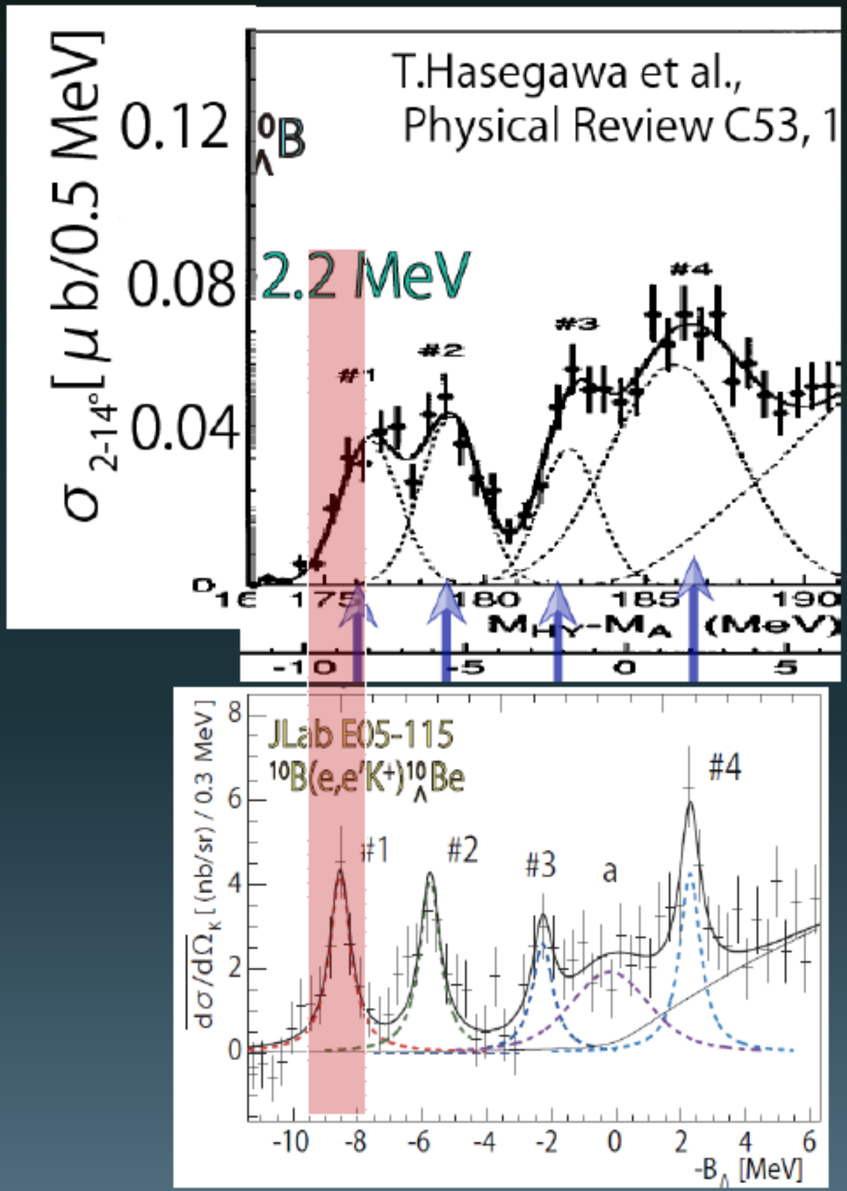
T.Hasegawa et al., Physical Review C53, 1

Comparison of the ground states (A=10)

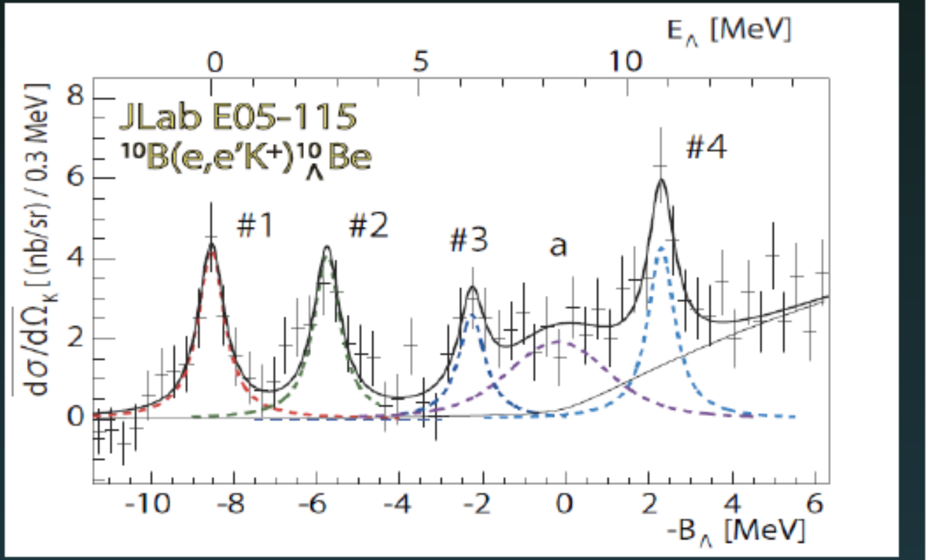

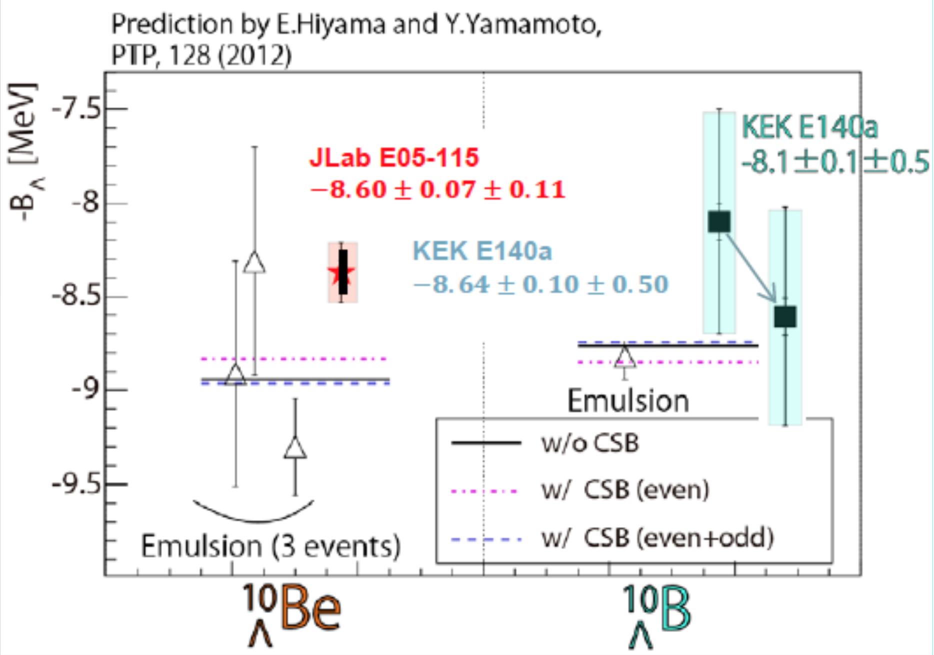

Hypernucleus	Experiment	Reported $B_{\Lambda}^{g.s.}$ [MeV]	Correction [MeV]	Corrected $B_{\Lambda}^{g.s.}$ [MeV]
$^{10}_{\Lambda}$Be	Present data	8.60 ± 0.07	-	8.60 ± 0.07
	Emulsion [24, 25]	9.11 ± 0.22	-	9.11 ± 0.22
$^{10}_{\Lambda}$B	KEK [31]	8.1 ± 0.1	$C_2 = +0.54$	8.64 ± 0.1
	Emulsion [16]	8.89 ± 0.12	-	8.89 ± 0.12
$^{12}_{\Lambda}$B	JLab [14]	11.529 ± 0.025	-	11.529 ± 0.025
	Emulsion [16]	11.37 ± 0.06	-	11.37 ± 0.06
$^{12}_{\Lambda}$C	Emulsion [16, 38]	10.76 ± 0.19	C_2	11.30 ± 0.19

$\Delta^{fit}_{emul\text{-}KEK}$ =+0.54 +- 005 MeV

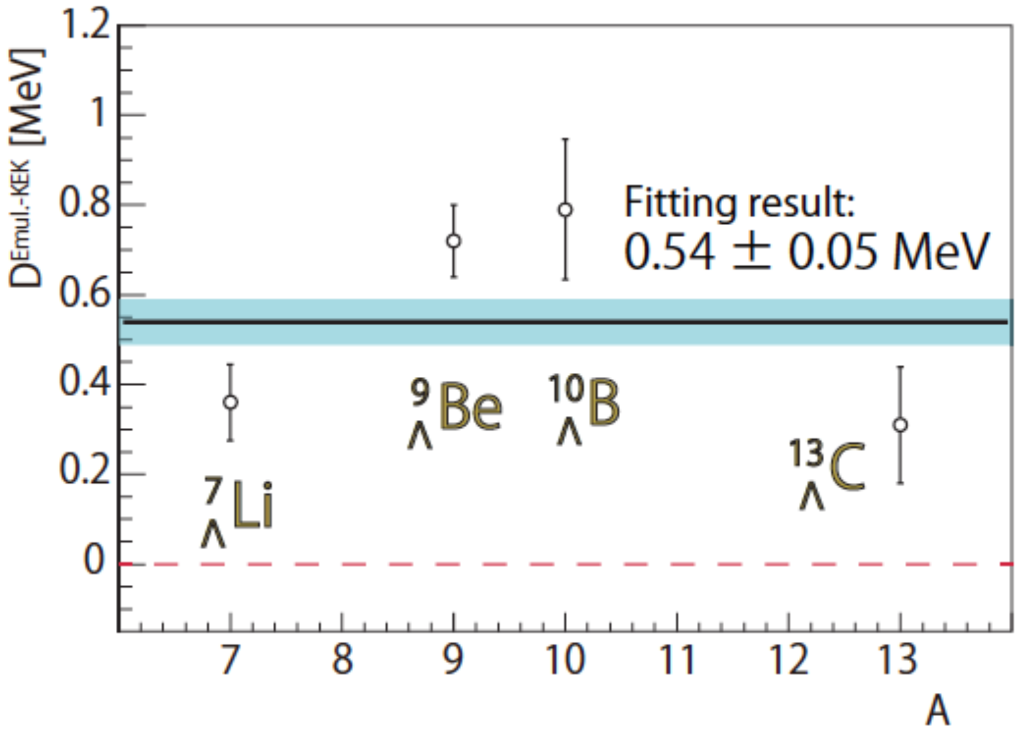

FIG. 6. The binding energy differences of $^{7}_{\Lambda}$Li, $^{9}_{\Lambda}$Be, $^{10}_{\Lambda}$B and $^{13}_{\Lambda}$C between the emulsion experiments [16] and the (π^+, K^+) experiments [2] with the statistical errors. The values of (π^+, K^+) experiments were subtracted from those of the emulsion experiments. The plots should be on a line of zero (dashed line) if the binding energies measured in the (π^+, K^+) and emulsion experiments are consistent.

A result of $^{12}_{\Lambda}$B comparing with $^{12}_{\Lambda}$C

H. Hotchi et al., PRC 64, 044302 (2001)

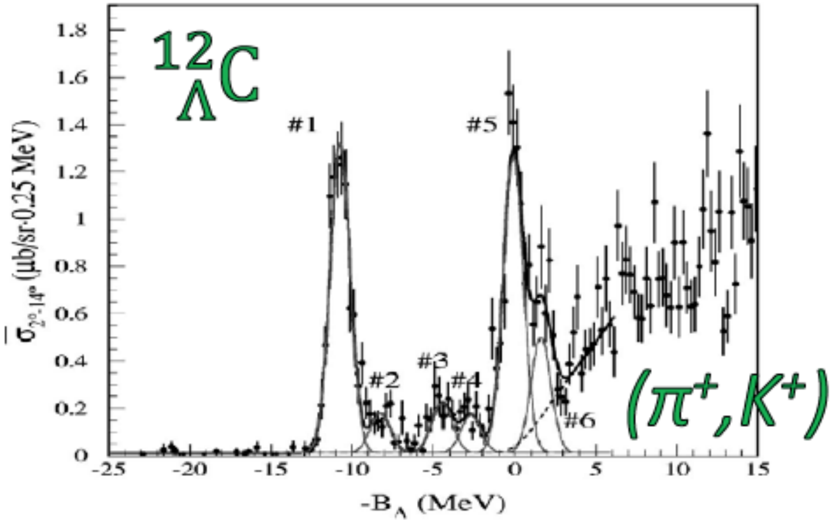

L.Tang et al., PRC 90, 034320 (2014)

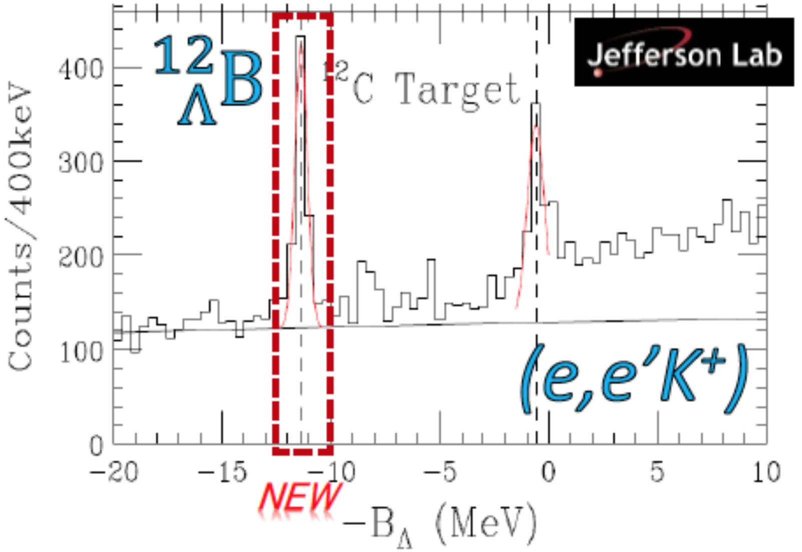

Hypernucleus	Experiment	B_Λ [MeV]	$\Delta B_\Lambda(^{12}_{\Lambda}\mathrm{C} - ^{12}_{\Lambda}\mathrm{B})$ [MeV]
$^{12}_{\Lambda}$C	Emulsion	$10.76 \pm 0.19^{*1)}$	
$^{12}_{\Lambda}$B	Emulsion	$11.37 \pm 0.06^{*1)}$	-0.61 ± 0.20
	JLab_2009	$11.529 \pm 0.025^{*2)}$	NEW -0.77 ± 0.19

$^{*1)}$ Systematic error = 0.04 MeV

$^{*2)}$ Systematic error = 0.11 MeV

A result of $^{12}{}_{\Lambda}$B comparing with $^{12}{}_{\Lambda}$C

H. Hotchi et al., PRC 64, 044302 (2001)

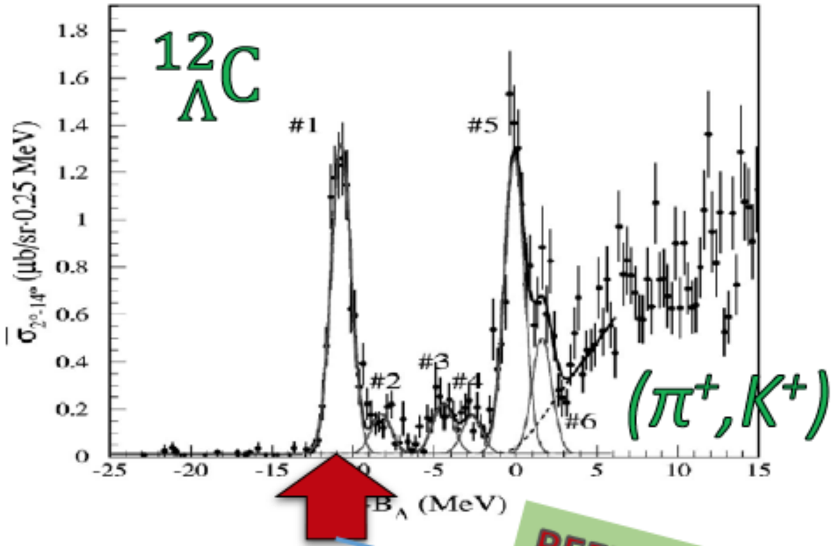

L.Tang et al., PRC 90, 034320 (2014)

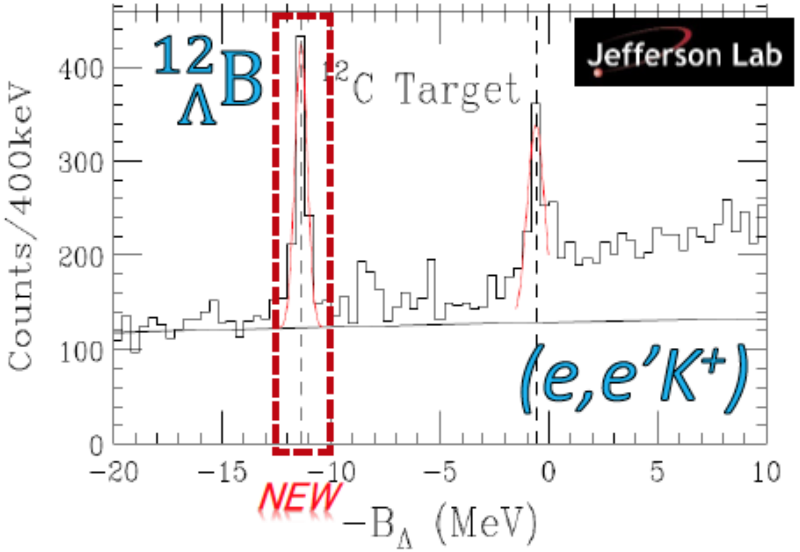

REFERENCE

Hypernucleus	Experiment	B_Λ [MeV]	$\Delta B_\Lambda(^{12}_{\Lambda}\text{C} - ^{12}_{\Lambda}\text{B})$ [MeV]
$^{12}_{\Lambda}$C	Emulsion	$10.76 \pm 0.19^{*1)}$	
$^{12}_{\Lambda}$B	Emulsion	$11.37 \pm 0.06^{*1)}$	-0.61 ± 0.20
	JLab_2009	$11.529 \pm 0.025^{*2)}$	NEW -0.77 ± 0.19

*1) Systematic error = 0.04 MeV

*2) Systematic error = 0.11 MeV

A result of $^{12}{}_{\Lambda}$B comparing with $^{12}{}_{\Lambda}$C

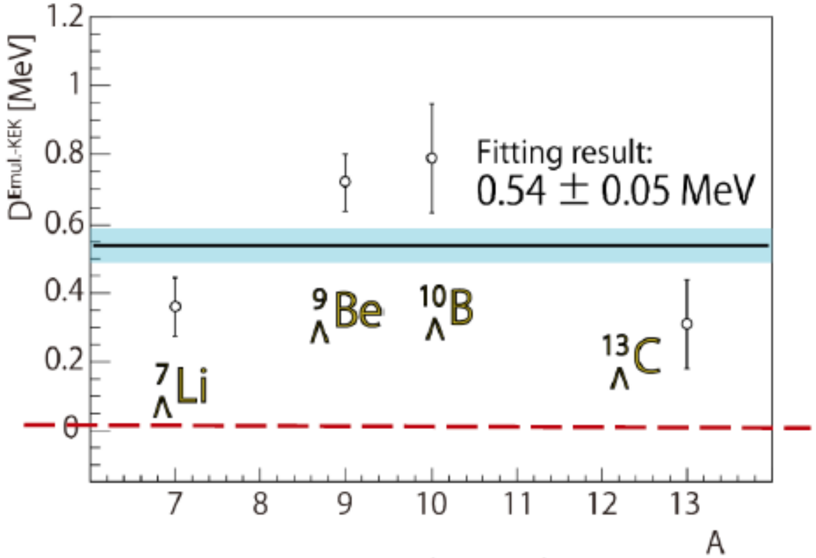

Difference between the (π^+,K$^+$) and emulsion exp.

Indicates that
the reported $B_\Lambda(^{12}_{\Lambda}\mathrm{C})$
is shifted by <u>0.54 MeV</u>!!

Hypernucleus	**Experiment**	B_Λ **[MeV]**	$\Delta B_\Lambda(^{12}_{\Lambda}\mathrm{C} - ^{12}_{\Lambda}\mathrm{B})$ **[MeV]**
$^{12}_{\Lambda}$C	Emulsion	$10.76 \pm 0.19^{*1)}$	
$^{12}_{\Lambda}$B	Emulsion	$11.37 \pm 0.06^{*1)}$	-0.61 ± 0.20
	JLab_2009	$11.529 \pm 0.025^{*2)}$	-0.77 ± 0.19

$^{*1)}$ Systematic error = 0.04 MeV
$^{*2)}$ Systematic error = 0.11 MeV

A result of ${}^{12}_{\Lambda}$B comparing with ${}^{12}_{\Lambda}$C

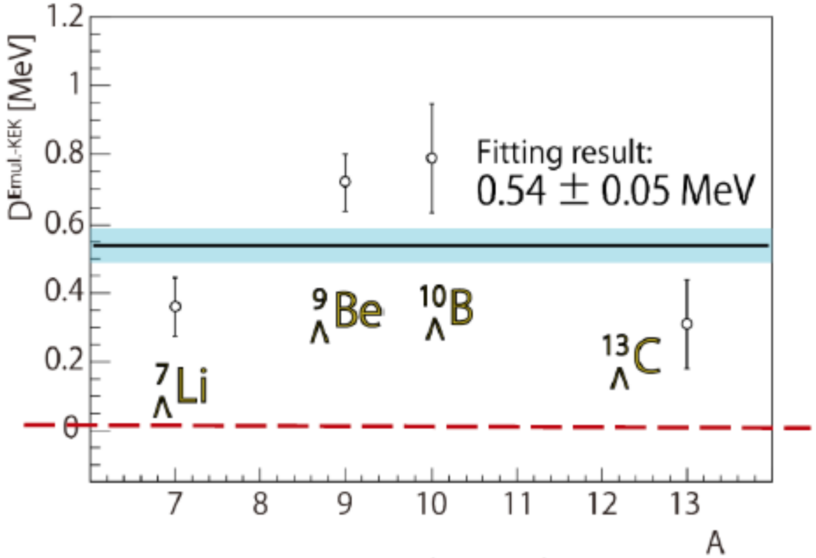

Difference between the (π^+,K$^+$) and emulsion exp.

Indicates that
the reported $B_\Lambda({}^{12}_{\Lambda}\mathrm{C})$
is shifted by **0.54 MeV**!!

Hypernucleus	**Experiment**	**B_Λ [MeV]**	**$\Delta B_\Lambda({}^{12}_{\Lambda}\mathrm{C} - {}^{12}_{\Lambda}\mathrm{B})$ [MeV]**
${}^{12}_{\Lambda}$C	Emulsion	~~10.76~~ ± 0.19*1) 11.30	
${}^{12}_{\Lambda}$B	Emulsion	11.37 ± 0.06*1)	~~0.61~~ ± 0.20 −0.07
	JLab_2009	11.529 ± 0.025*2)	~~0.77~~ ± 0.19 −0.23

*1) Systematic error = 0.04 MeV

*2) Systematic error = 0.11 MeV

ΔB_{Λ} of isotopic mirror pairs (g.s.) w/ correction

Mirror pairs	$\Delta B_{\Lambda}^{theor.}$ [MeV]	Experiment	$\Delta B_{\Lambda}^{exp.}$ [MeV]
$^{4}_{\Lambda}\mathrm{He} - ^{4}_{\Lambda}\mathrm{H}$	$+0.226$[1]	Emul. - Emul.	$+0.35 \pm 0.06$
		Emul. - MAMI	$+0.27 \pm 0.10$
$^{7}_{\Lambda}\mathrm{Be} - ^{7}_{\Lambda}\mathrm{Li}^{*}$	-0.017[1], -0.070[2]	Emul. - (Emul.+ γ)	-0.10 ± 0.09
$^{7}_{\Lambda}\mathrm{Li}^{*} - ^{7}_{\Lambda}\mathrm{He}$	-0.080[2]	(Emul.+ γ) - JLab_2005	-0.42 ± 0.04
		(Emul.+ γ) - *JLab_2009*	*NEW*
$^{8}_{\Lambda}\mathrm{Be}$ [illegible]	[illegible]	[illegible]	$+0.04 \pm 0.06$
$^{9}_{\Lambda}\mathrm{B}$ [illegible]	[illegible]	[illegible]	-0.21 ± 0.22
		Emul. - JLab_A	-0.07 ± 0.20
$^{10}_{\Lambda}\mathrm{B} - ^{10}_{\Lambda}\mathrm{Be}$	-0.136[1], -0.180[3]	Emul. - Emul.	-0.22 ± 0.25
		Emul. - *JLab_2009*	*NEW*
$^{12}_{\Lambda}\mathbf{C} - ^{12}_{\Lambda}\mathrm{B}$		**Emul.'** - Emul.	$\mathbf{-0.07} \pm 0.20$
		Emul.' - Other_(e,e'K^{+})	Consistent with above
		Emul.' - *JLab_2009*	$\mathbf{-0.23} \pm 0.19$

Support small CSB in A=12

[1] A.Gal, PLB 744, 352 (2015)

[2] E.Hiyama *et al.*, PRC 80, 054321 (2009), w/o CSB

[3] E.Hiyama and Y.Yamamoto., PTP 128, 1 (2012), w/o CSB

Possible shift of $^{12}{}_{\Lambda}C_{gs}$ B_{Λ}

$^{12}{}_{\Lambda}B$ - $^{12}{}_{\Lambda}C$: 0.57 ± 0.19 MeV (emulsion)
0.62 ± 0.19 MeV (E05-115 – emulsion)

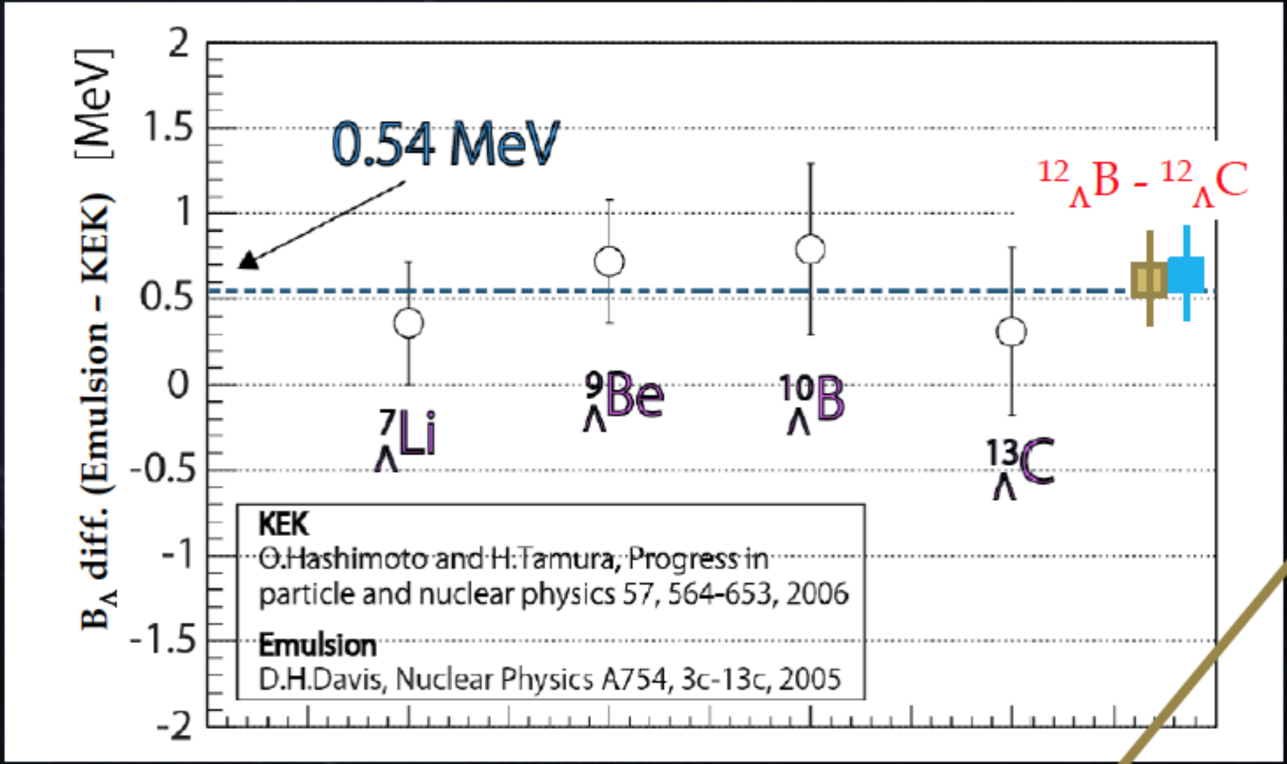

T. Gogami, Doctor thesis, (2014) Tohoku U.

Large CSB
or
CSB ~ 0 with

$^{12}{}_{\Lambda}C$ is very special or B_{Λ} ($^{12}{}_{\Lambda}C_{gs}$) is shifted by ~0.5 MeV.

The possible correction of 0.54 MeV on $^{12}{}_{\Lambda}C$ binding energy makes results in the emulsions and (π,K) experiments consistent, and support small CSB effect in the A = 10 and A = 12 hypernuclear system as expected from theory

The binding energy of $^{12}{}_{\Lambda}C$ was used as a reference of the binding energy measurements for all the (π^+,K^+) experiments in which most energy levels of hypernuclei with A > 16 were obtained and used as theoretical inputs for the study of Λ - N potential.

Therefore, well calibrated binding energy measurements particularly for medium to heavy mass region are needed, and only the (e, e'K^+) experiment would be suitable for the purpose

Update: Millener, Dover, Gal PRC 38, 2700 (1988)

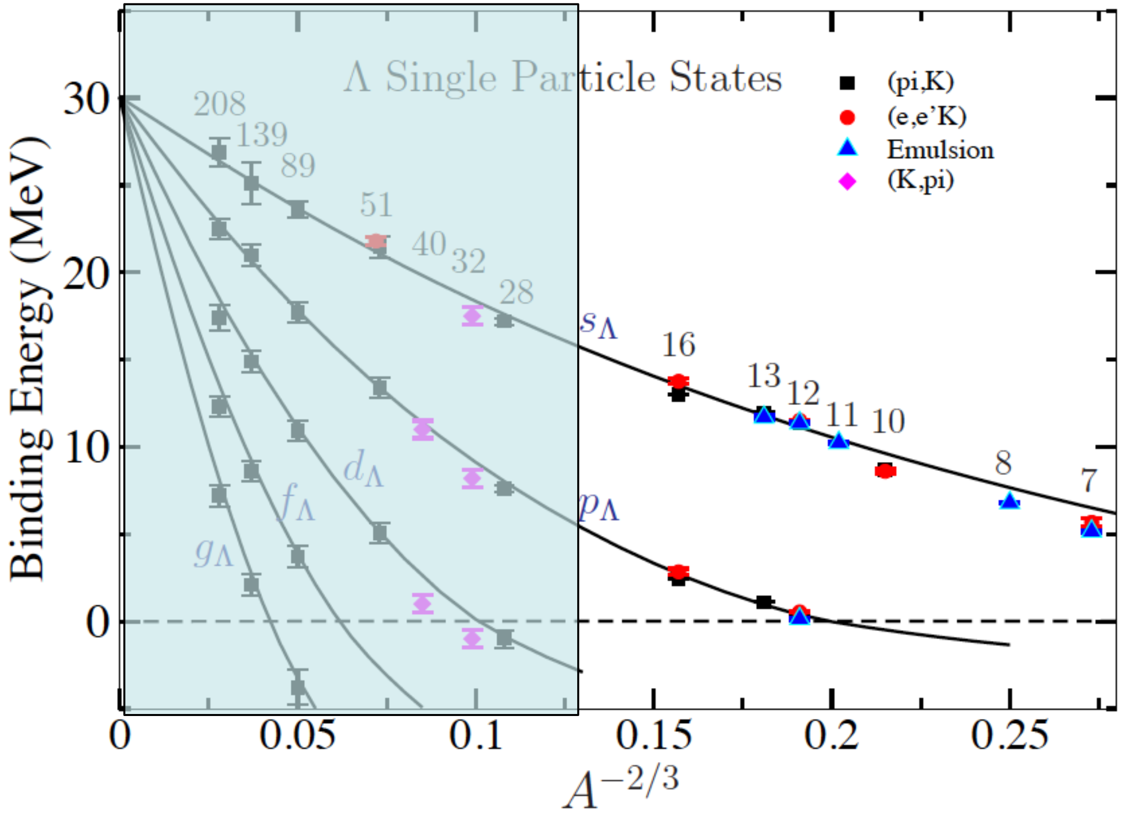

Woods-Saxon $V = 30.05$ MeV, $r = 1.165$ fm, $a = 0.6$ fm

Data to be shifted by 0.54 MeV

Do all data in medium to heavy mass region need this correction ?

To be confirmed by (e,e'K) experiments

Conclusions (I part)

- Good results from the Hall A (^{9}Be, ^{12}C, ^{16}O) and Hall C (^{7}He, ^{10}B, ^{12}C) data *(huge experimental effort)*

- Absolute binding energy calibration is one of the great advantages of the (e,e'K) hypernuclear spetroscopy

- Some calculation still to be done for interpretation of the data

- CSB has to be studied and understood

- B_Λ measurements should be extended to medium-heavy mass nuclei

Prospectives

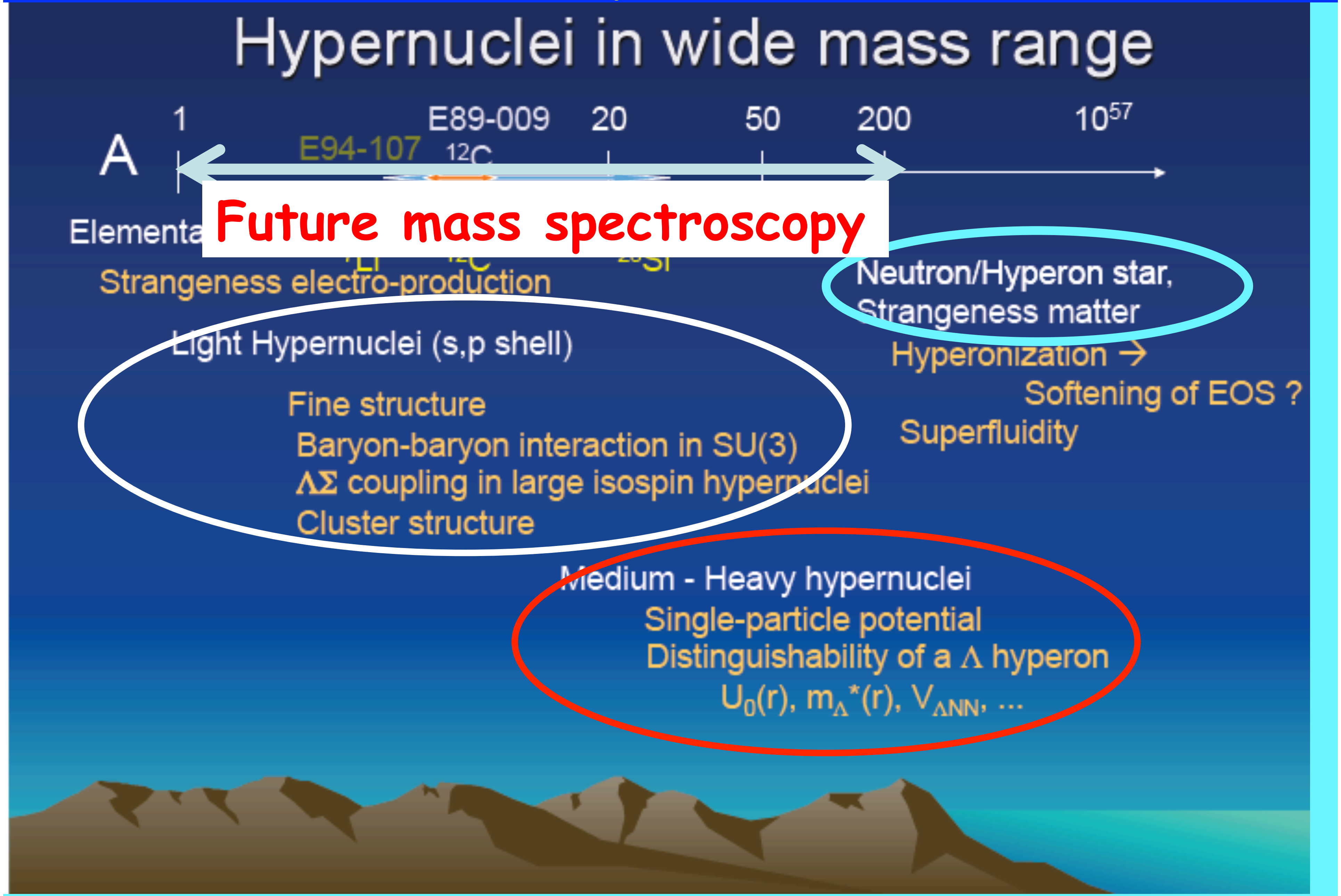

Hypernuclei in wide mass range

Future mass spectroscopy

Elementa

Strangeness electro-production

Light Hypernuclei (s,p shell)

Fine structure

Baryon-baryon interaction in SU(3)

$\Lambda\Sigma$ coupling in large isospin hypernuclei

Cluster structure

Neutron/Hyperon star,
Strangeness matter

Hyperonization →
Softening of EOS ?

Superfluidity

Medium - Heavy hypernuclei

Single-particle potential

Distinguishability of a Λ hyperon

$U_0(r)$, $m_\Lambda{}^*(r)$, $V_{\Lambda NN}$, ...

Proposal to Jlab PAC

A study of the ΛN interaction through
the high precision spectroscopy of
Λ-hypernuclei with electron beam

Charge symmetry breaking
(part I)

Hyperon puzzle
(part II)

Light hypernuclear spectroscopy

Mid-Heavy Hyp.Nucl

${}^{4}_{\Lambda}H$ spectroscopy

P(e,e'K⁺) $\Lambda\Sigma_0$ (small θγκ)

A dependence of B_{Λ}

${}^{40}_{\Lambda}K$, ${}^{89}_{\Lambda}SC$, ${}^{208}_{\Lambda}Tl$

Exotic systems ([nΛ], [nnΛ])

Isospin dependence (${}^{48}_{\Lambda}$ K)

Established lightest HY (${}^{3}_{\Lambda}H$)

A coherent series of measurements on Λ hypernuclei in a wide mass range of targets to investigate the ΛN interaction and various forms of quantum many body systems bound by strong interaction

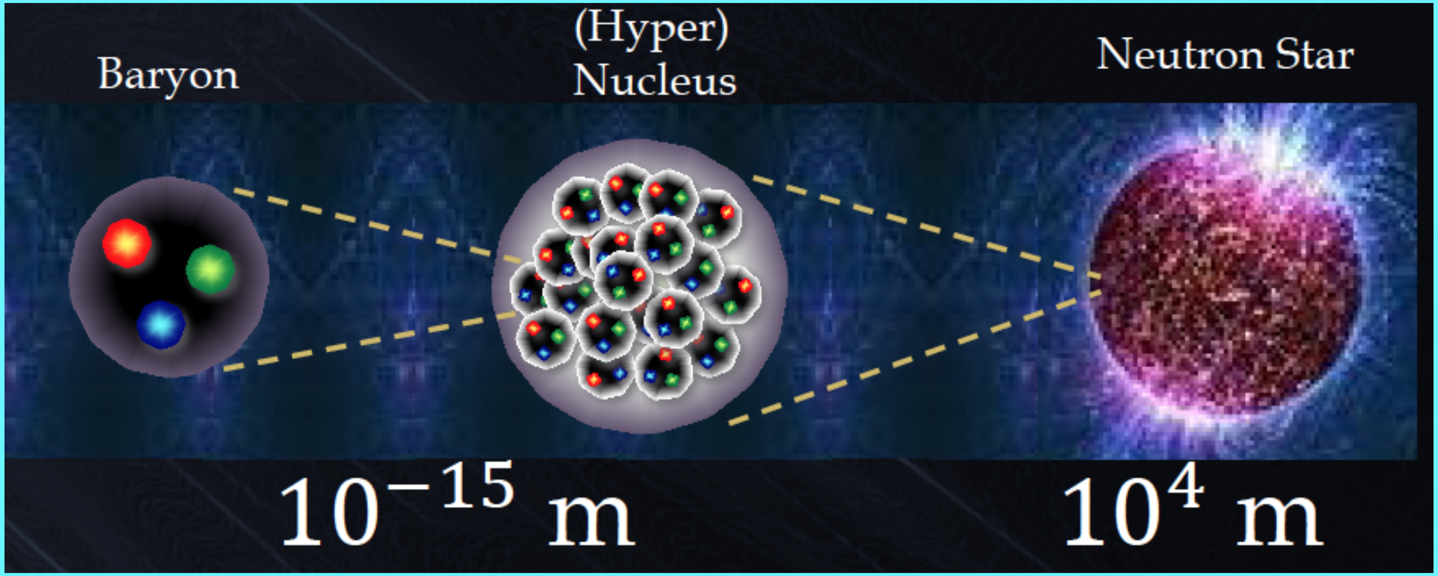

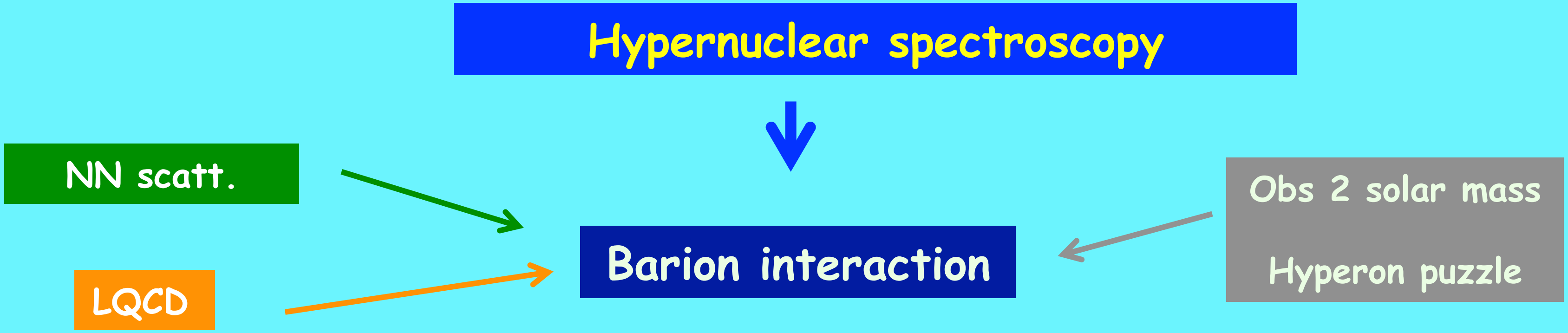

Hypernuclear spectroscopy

NN scatt.

LQCD

Barion interaction

Obs 2 solar mass

Hyperon puzzle

Proposed Setup

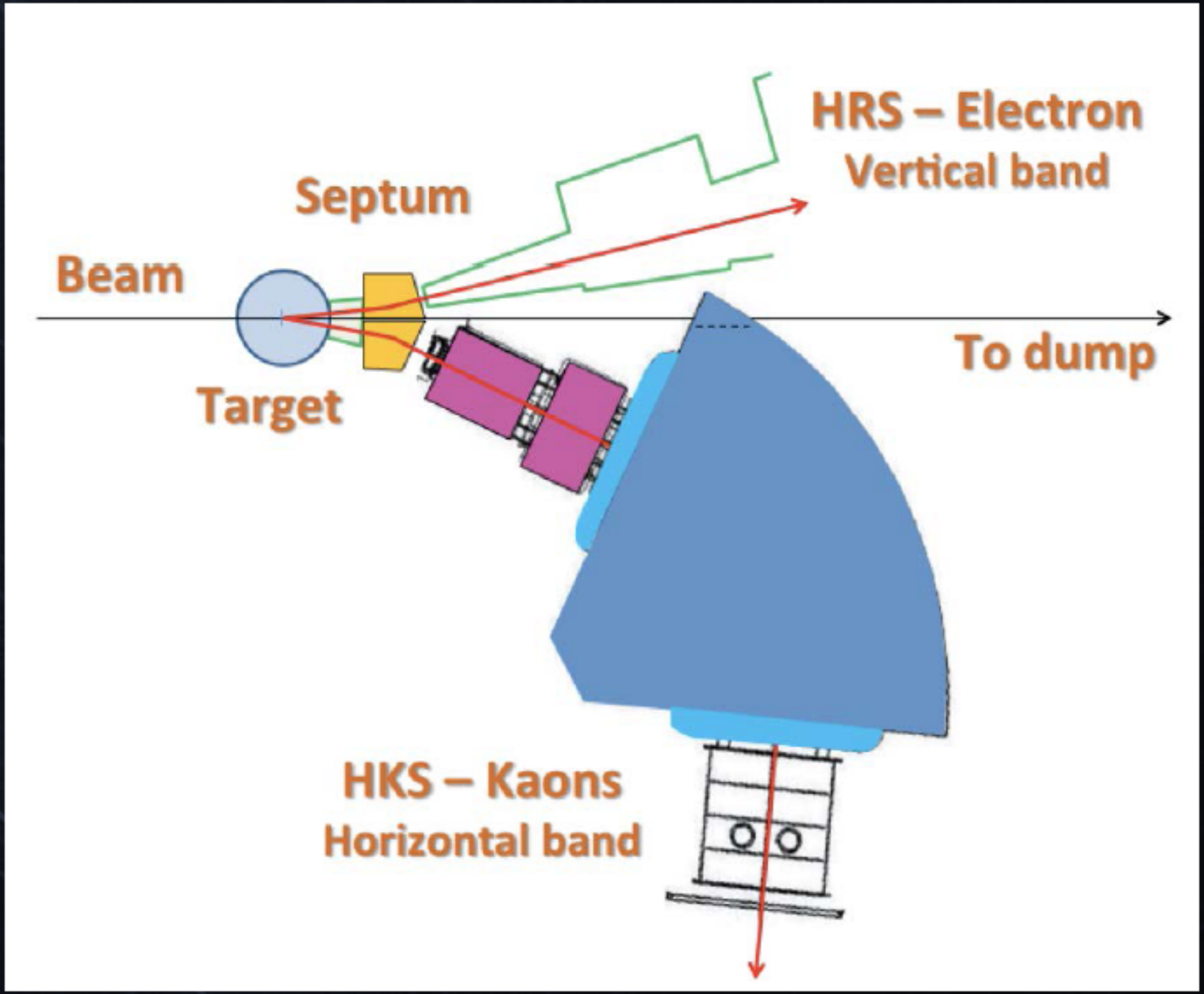

K(HKS) x HRS (e′)

Only **JLab** : Beam + Spectrometers for (e,e′K^+)

Advantage of the proposed setup over previous experiments.

Higher Pe′ with HRS

Established in Hall-A

Excellent momentum resolution (2x10^{-4})

Orbit is long but no problem for e′

Allow to use higher (4.5 GeV) incoming electron beam.

Background from Bremsstrahlung will be boosted to forward.

Introduction of Septum magnet

Easier and more reliable calibration of HKS-HRS systems separately.

Good Signal to Noise ratio

Electron BG will be 1/40 of Hall-C exps.

HKS

Established in Hall-C

Excellent momentum resolution (2x10^{-4}) with short orbit to avoid decay loss of kaons with lower momentum (1.2 GeV/c).

Large solid angle as well as momentum acceptance.

High resolution

Large Yield (best virtual photon energy & HKS acceptance)

Keep resolution and 5.4 times larger yield than Hall-A exp.

Req. beamtime in proposal

Target	Purpose	Req. BT (hours)
Engineering	Beam, target, spectrometers, detectors and DAQ	1 calendar month
Calibrations Various targets	Optics, kinematics for energy resolution and absolute energy scale	167
Physics I : Few-body	Direct ΛN int. study (CSB,FSI)	
$^{4}\mathrm{He}$ ($^{4}_{\Lambda}\mathrm{H}$)	CSB for A=4 system	266
H_2 (Λ, Σ^0)	Elementary, calibration	52
D_2 and $^{3}\mathrm{He}$ ($^{2}_{\Lambda}\mathrm{n}$, $^{3}_{\Lambda}\mathrm{H}$)	ΛN int. study through FSI	210
$^{3}\mathrm{T}$ ($^{3}_{\Lambda}\mathrm{n}$)	Exotic bound state search	130
Subtotal		658
Physics II : Mid-Heavy	3B force study – EoS w/ Y	
$^{40}\mathrm{Ca}$ ($^{40}_{\Lambda}\mathrm{K}$)	High precision exp. Reliable Calc.	124
$^{48}\mathrm{Ca}$ ($^{48}_{\Lambda}\mathrm{K}$)	Iso-spin dep.	148
$^{208}\mathrm{Pb}$ ($^{208}_{\Lambda}\mathrm{Tl}$)	Heaviest HY	642
Subtotal		914
Total		1739

51 days (1224h) option for high priority targets

Target	Purpose	High Priority (hours)
Engineering	Beam, target, spectrometers, detectors DAQ	1 calendar month
Calibrations Various targets	Optics, kinematics, absolute energy scale	**167**
Physics I : Few-body	**Direct ΛN int. study (CSB,FSI)**	
^{4}He ($^4_\Lambda$H)	CSB for A=4 system	**177**
H_2 (Λ, Σ^0)	Elementary, calibration	35
D_2 and ^{3}He ($^2_\Lambda$n, $^3_\Lambda$H)	ΛN int. study through FSI	140
~~^{3}T ($^3_\Lambda$n)~~	~~Exotic bound state search~~	
Subtotal		352
Physics II : Mid-Heavy	**3B force study – EoS w/ Y**	
^{40}Ca ($^{40}_\Lambda$K)	High prec. exp. Reliable Calc.	**103**
~~^{48}Ca ($^{48}_\Lambda$K)~~	~~Iso-spin dep.~~	
^{89}Y ($^{89}_\Lambda$Sr)	Heavy HY	**124**
^{208}Pb ($^{208}_\Lambda$Tl)	Heaviest HY	**478**
Subtotal		705
Total	Fit in 51 PAC days (1224h)	**1224**

CSB interaction test in A=7

CSB potential is not necessary for A=7

Assumed CSB potential is too naïve or problem for A=4 data

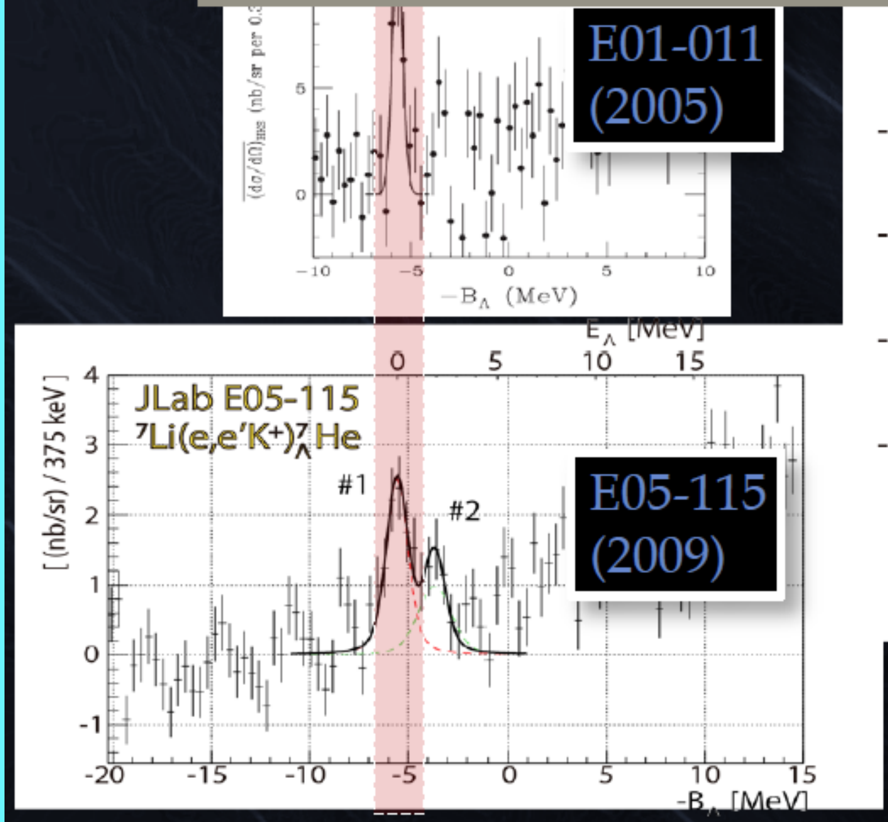

T.Gogami, Doctor Thesis (2014) Tohoku Univ.

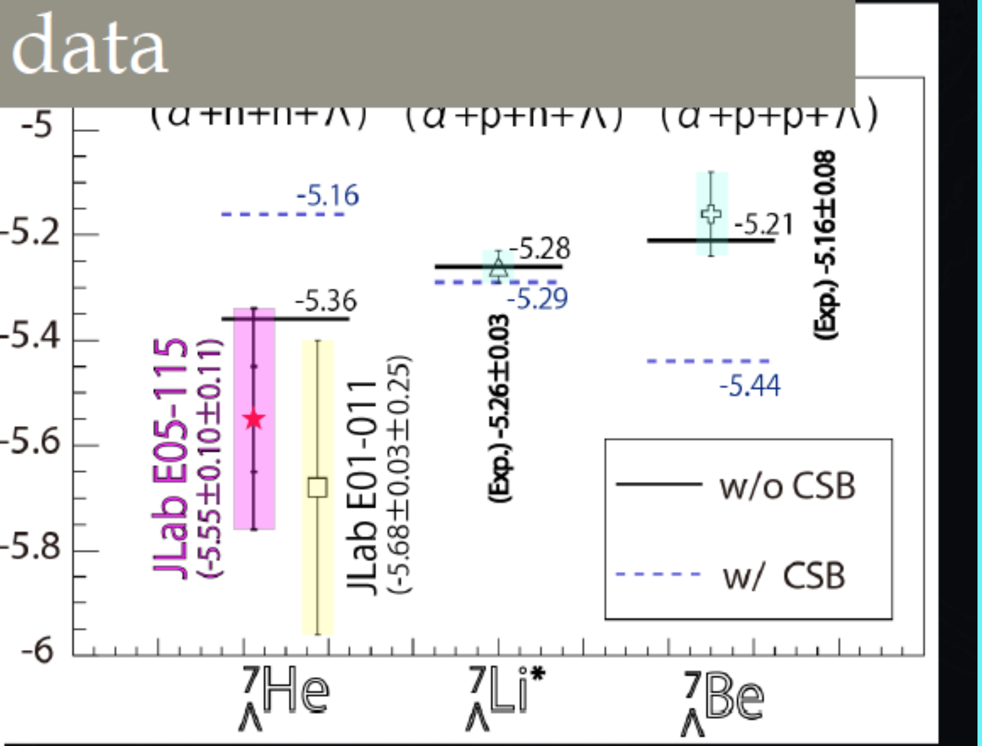

A = 4 Systems
CSB ΛN potential

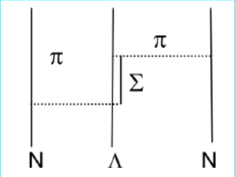

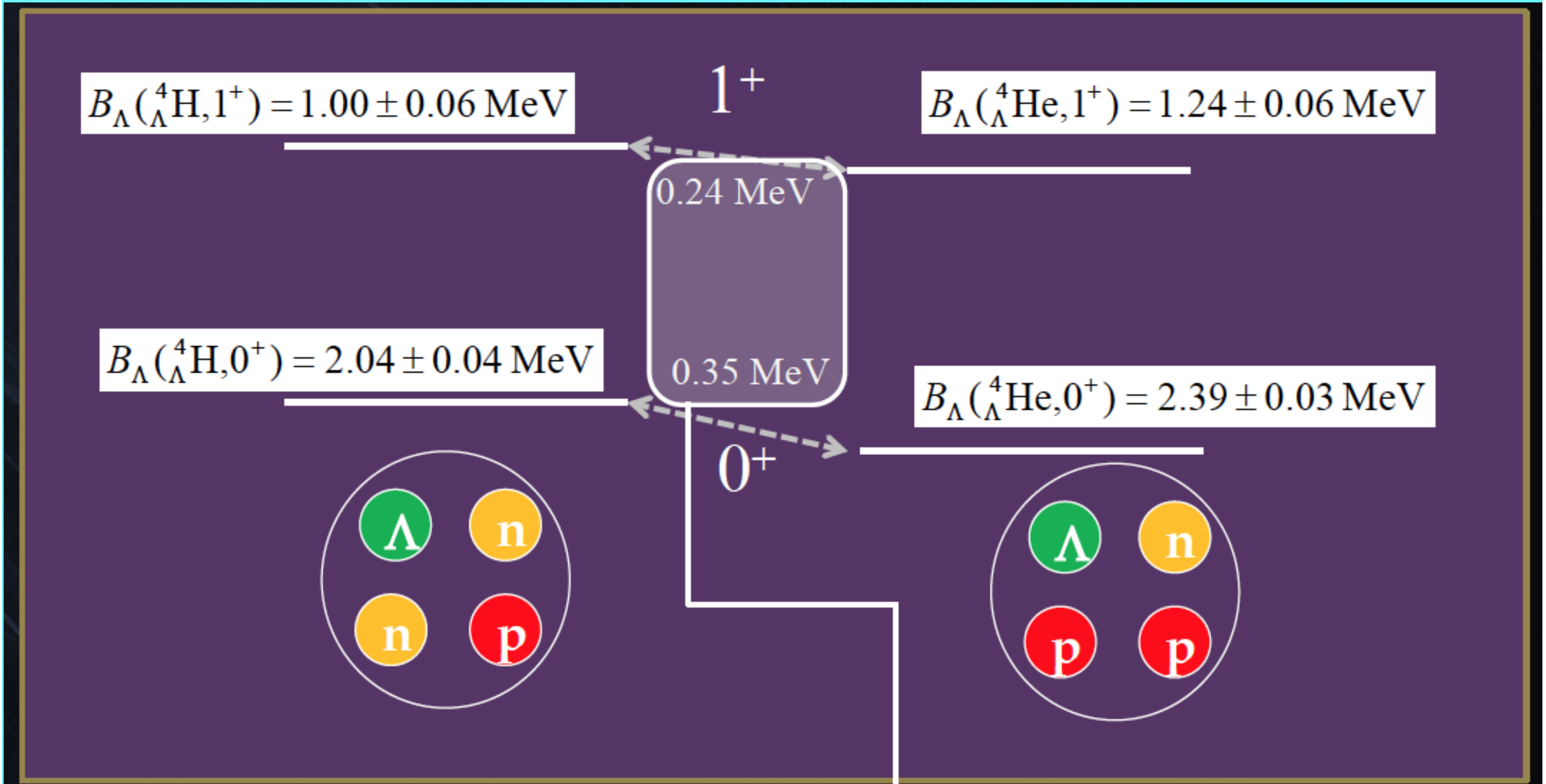

$$B_\Lambda({}^4_\Lambda\mathrm{H},1^+) = 1.00 \pm 0.06\ \mathrm{MeV}$$

$$B_\Lambda({}^4_\Lambda\mathrm{He},1^+) = 1.24 \pm 0.06\ \mathrm{MeV}$$

$$B_\Lambda({}^4_\Lambda\mathrm{H},0^+) = 2.04 \pm 0.04\ \mathrm{MeV}$$

$$B_\Lambda({}^4_\Lambda\mathrm{He},0^+) = 2.39 \pm 0.03\ \mathrm{MeV}$$

Coulomb effect is very small.

$$-\Delta B_c = 0.050 \pm 0.02\ \mathrm{MeV}\ ,$$

$$-\Delta B_c^* = 0.025 \pm 0.015\ \mathrm{MeV}$$

Charge Symmetry Breaking

cf) $B({}^3\mathrm{H})$-$B({}^3\mathrm{He})$-ΔB_c ~ 70 keV

Three-body ΛNN force

Modern ChPT-NLO calculation predicts 3NF effect is < 100keV
NLO calculation cannot explain experimental results for A=4, T=1/2, hypernuclei.
(Nogga, HYP2012)

ΛΣ mass difference ~ 80 MeV < NΔ mass difference ~ 300MeV

$M(\Sigma^+) < M(\Sigma^0) < M(\Sigma^-)$, $\Delta M(\Sigma^- - \Sigma^+)$~8MeV

Consistent ~~understanding of 0^+, 1^+ of ${}^4_\Lambda$H, ${}^4_\Lambda$He~~

Phenomenological potential :

A.R.Bodmer&Q.N.Usmani, PRC 31(1985)1400.

$$V^{\mathrm{CSB}} = -\tau_3 T_\pi^2 \tfrac{1}{8}[(0.568\Delta B_\Lambda + 0.756\Delta B^*_\Lambda) + (0.568\Delta B_\Lambda - 0.756\Delta B^*_\Lambda)\sigma_\Lambda\cdot\sigma_N]$$

Study of A=4 system

Only accessible by the $^4He(e,e'K^+)^4{}_\Lambda H$ at JLab

γ-ray : level spacing
Decay π: ground state

$B_\Lambda({}^4_\Lambda H, 1^+)$ = New data necessary

Mainz New data :
PRL **114**, 232501 (2015)

$B_\Lambda({}^4_\Lambda H, 0^+) = 2.12 \pm 0.09$ MeV

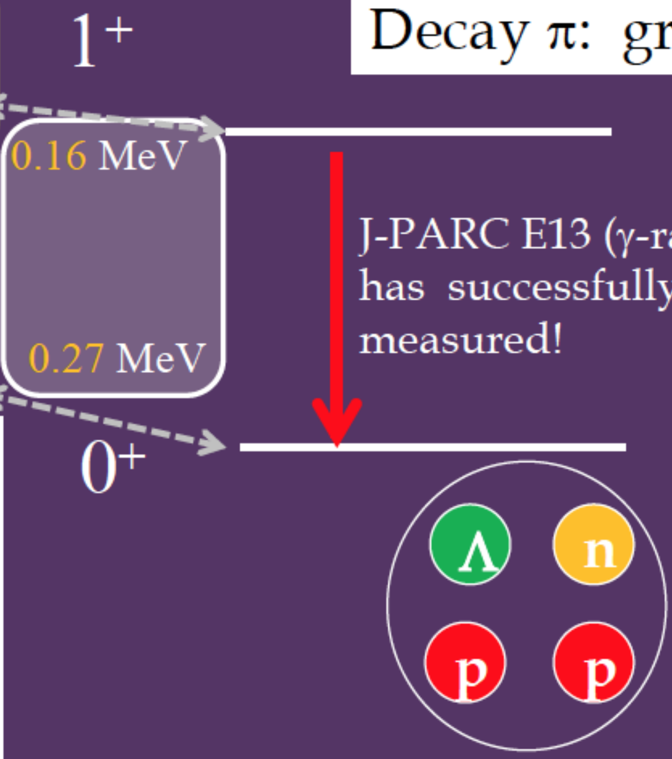

J-PARC E13 (γ-ray; hyperball) has successfully measured!

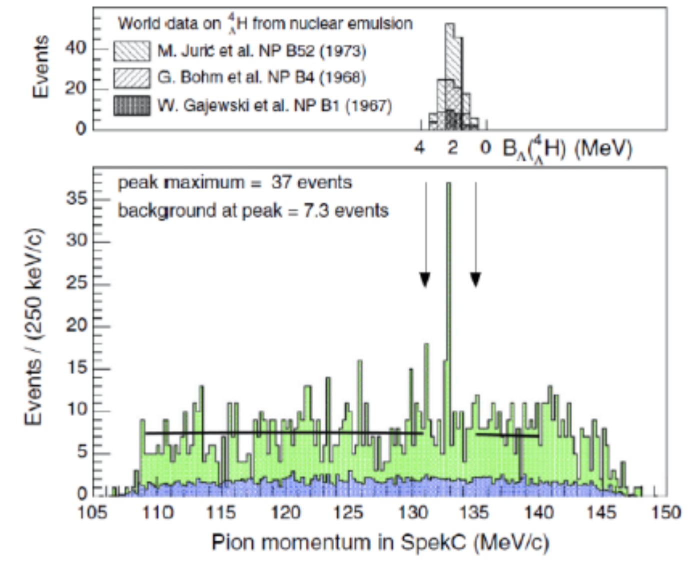

3B/4B Repulsive Hyperon Interaction for EOS of Neutron Stars

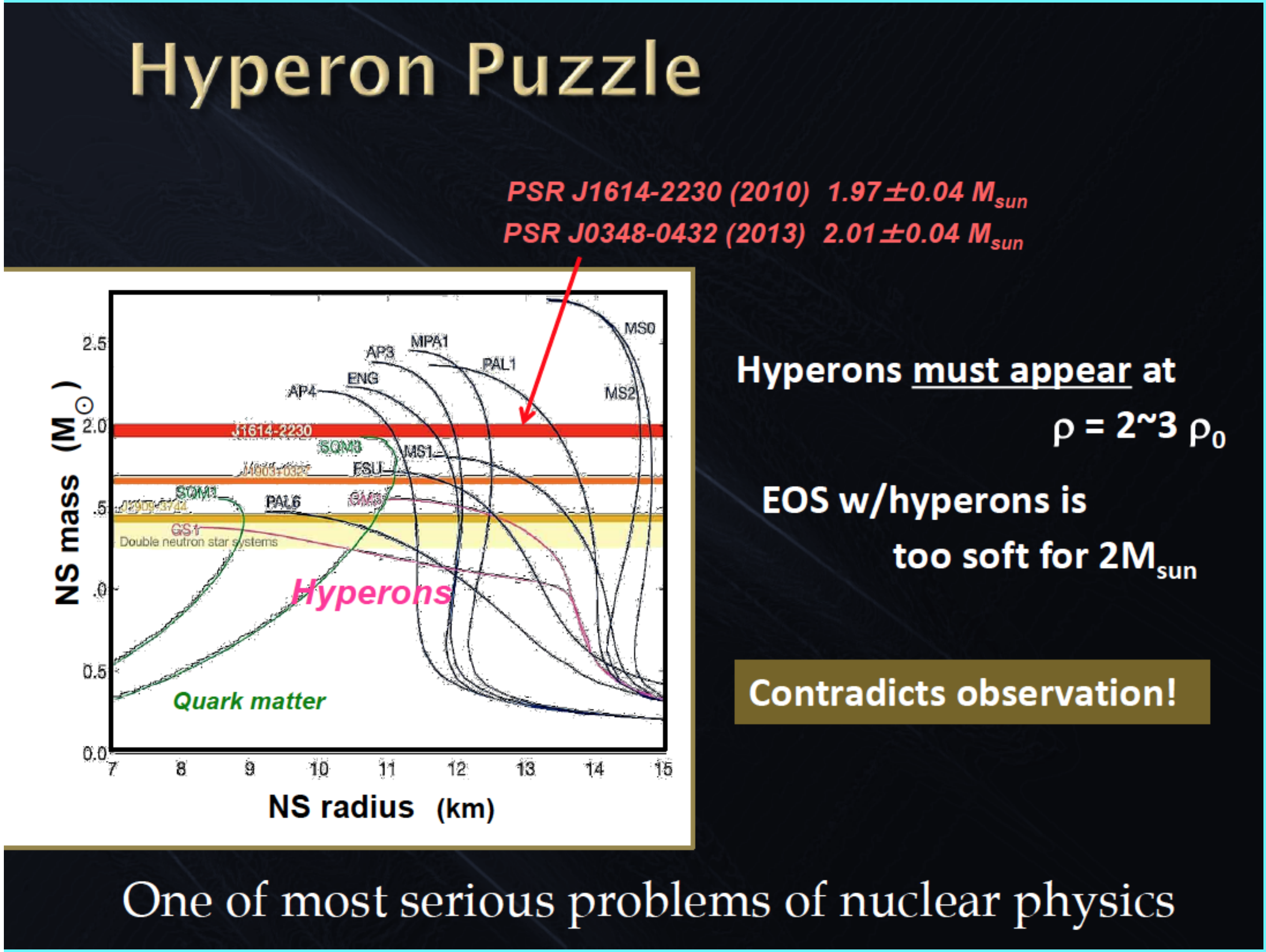

Hyperon Puzzle

PSR J1614-2230 (2010) 1.97±0.04 M_{sun}

PSR J0348-0432 (2013) 2.01±0.04 M_{sun}

Hyperons <u>must appear</u> at $\rho = 2 \sim 3\ \rho_0$

EOS w/hyperons is too soft for 2M_{sun}

Contradicts observation!

One of most serious problems of nuclear physics

Key points to understand neutron stars

Hyperon force under high ρ

↓

3B repulsive force

↑

Inclusion of hyperons soften EOS

In the degenerate dense matter forming the inner core of a NS, Pauli blocking would prevent hyperons from decaying by limiting the phase space available to nucleons. When the nucleon chemical potential is large enough, the conversion of nucleons into hyperons becomes energetically favorable. This results in a reduction of the Fermi pressure exerted by the baryons and a softening of the equation of state (EOS).

Currently there is no general agreement among the predicted results for the EOS and the maximum mass of NS including hyperons. This has to be ascribed to the combination of an incomplete knowledge of the forces governing the system (in the hypernuclear case both two- and three-body forces), and to the concurrent use of approximated theoretical many-body techniques.

However, the most accurate phenomenological three-body force (Illinois 7), while providing a satisfactory description of the spectrum of light nuclei up to 12C [PIE08] yields to a pathological EOS for pure neutron matter (PNM) [MAR13]. On the other hand, when additional information on the three-nucleon interaction is inferred from saturation properties of symmetric nuclear matter (Urbana IX force), the resulting PNM EOS turns out to be compatible with astrophysical observations

Recent analysis of ^{16}O-^{16}O scattering data shows that the established meson exchange potential model (Nijmegen ESC08c) cannot reproduce the cross section at large scattering angles and inclusion of 3-body/4-body repulsive forces solves the problem [FUR09]. This is also an indication that 3-body/4-body repulsive forces become more significant at higher density.

Behavior of such repulsive forces at higher density can be studied more clearly in heavier hypernuclear system. Additional information must necessarily be inferred from the properties of medium and heavy hypernuclei in order to extrapolate to the infinite limit.

EOS of Nuclear Matter (with hyperons)

Microscopic nuclear force model at $2\rho_0$

Density dependence (Yamamoto et al, Bruckner + G matrix calulations)

Importance of repulsive 3 body forces

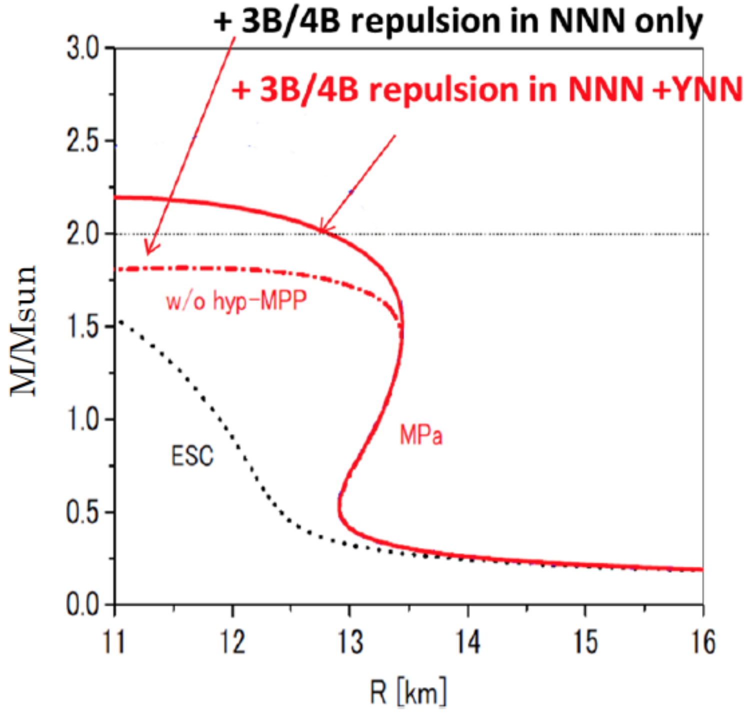

Figure 2-6: Calculated neutron star mass as a function of radii [YAM14]. The result with only Nijmegen ESC08c makes EOS too soft (dots), but inclusion of 3/4 body repulsion force in nucleon sector makes it harder (dot-line) and inclusion of it in hyperon sector as well as normal sector solve the hyperon puzzle (solid).

3 body, strong effect at high densities

An approach to solve the hyperon puzzle

It is expected that such 3/4-body YN forces make systematic shifts to the energy levels of medium to heavy hypernuclei at the few 100 keV level, which affects calculated maximum neutron star mass by ~30%.

Therefore, precise Λ binding energy measurements of hypernuclei should be determined in medium to heavy hypernuclei.

Auxiliary Field Diffusion Monte Carlo (AFDMC) (Lonardoni et al.)

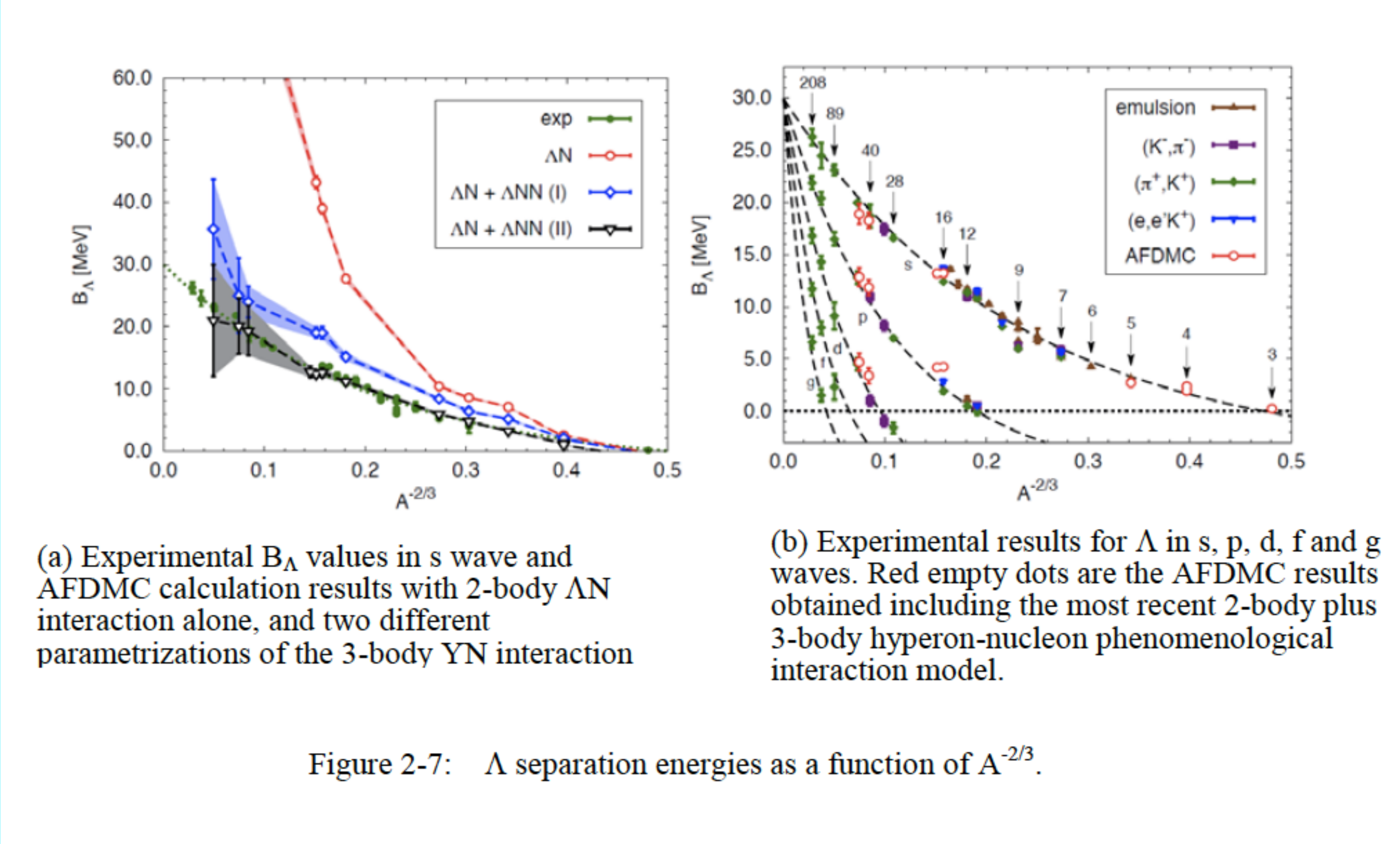

(a) Experimental B_Λ values in s wave and AFDMC calculation results with 2-body ΛN interaction alone, and two different parametrizations of the 3-body YN interaction

(b) Experimental results for Λ in s, p, d, f and g waves. Red empty dots are the AFDMC results obtained including the most recent 2-body plus 3-body hyperon-nucleon phenomenological interaction model.

Figure 2-7: Λ separation energies as a function of $A^{-2/3}$.

Auxiliary Field Diffusion Monte Carlo (AFDMC) (Lonardoni et al.

Potential models predicting relatively small differences in the Λ separation energies of hypernuclei give dramatically different results for the properties of an infinite medium

EOS spans all the regimes from the appearance of a substantial fraction of hyperons at $\sim 2\ \rho_0 \approx 0.32$ fm^{-3} to the absence of Λ particles in the whole density range of the star

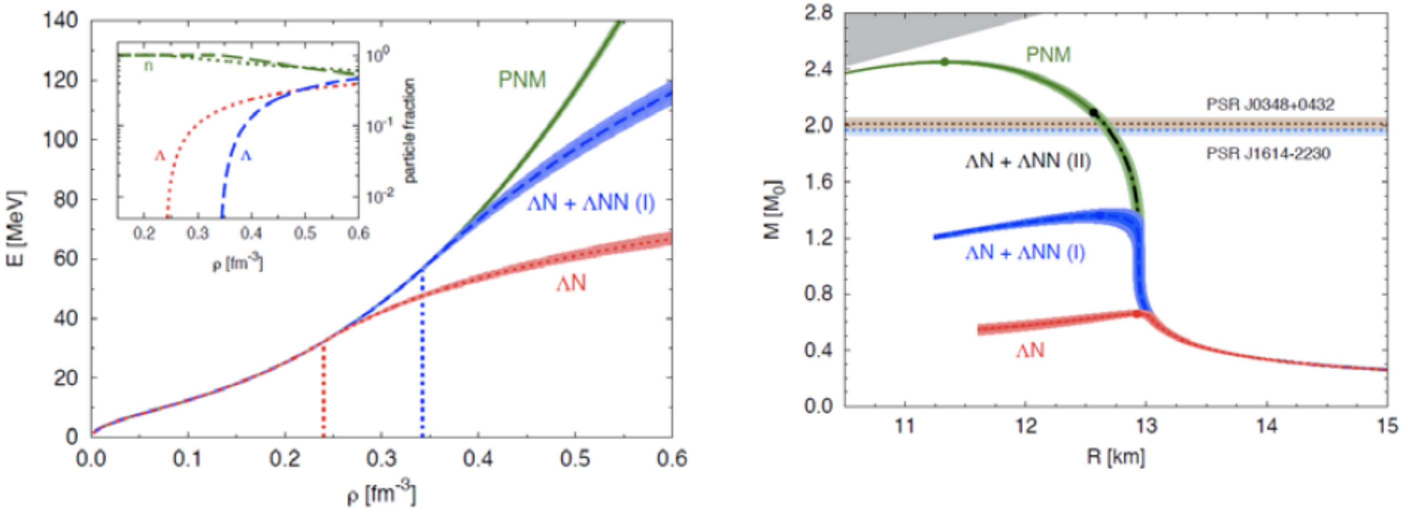

(a) Equations of state. The vertical dotted lines indicate the Λ threshold densities. In the inset, neutron and Λ fractions corresponding to the two hyper-neutron matter EOSs.

(b) Mass-radius relations given by AFDMC. Full dots represent the predicted maximum masses. Horizontal bands at $2M_\odot$ are the observed masses of the heavy neutron stars [DEM10,ANT13].

Figure 2-8: EOS and neutron star mass-radius relations calculated by AFDMC.

Medium mass hyperuclei

Systems with A≤50 are similar to the infinite medium for which ab-initio many-body calculations are feasible. However, present experimental information in the mass region 40≤ A≤50 relies uniquely on the data measured by the (π+, K+) reaction

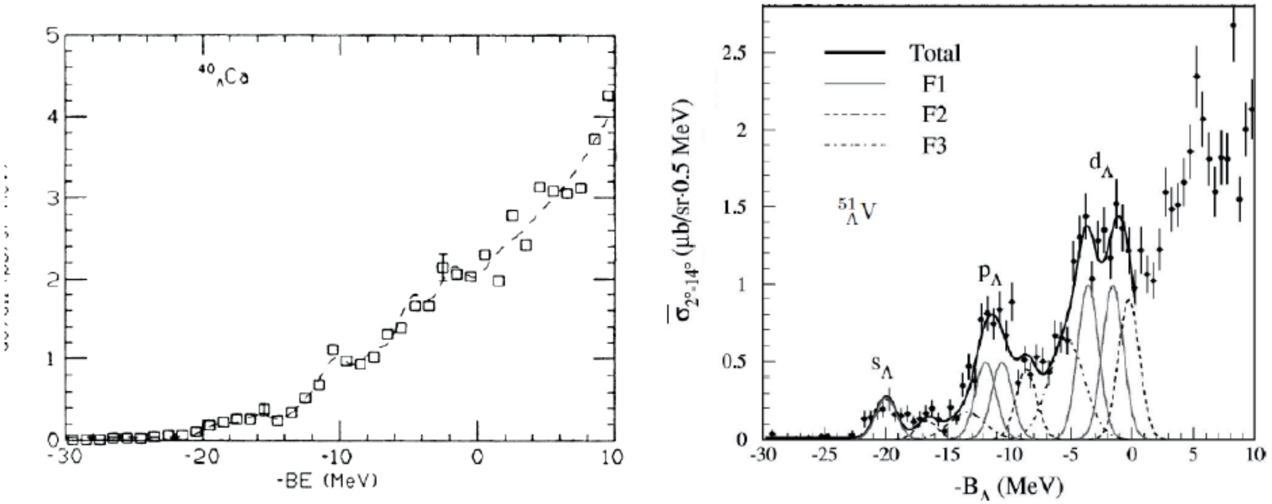

Figure 2-9: $^{40}{}_{\Lambda}$Ca [PIL91] and $^{51}{}_{\Lambda}$V [HOT01] spectra obtained by the (π,K) reaction.

New accurate (e,e'K^{+}) measurements of the Λ separation energies are necessary to constrain the behavior of hypernuclear interactions at densities relevant for neutron star matter

Experimental data suitable to establish a possible asymmetry between the Λnp and the Λnn interactions are rather scarce

Precise measurements of B_{Λ} in ^{40}Ca(e, e'K+)$^{40}{}_{\Lambda}$K and ^{48}Ca(e, e'K+)$^{48}{}_{\Lambda}$K could provide such data as well as assess the isospin dependence of the phenomenological three-body hyperon-nucleon force

The present parametrization of the ΛNN potential, based on a fit to symmetric hypernuclei, includes a contribution that can be written in terms of projectors on the triplet (T = 1) and singlet (T = 0) nucleon isospin channels. Introducing an additional parameter CT, it is possible to gauge the strength and the sign of the Λnn contribution.

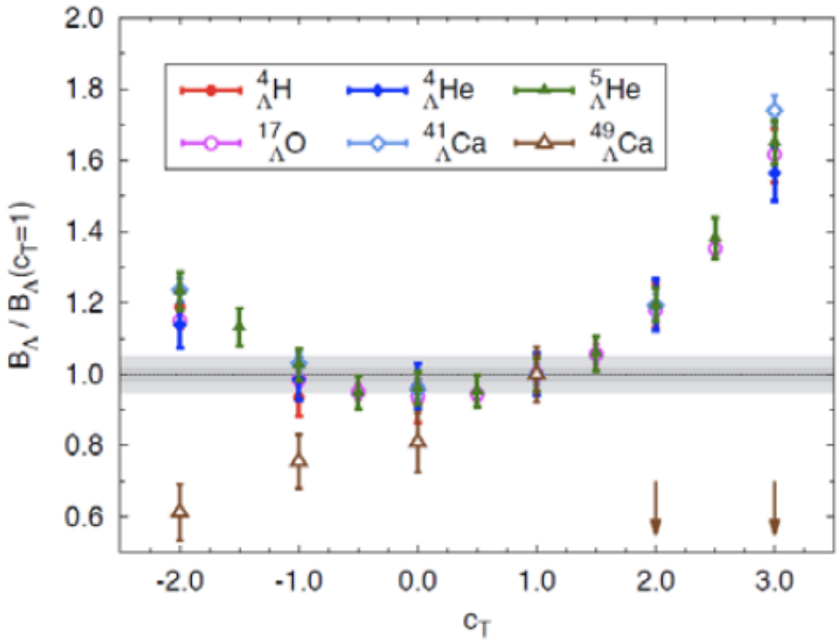

Figure 2-10: Λ separation energies normalized with respect to the $C_T = 1$ case as a function of C_T. Grey bands represent the 2% and 5% variations of the ratio B_Λ/B_Λ ($C_T = 1$). Brown vertical arrows indicate the results for ^{49}Ca in the case of $C_T = 2$ and $C_T = 3$, outside the scale of the plot.

Preliminary results for the Λ separation energies obtained by the AFDMC calculation varying CT from -2 to 3. The B_Λ are normalized with respect to the CT = 1 case for which the original three-body force is recovered. The grey bands represent the 2% and 5% variations of the ratio B_Λ/B_Λ(CT = 1).

No scattering data exist in the YY sector (a ΣN scattering experiment is currently in preparation at J-PARC)

Therefore, the realistic YN interaction models use the measured binding energies of hypernuclei as constraints

Mass dependence of B_Λ

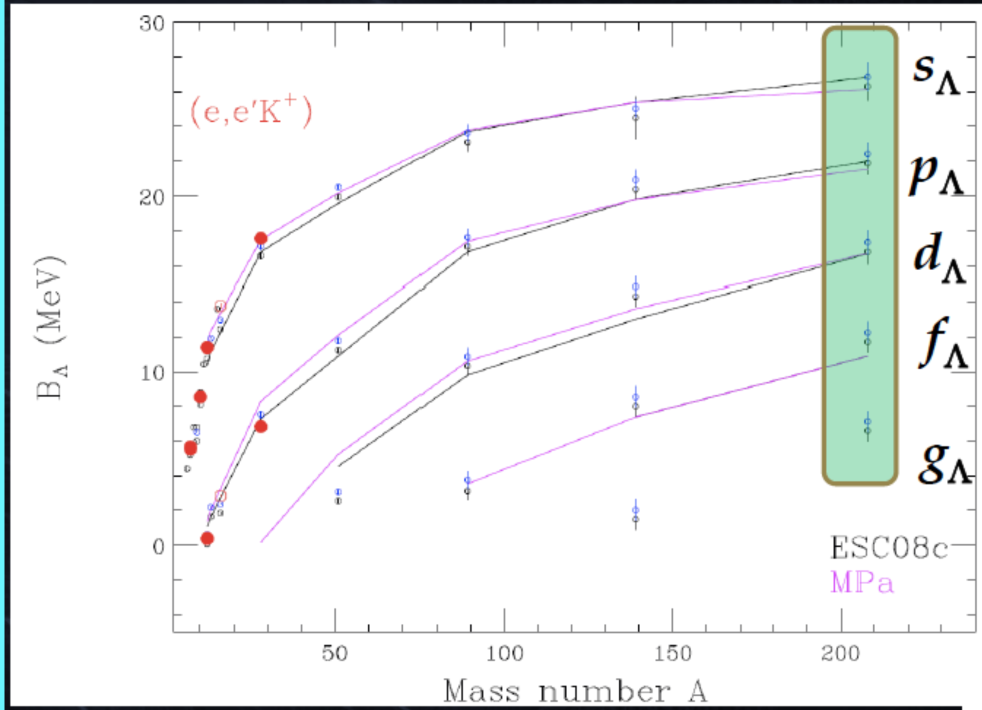

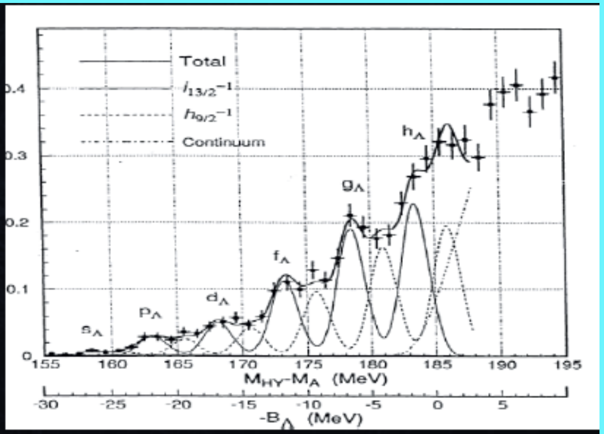

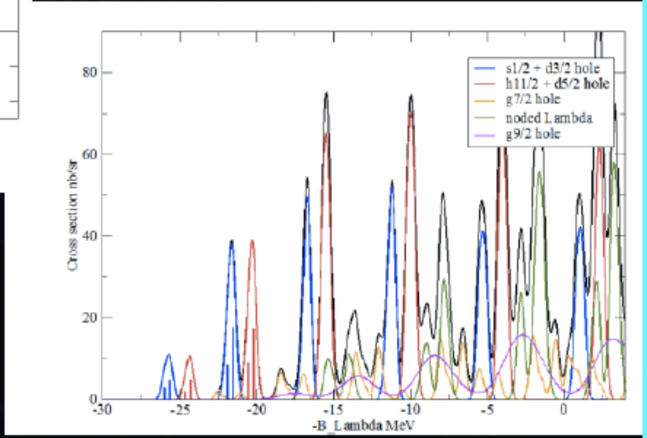

Lines: Calc. by Yamamoto & Rijken

Nijmegen ESC08c : Commonly used realistic YN

MPa : ESC08c + 3B/4B RF

Mass dependence of B_Λ

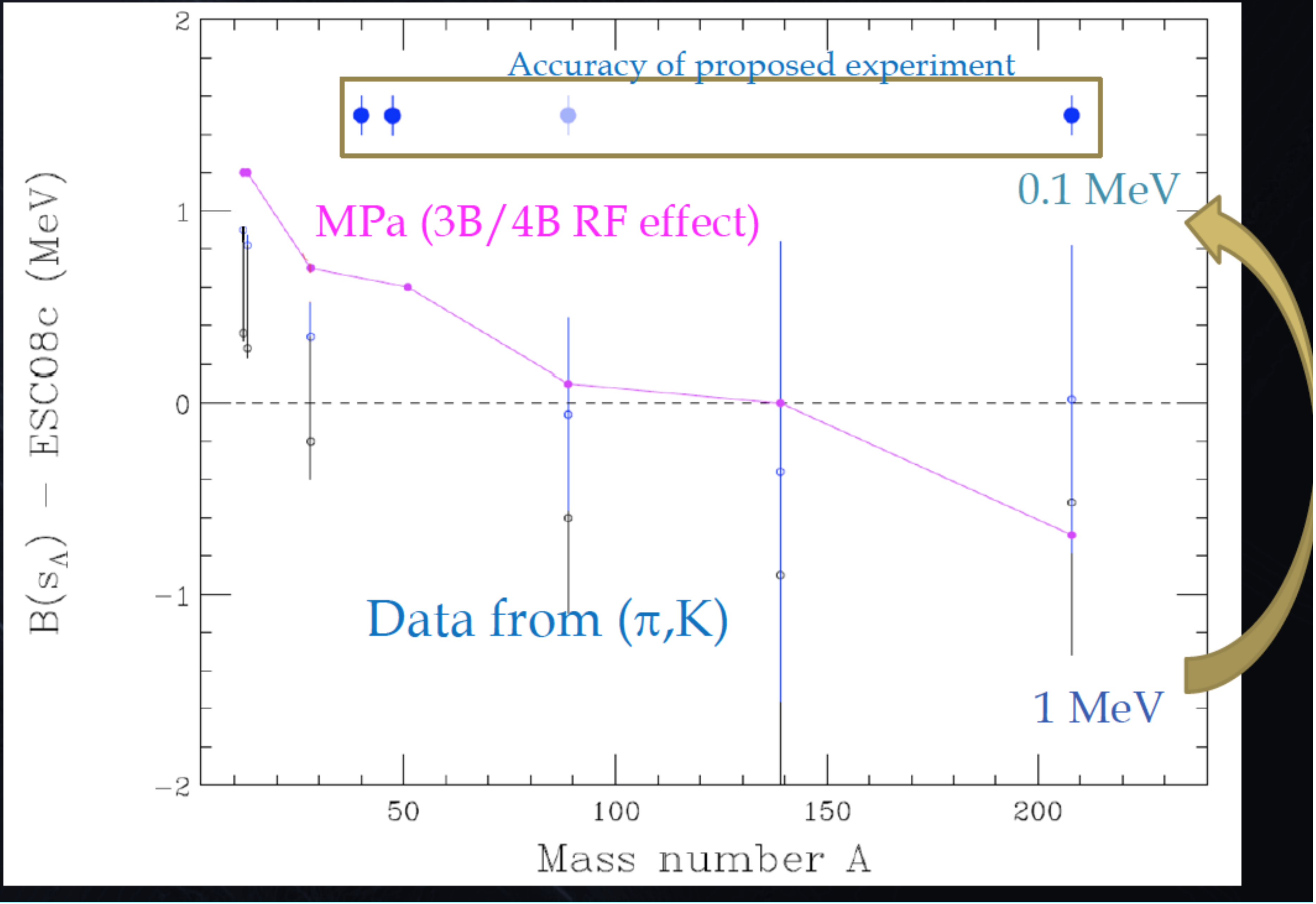

Mass dependence of B_Λ

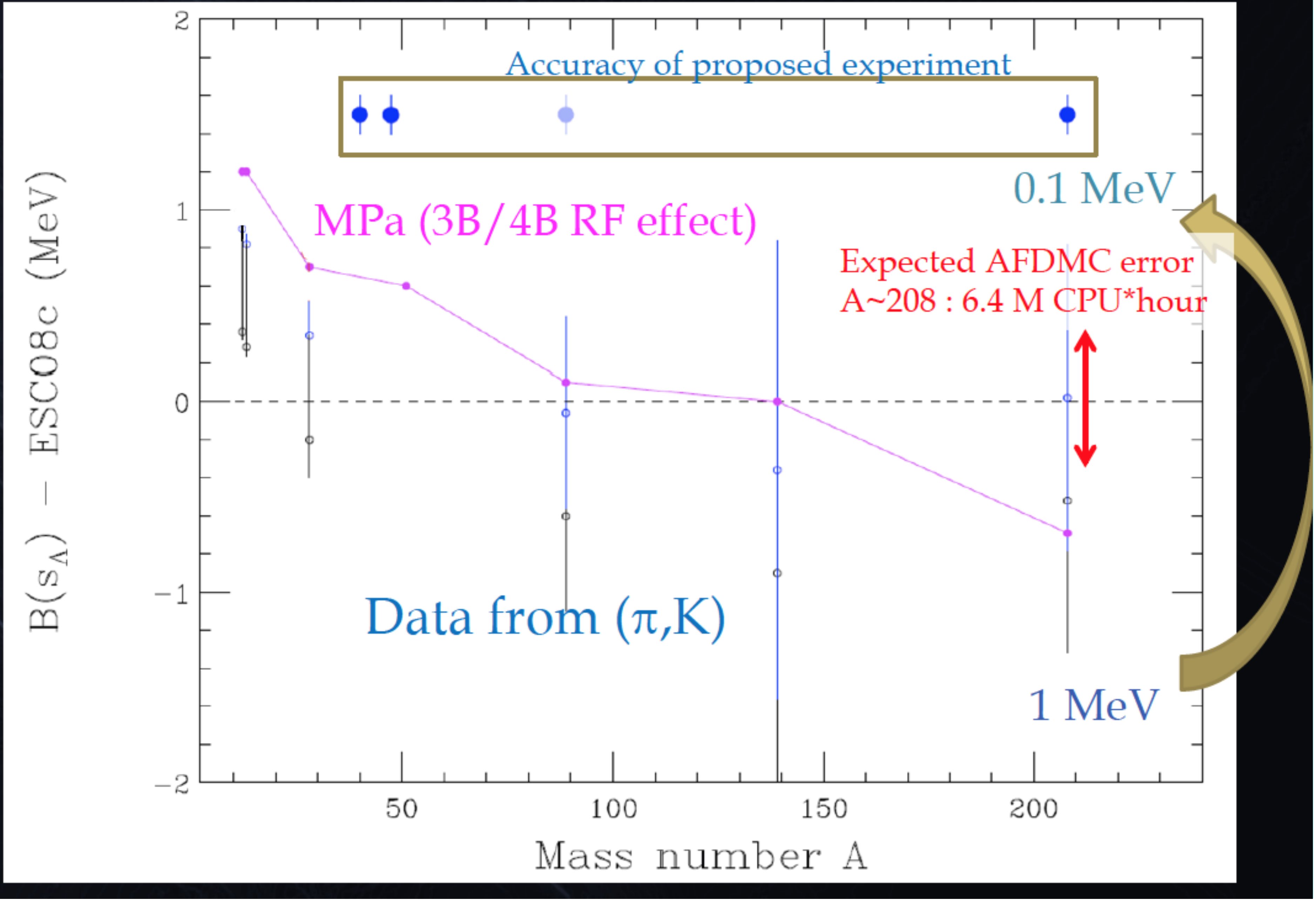

Theoretical cost for more sophisticated calculation

D.Lonardoni @ JLab Hypernuclear WS, May (2014)

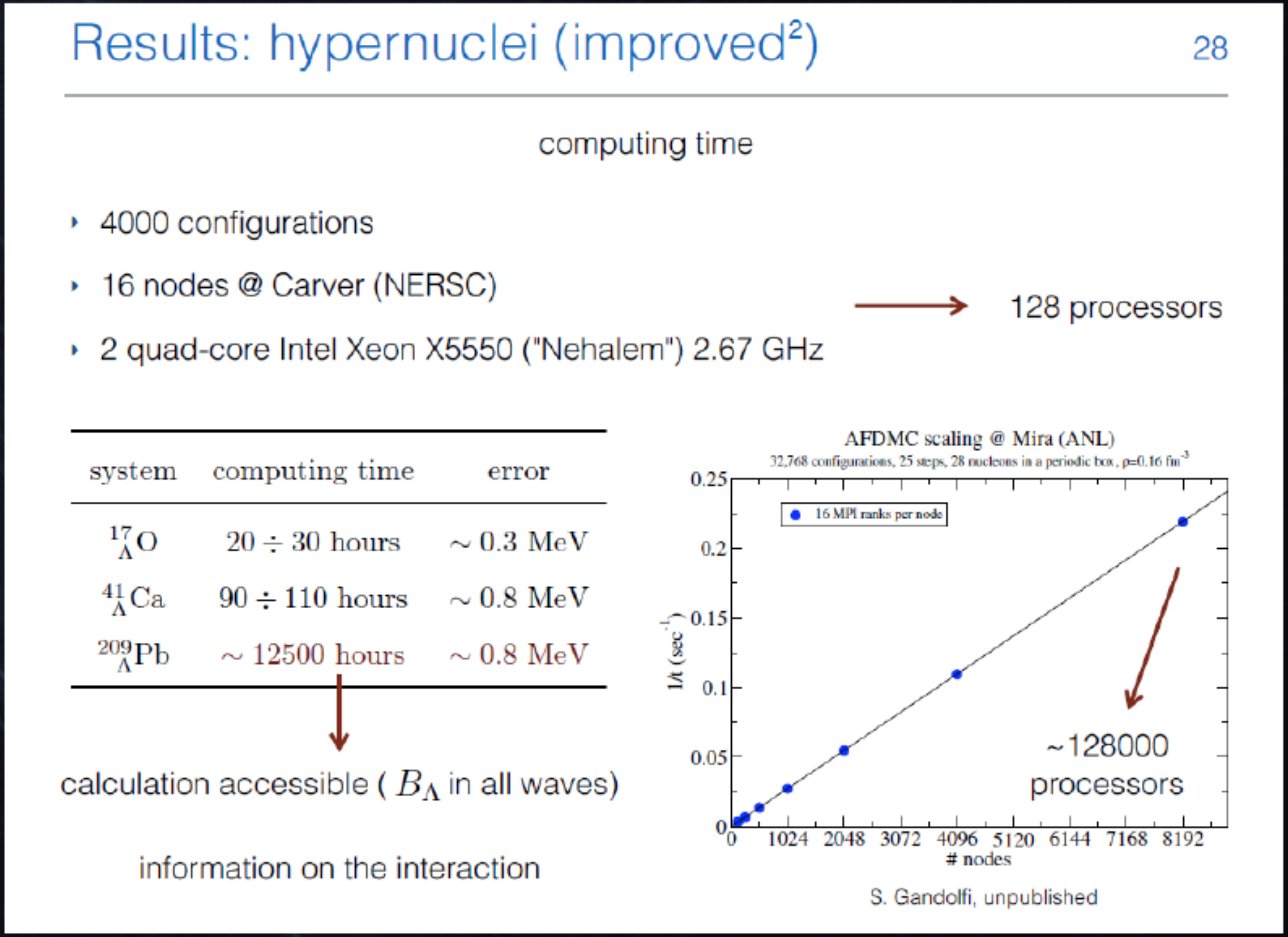

Results: hypernuclei (improved²)

computing time

- 4000 configurations
- 16 nodes @ Carver (NERSC)
- 2 quad-core Intel Xeon X5550 ("Nehalem") 2.67 GHz

→ 128 processors

system	computing time	error
$^{17}_{\Lambda}$O	$20 \div 30$ hours	~ 0.3 MeV
$^{41}_{\Lambda}$Ca	$90 \div 110$ hours	~ 0.8 MeV
$^{209}_{\Lambda}$Pb	~ 12500 hours	~ 0.8 MeV

calculation accessible (B_Λ in all waves)

information on the interaction

AFDMC scaling @ Mira (ANL)

32,768 configurations, 25 steps, 28 nucleons in a periodic box, ρ=0.16 fm^{-3}

~128000 processors

S. Gandolfi, unpublished

Calc. w/ 0.4 MeV error for A=208 requires 12500 x $(0.8/0.4)^2$ x 128 (CPU * hours)
= 6.4 M CPU hours = 130 days * 2048 CPU

Hyperon in heavier nuclei – ^{208}(e,e'K+)$^{208}{}_{\Lambda}$Ti

✔ A range of the mass spectroscopy to its extreme

✔ Studied with (π,k) reaction, levels barely visible (poor energy resolution)

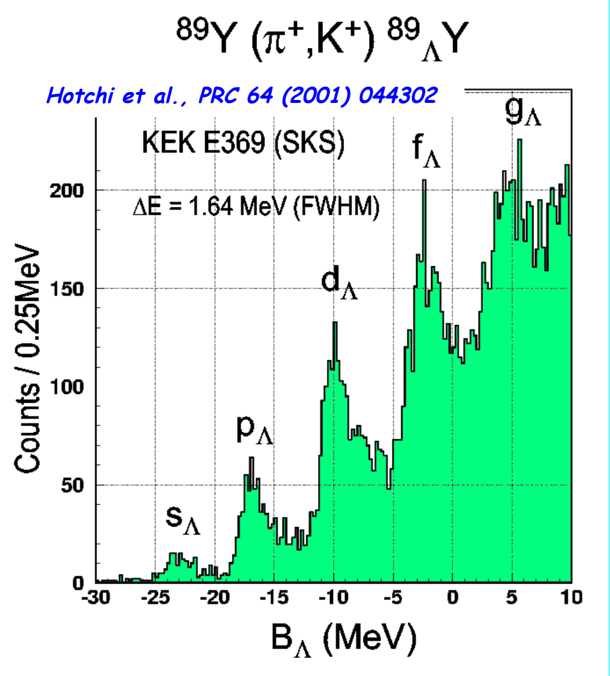

^{89}Y (π$^+$,K$^+$) $^{89}{}_{\Lambda}$Y

Hotchi et al., PRC 64 (2001) 044302

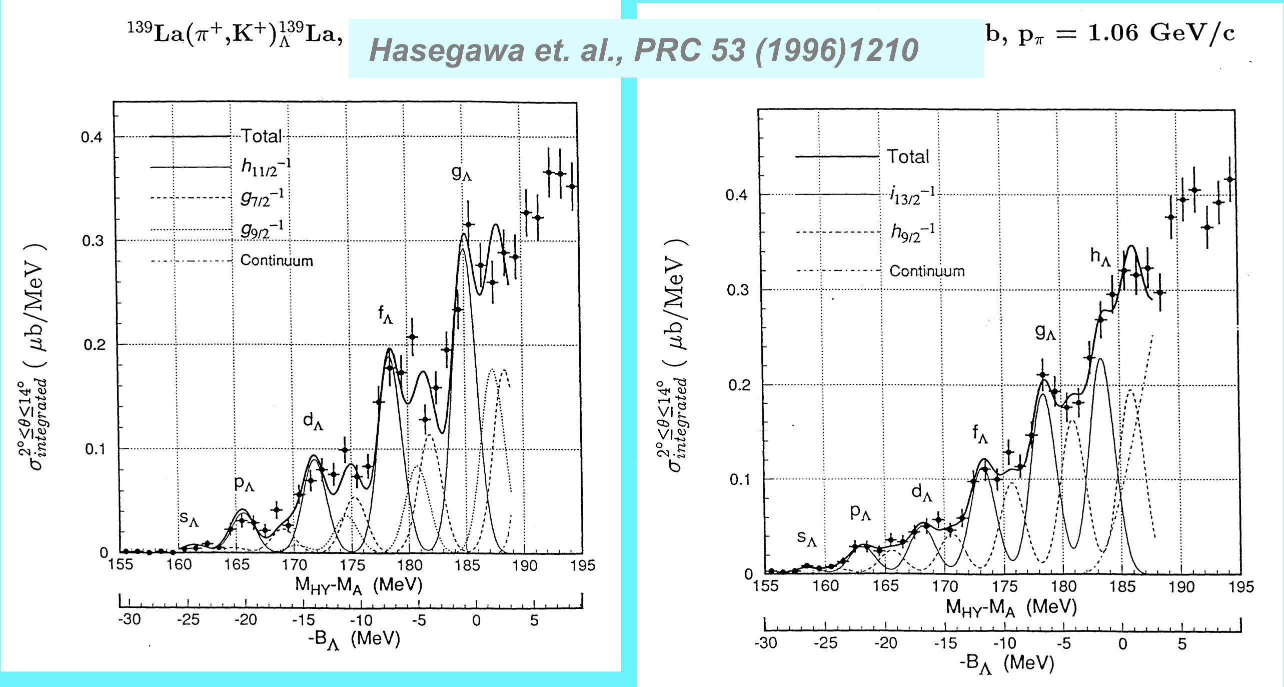

^{139}La(π$^+$,K$^+$)$^{139}_{\Lambda}$La,

b, p_π = 1.06 GeV/c

Hasegawa et. al., PRC 53 (1996)1210

✔(e,e'K) reaction can do much better

Energy resolution → Much more precise Λ single particle energies. Complementarity with (π,k) reaction

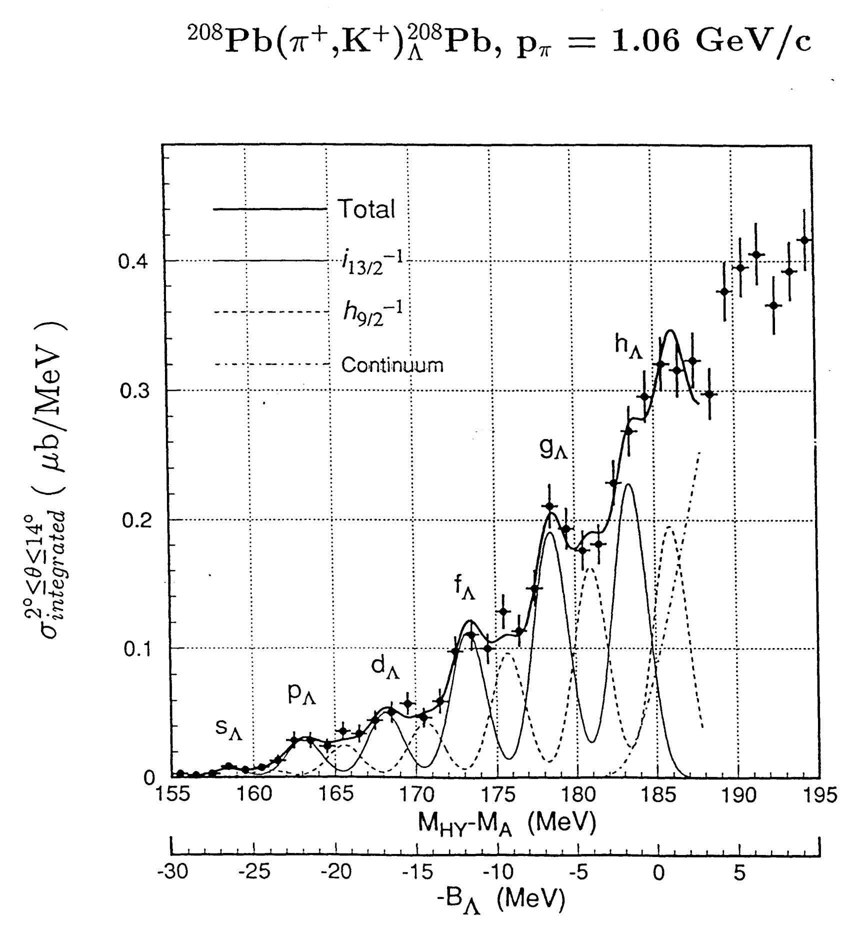

"Up to now these data are the best proof ever of quasi particle motion in a strongly interacting system"

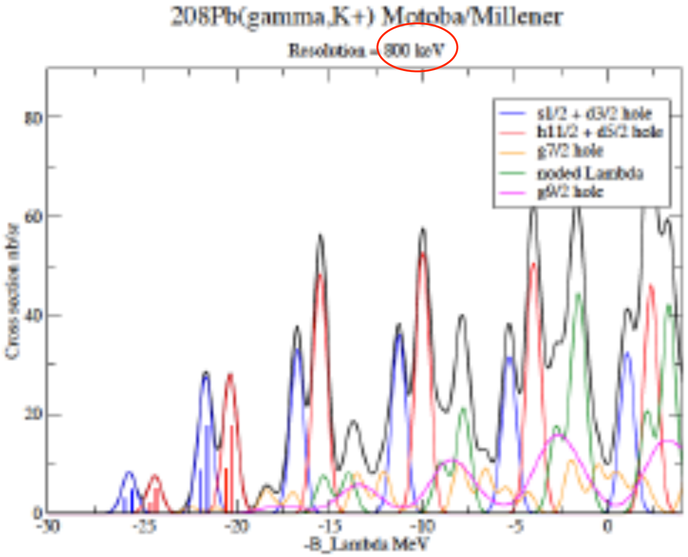

Fig. 5 a Excitation energy plot (Millener Motoba calculation (see text))

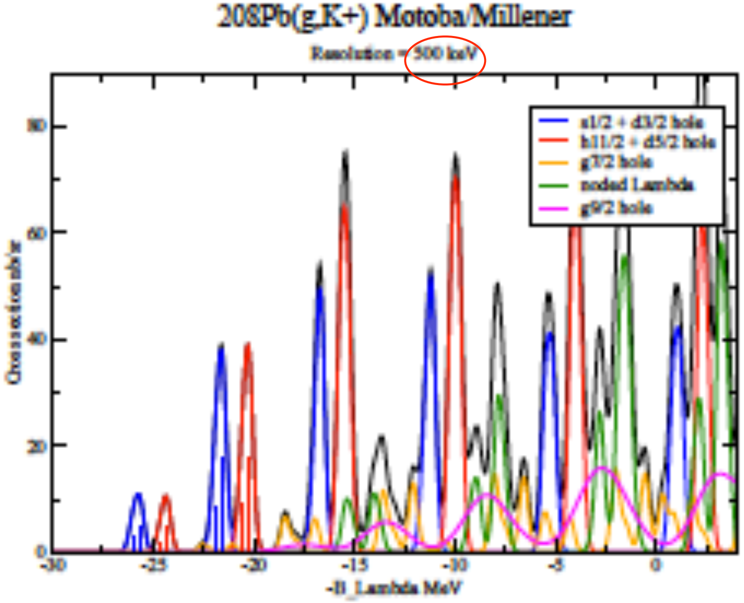

Fig. 5 b Excitation energy plot with 500 keV Energy Resolution

Millener-Motoba calculations

- particle hole calculation, weak-coupling of the Λ hyperon to the hole states of the core (i.e. no residual Λ-N interaction).

- Each peak does correspond to more than one proton-hole state

- Interpretation will not be difficult because configuration mixing effects should be small

- Comparison will be made with many-body calculations using the Auxiliary Field Diffusion Monte Carlo (AFDMC) that include explicitely the three body forces.

- Once the Λ single particle energies are known the AMDC can be used to try to determine the balance between the spin dependent components of the ΛN and ΛNN interactions required to fit Λ single-particle energies across the entire periodic table.

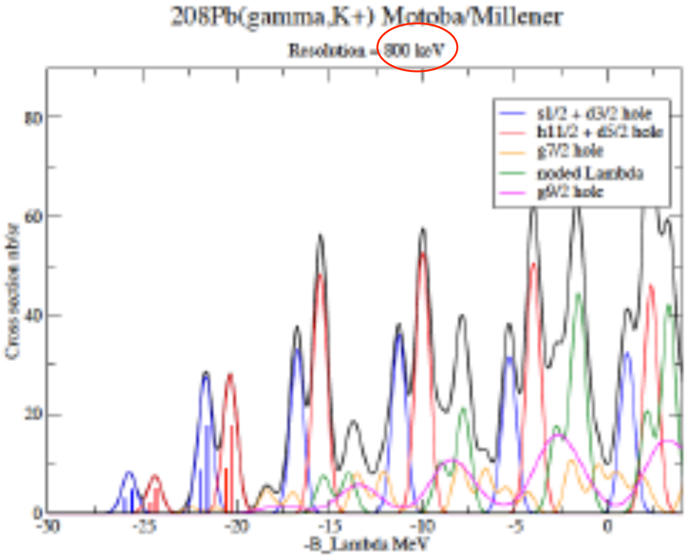

Fig. 5 a Excitation energy plot (Millener Motoba calculation (see text))

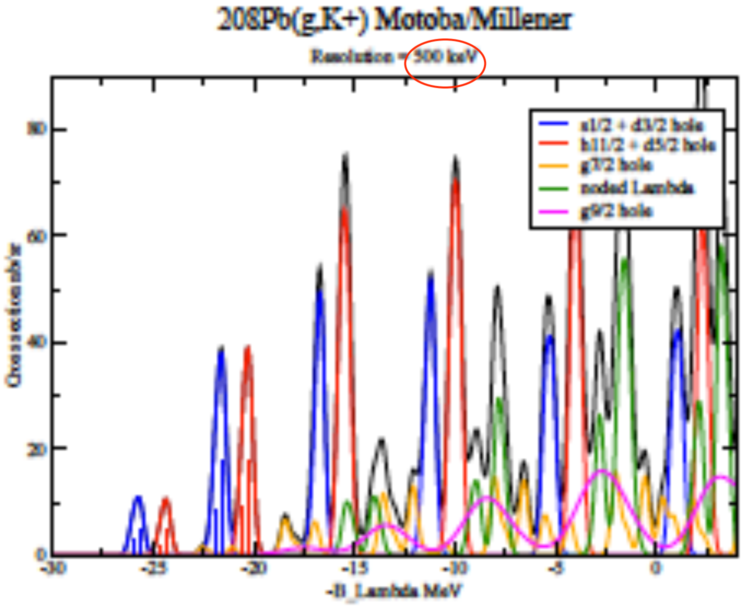

Fig. 5 b Excitation energy plot with 500 keV Energy Resolution

<I> (μA)	Target thickness (mg/cm²)	Peak significance	Peak
10	100	3.48	s-shell
10	200	4.13	s-shell
10	300	4.48	s-shell
10	100	7.54	p-shell
10	200	9.21	p-shell
10	300	11.52	p-shell
20	100	4.13	s-shell
20	200	4.63	s-shell
20	300	4.84	s-shell
25	100	4.3	s-shell
25	200	4.7	s-shell
25	300	4.9	s-shell
25	100	10.5	p-shell
25	200	12.8	p-shell
25	300	14.0	p-shell

The target

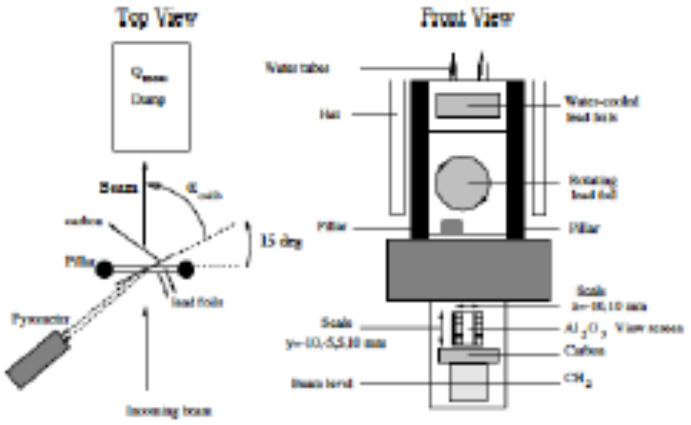

Fig. 7 The NIKHEF ^{208}Pb target layout

(15 °C) of up to 95 dm³/h during the actual data taking.

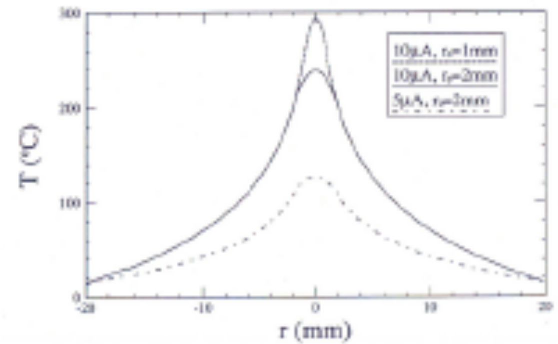

$<i>$ = 25 μA – 100 mg/cm² (cryocooling)

$$< i_{max}> = 2\pi k\,(T_{melting} - T_0)/\{[\ln(r_1/r_0) + ½]\,\rho dE/dx\}$$

but

With rotating target we can run higher current

Target calibration and monitoring

Elastic scattering measurement off Pb-208 to know the actual thickness of the target then monitor continuously by measuring the electron scattering rate as a function of two-dimensional positions by using raster information.

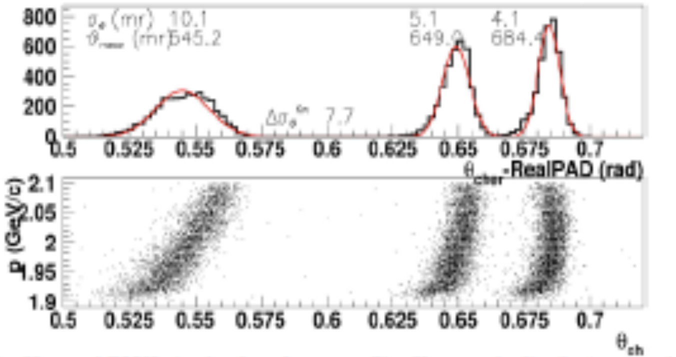

Fig. 11 Upgraded RICH simulated performance. Pion/Kaon angle distribution (equal

Rich detector upgrated for transversity experiment

PID π rejection ratio ~ 10^{-10} (threshold + RICH)

RICH Detector

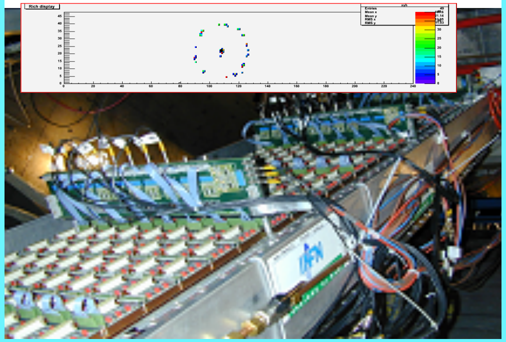

Advantages of Pb

In view of the astrophysical implications, experimental studies of hyper nuclei should focus on heavy targets, such as ^{208}Pb, in which the region of constant density accounts for a large fraction (~70%) of the nuclear volume (see figure) thus suggesting that its properties may be largely inferred from those of uniform nuclear matter

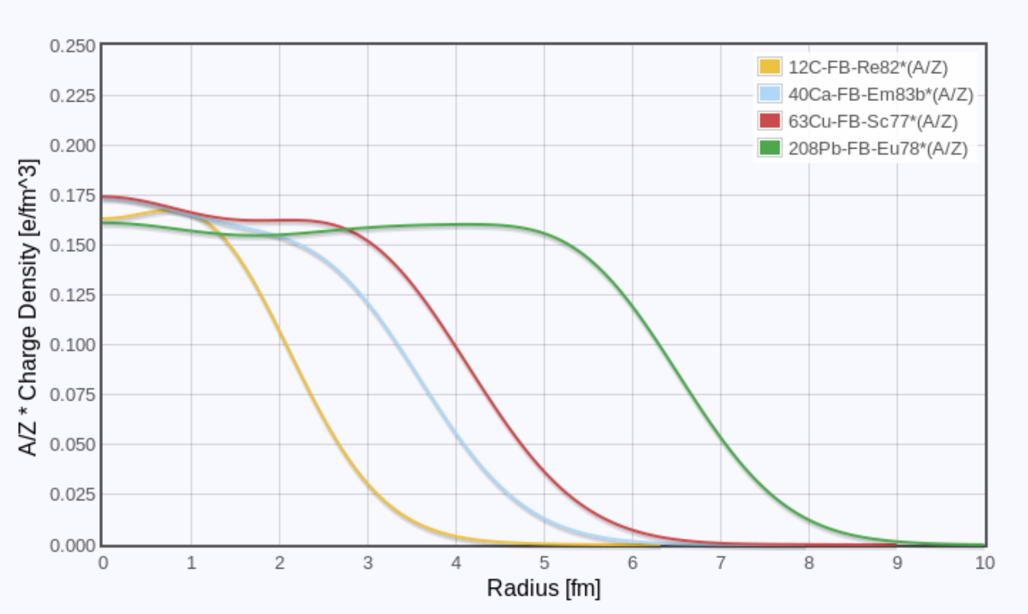

The possibility of using lead as a model of uniform nuclear matter has been confirmed by (e,e'p) experiments, showing that the observed spectroscopic factors of deeply bound shell model states of lead are very close to the results of nuclear matter calculations

In ^{208} Pb the properties of a bound hyperon are likely to be little affected by surface effects

Summary and conclusions

- The (e,e'K) experiments in the 6 GeV era confirmed the specific, crucial role of this technique

The new experiments would allow to obtain important information on

– ΛN interaction

-Charge Symmetry Breaking (CSB) in the Λ-N interaction

- Λ binding energy as a function of A for different nuclei than those probed with hadrons with much better energy resolution and accuracy

- The role of the 3 body ΛNN interaction in Hypernuclei and Neutron Stars, key point to solve the hyperon puzzle

Backup slides

Measurement and Feasibility: The experimental setup requires a combination of the HRS and HKS spectrometers. While there is a large lead-time associated with preparing for the experiments, no new equipment is required. Requested beam time for the main experiments discussed in the presentation is 147 hours for calibrations, 346 hours to test the CSB, 272 hours to investigate the ground states of $^{40}\Lambda$K and $^{48}\Lambda$K, 642 hours to measure the ground state of $^{208}\Lambda$Tl. The nnΛ re-measurement requires 130 hours.

Issues: The PAC views the most compelling science presented as the measurements of binding energy of the medium mass nuclei $^{48}\Lambda$K and $^{40}\Lambda$K. It is these measurements, along with the calibration measurements, that are conditionally approved. The PAC believes there should be a strong connection between understanding the ΛNN force and the 2 solar mass neutron star observations. However, the science case even for these measurements still needs refinement, and the connection has not been well articulated. Theoretical calculations are possible in the 40,48 nuclei, as well as in neutron matter. While AFDMC (Pederiva et al, arXiv:1506.04042) calculations have been performed with simplified interactions (AV4' + one term in UIX, and a ΛN and ΛNN interaction), a more complete picture may be feasibly obtained. Even using the simplified interaction in AFDMC, the calculations indicate that the tensor parameter could be well constrained by a measurement of BΛ in an asymmetric nucleus. This argument should be strengthened and explored, possibly by a workshop. The PAC believes the collaboration would benefit from a more integrated theoretical effort in this area.

The collaboration should submit an updated proposal to study $^{48}\Lambda$K and $^{40}\Lambda$K along with a stronger theoretical connection to neutron star physics.

The PAC is not convinced that measurements of the A dependence of BΛ will provide meaningful input to theoretical calculations of the equation of state for neutron stars. Therefore the ^{208}Pb measurements and other parts of this proposed work, including CSB efforts, are deferred. Completely new proposals would need to be submitted to the PAC in order to address these additional physics topics.

CSB interaction test in A=7 iso-triplet comparison

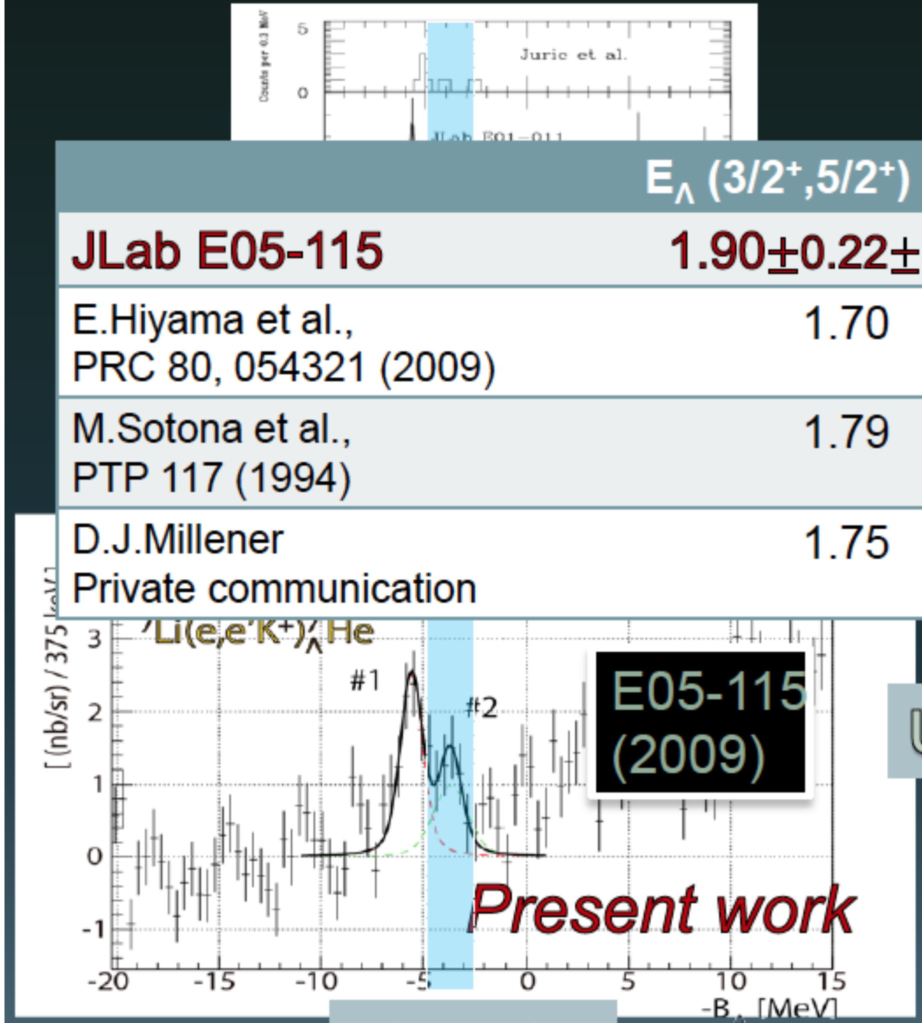

	E_Λ ($3/2^+$,$5/2^+$) [MeV]
JLab E05-115	**1.90±0.22± 0.05**
E.Hiyama et al., PRC 80, 054321 (2009)	1.70
M.Sotona et al., PTP 117 (1994)	1.79
D.J.Millener Private communication	1.75

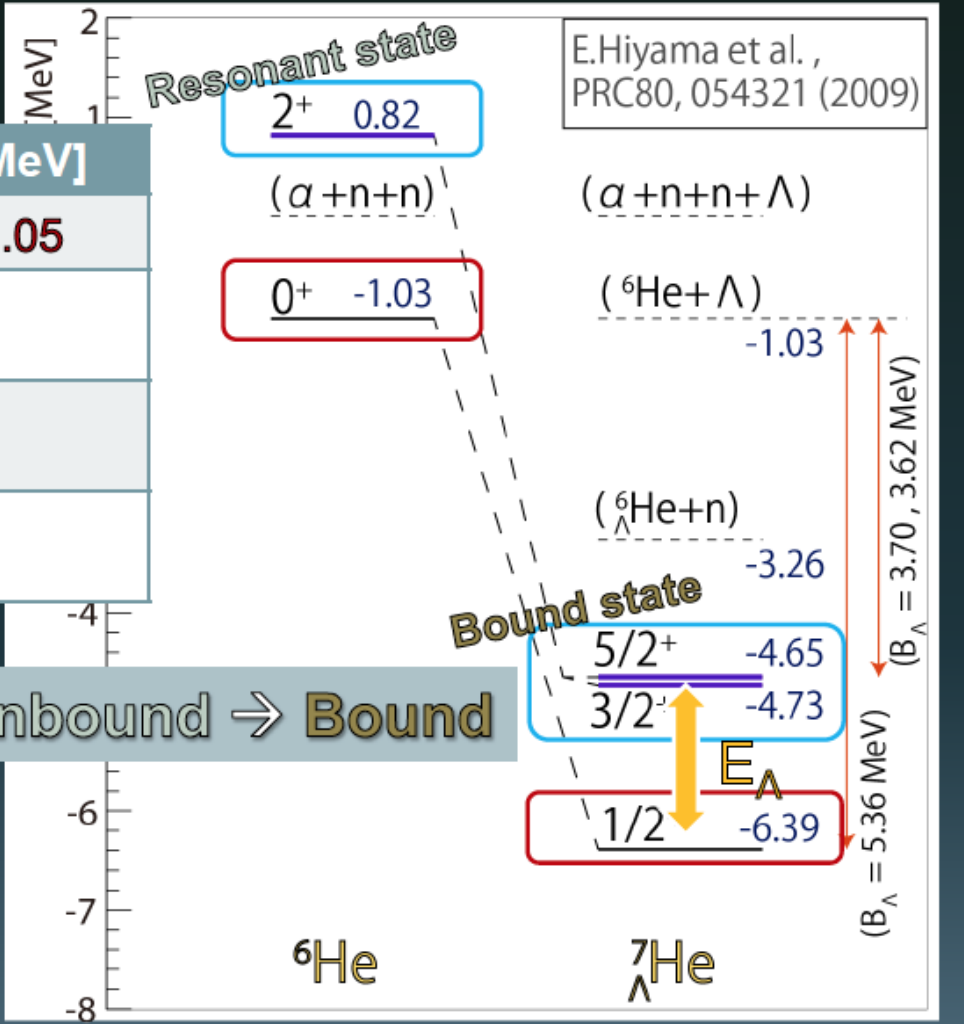

Unbound → Bound

T.Gogami, Doctor Thesis (2014) Tohoku Univ.

The theoretical calculation of the (e, e'K+) cross section involves three ingredients: (i) the known cross section of the elementary ep→e'K+Λ process, (ii) the spectral function, describing the nucleon momentum and energy distribution in the ^{208}Pb ground state, and (iii) the spectral function containing the information of the bound hyperon. In this context, using a realistic model of the nucleon spectral function, such as the one employed to obtain the results displayed in Fig would greatly reduce the systematic error associated with the treatment of the non-strange sector.

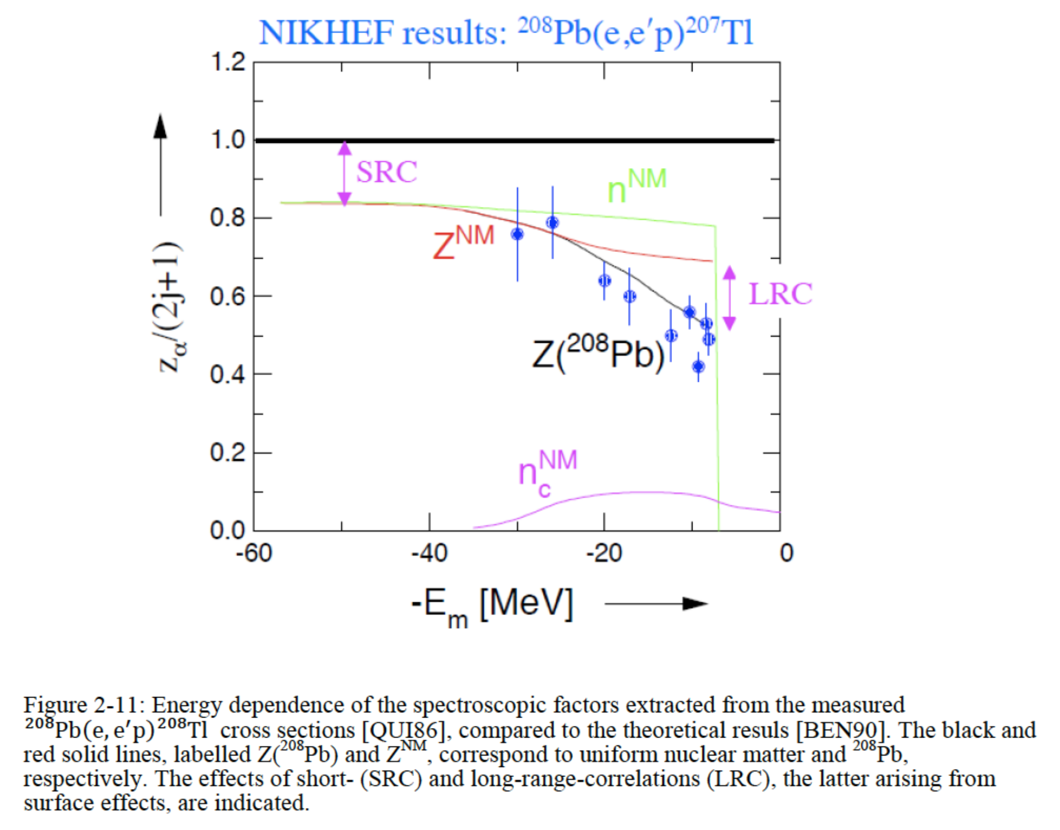

Figure 2-11: Energy dependence of the spectroscopic factors extracted from the measured ^{208}Pb(e, e′p)^{208}Tl cross sections [QUI86], compared to the theoretical resuls [BEN90]. The black and red solid lines, labelled Z(^{208}Pb) and Z^{NM}, correspond to uniform nuclear matter and ^{208}Pb, respectively. The effects of short- (SRC) and long-range-correlations (LRC), the latter arising from surface effects, are indicated.

Energy dependence of the spectroscopic factors extracted from the measured Pb 208(e,e'p)Tl 208 cross sections [QUI86], compared to the theoretical resuls [BEN90]. The black and red solid lines, labelled Z(^{208}Pb) and Z^{NM}, correspond to uniform nuclear matter and ^{208}Pb, respectively.

The effects of short- (SRC) and long-range-correlations (LRC), the latter arising from surface effects, are indicated.

N. of detected photoelectrons

$$N_{p.e.} = 370 L \sin^2 \overline{\vartheta}_c \prod_i \varepsilon_i \Delta E \approx 20 - 50$$

Separation power

$$\vartheta_2 - \vartheta_1 = n_\sigma \sigma_{\vartheta_c}$$

Particle mass m_1 **Particle mass m_2**

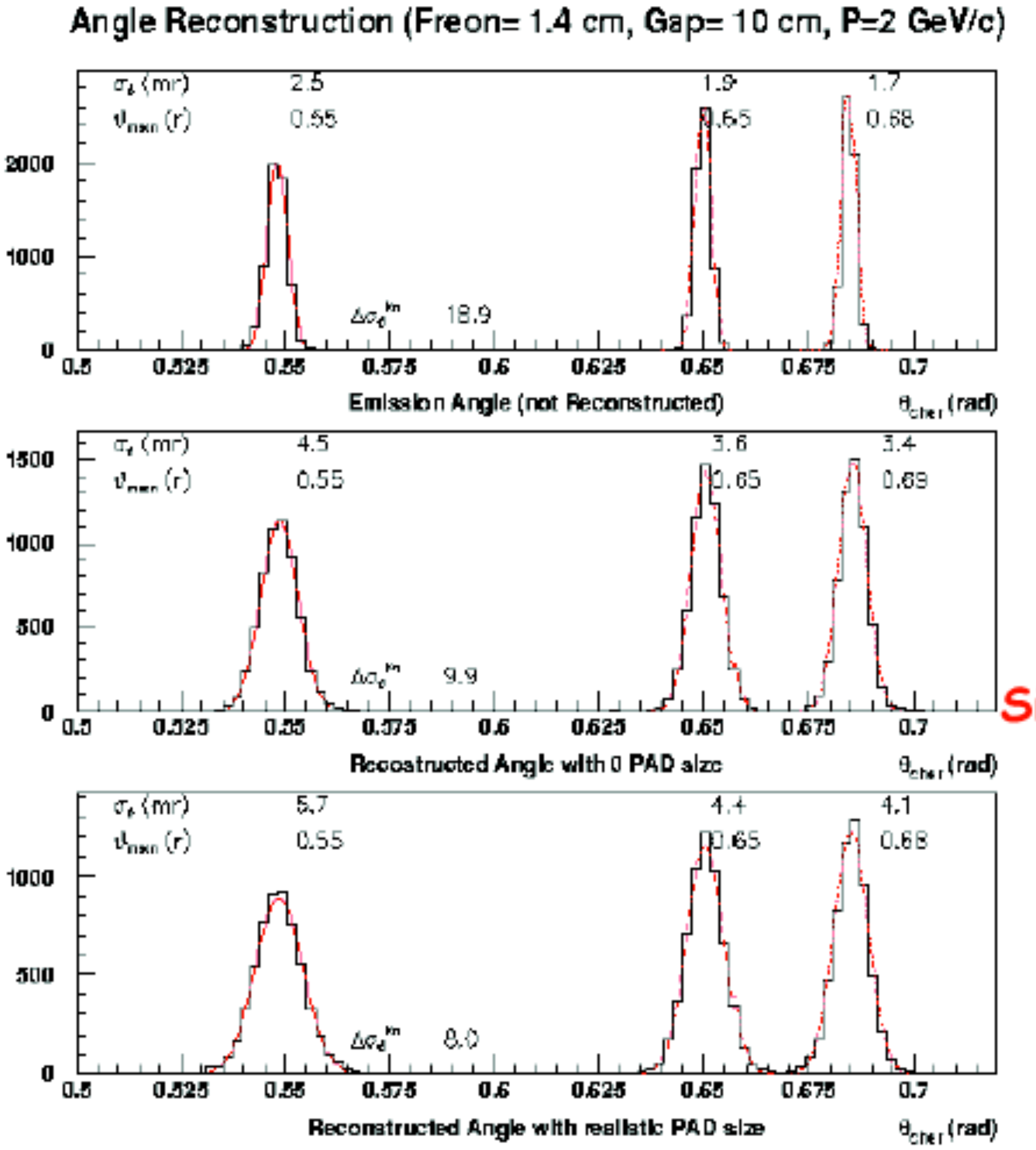

Cherenkov angle resolution

$$\sigma_{\vartheta_c} = \frac{\sigma_\vartheta^{p.e.}}{\sqrt{N_{p.e.}}}$$

Minimize

Maximize

π, K separated by 30 mrad

with 3 mrad: 10 σ

Simulation (spectra) done with 5 σ

Rich Performances
'key parameters':

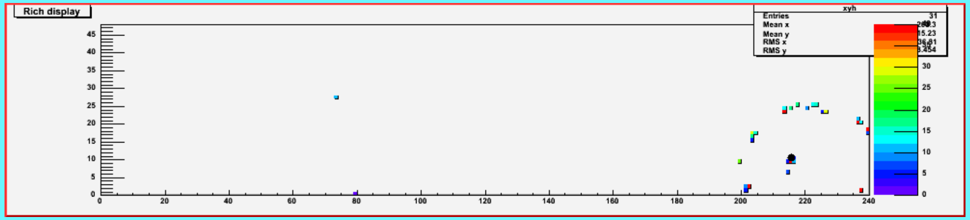

N_{pe} for π and p

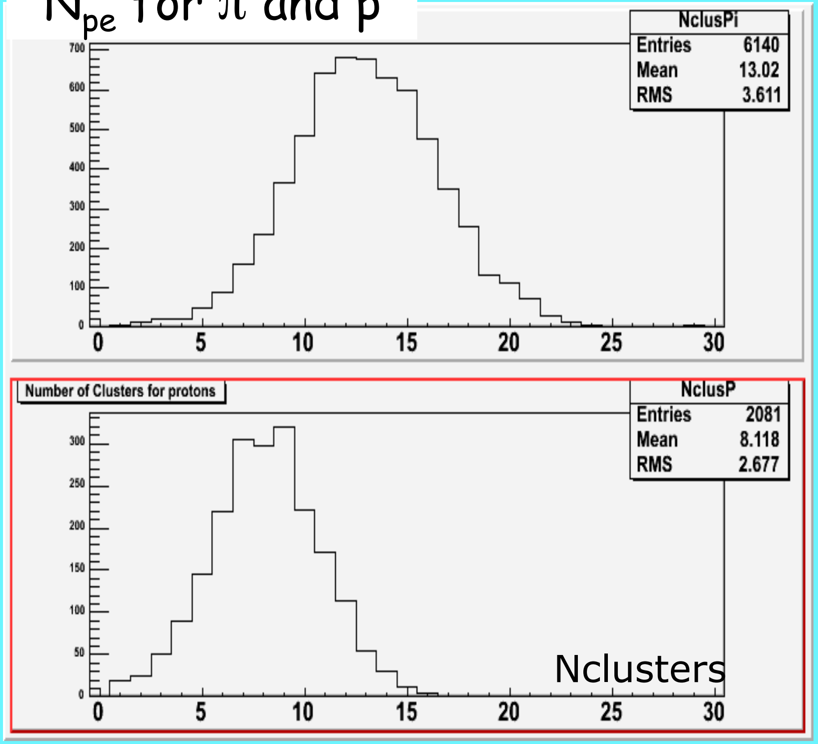

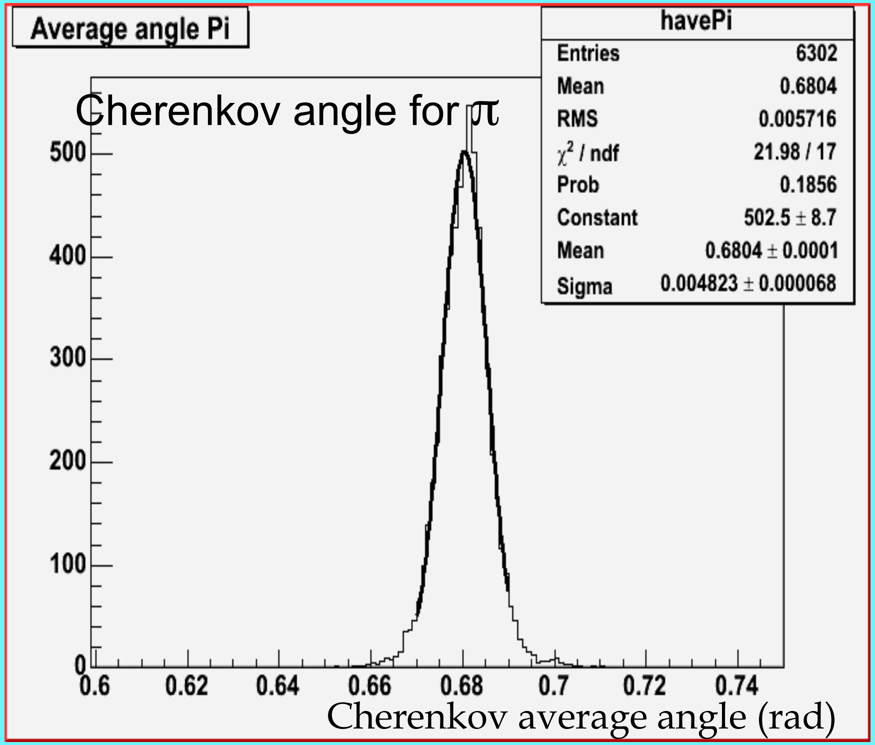

N_{pe} π/p ratio:

$$\frac{N^{P}_{clus}}{N^{\pi}_{clus}} = \frac{1-\beta_P^2 n^2}{1-\beta_\pi^2 n^2} = 0.66$$

Mean number of photoelectrons

$$N_\pi = 13$$

Angular resolution

$$\sigma_{\theta_\pi} = 5 \textbf{ mrad}$$

$$\Downarrow$$

$$\theta_\pi - \theta_K \sim 6 \cdot \sigma_{\theta_\pi}$$

Radiator: the Freon Vessel

Most fragile component of the detector

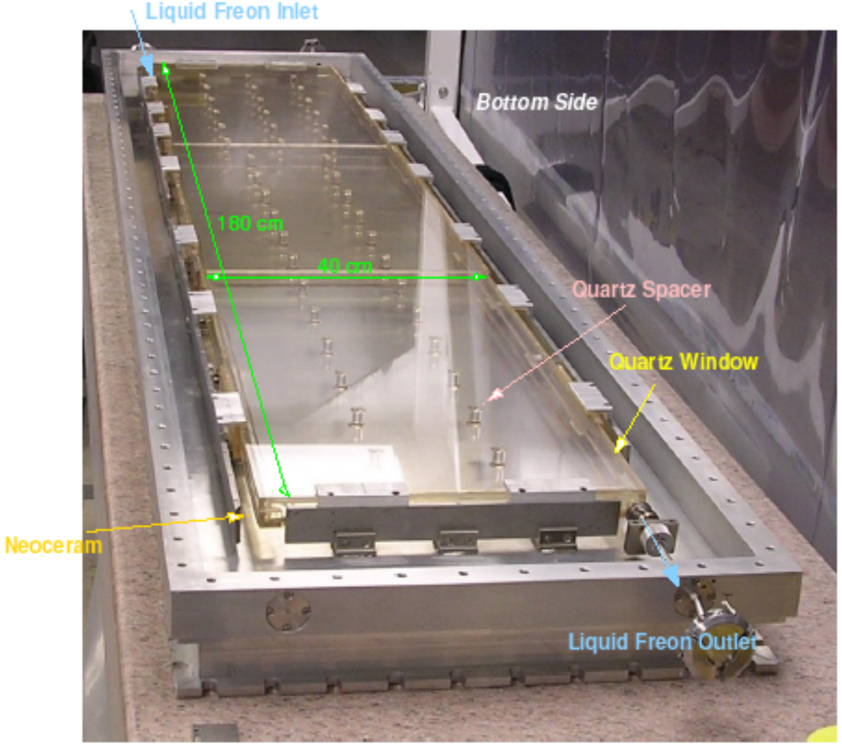

Freon pressure partially compensated by the glued spacers

Tracks without photon clusters

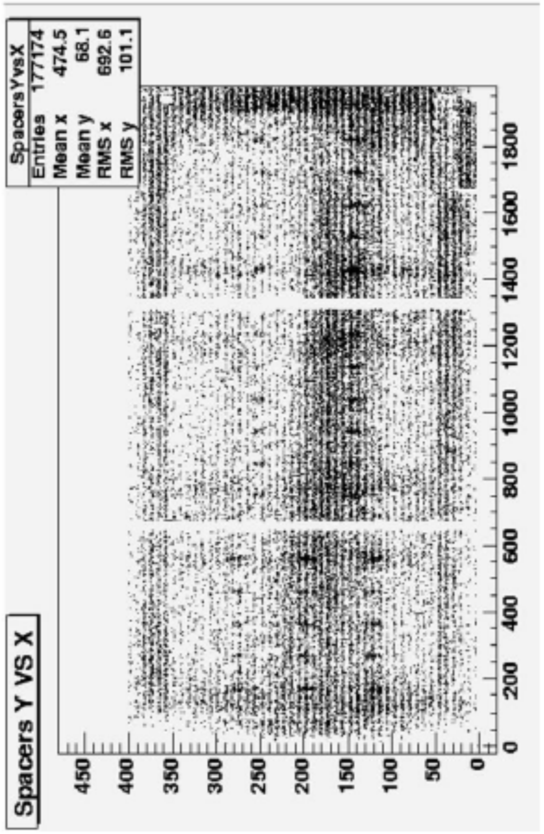

[Garibaldi et al NIMA 2003] for details on the freon recirculating system

Many parameters affect the detector performances (# p.e.)

- quartz transparency in the v.w. region of interest (160 - 220 nm)

- freon purity to not absorb the emitted Cherenkov light
  - freon purity circuit + continuously monitoring

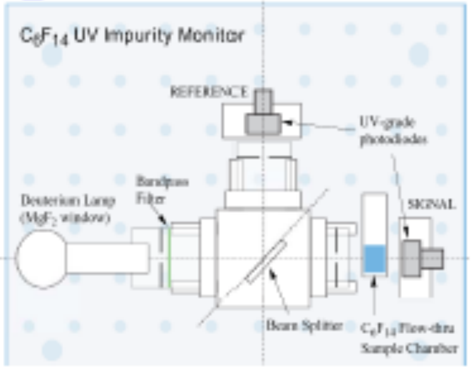

- CsI photocathode
  - evaporation + on line QE absolute measurement
  - QE is strongly affected by oxygen and moisture
    - Careful handling of photocathodes after evaporation
    - Continuous monitoring of gas "purity"

The RICH detector at Jefferson Lab

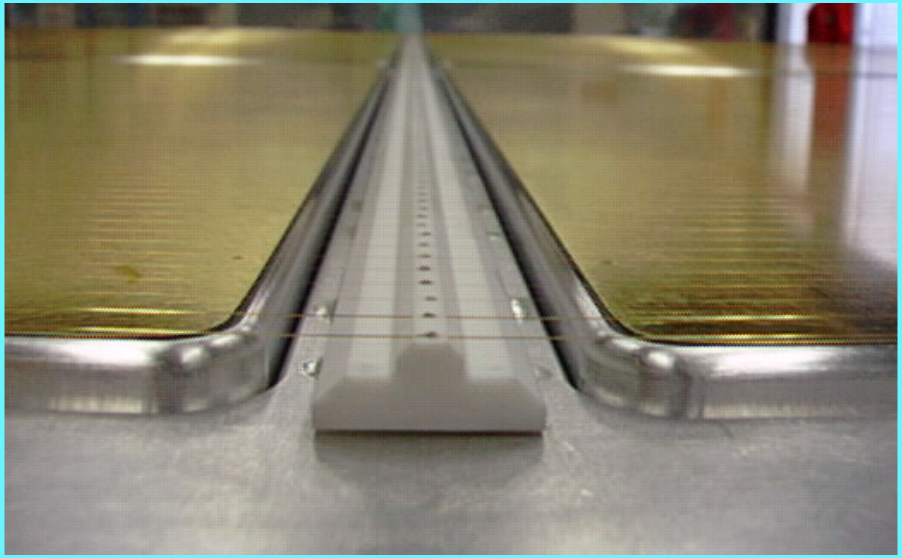

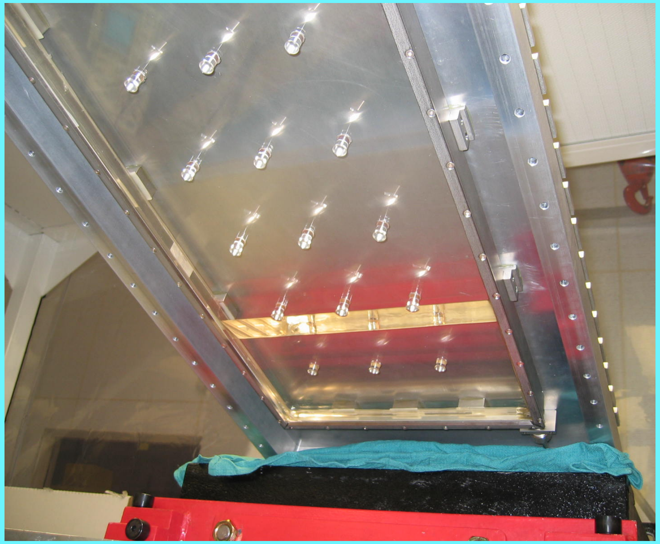

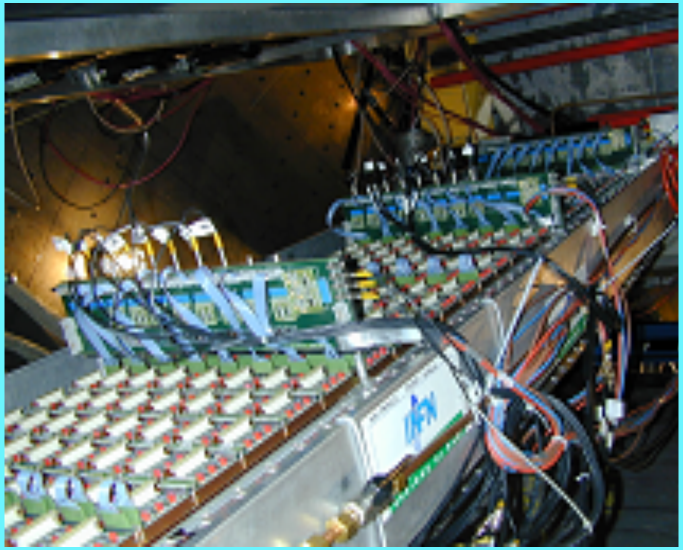

RICH photocathode installation

JLAB Hall A RICH flying to hunt kaons into the detector hut

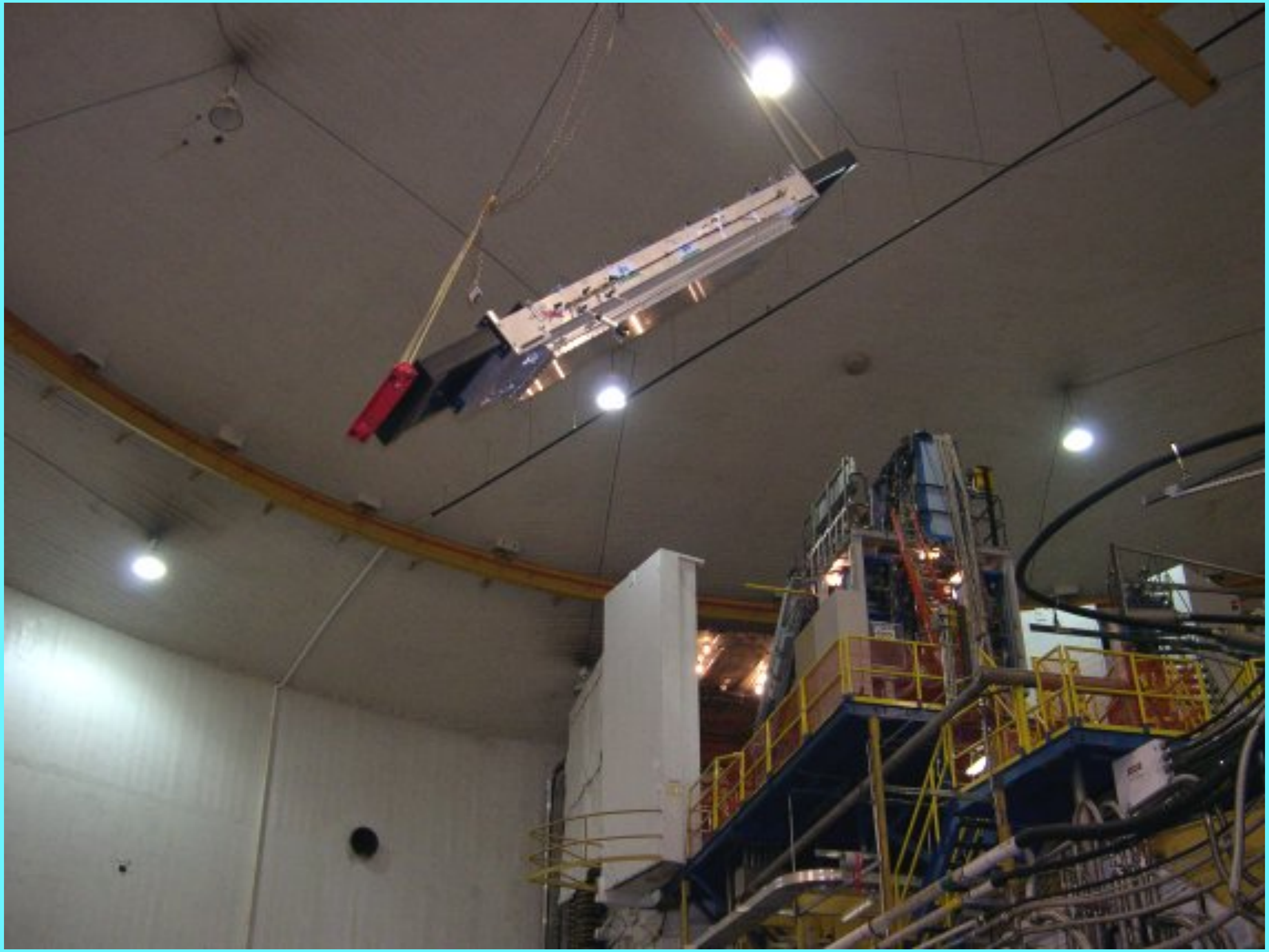

Evaporation Facility for large area photocathode

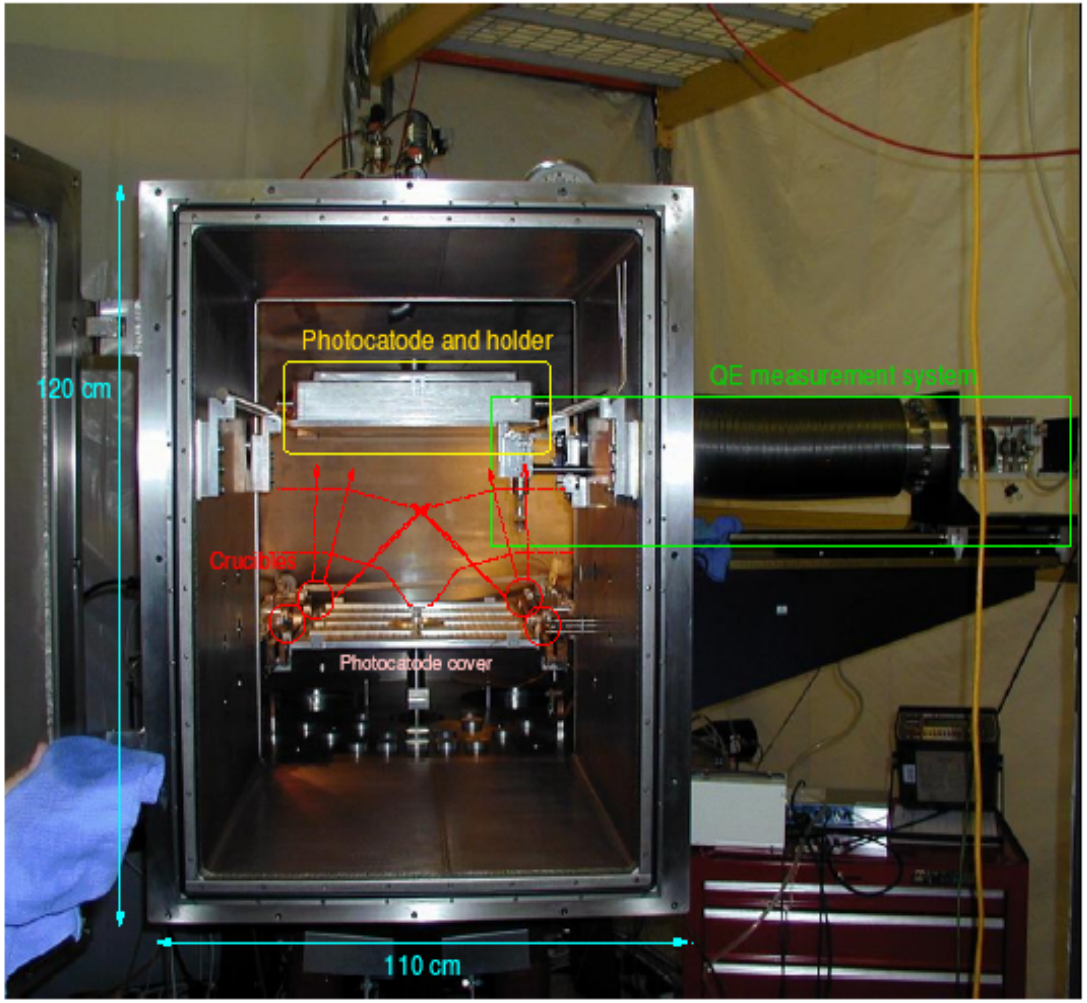

- Stainless steel cylindrical vessel
- 3 pumps (scroll + molecular + cryogenic) provide vacuum of $5 \cdot 10^{-7}$ mbar in < 24 h
- 4 crucibles → thickness uniformity $\sim 10\%$
- CsI powder (from CERN) evaporated at $\sim 500\ ^{o}$C

Evaporation station is temporary moved to Stony Brook University (Long Island) for R&D on GEM

The evaporator system

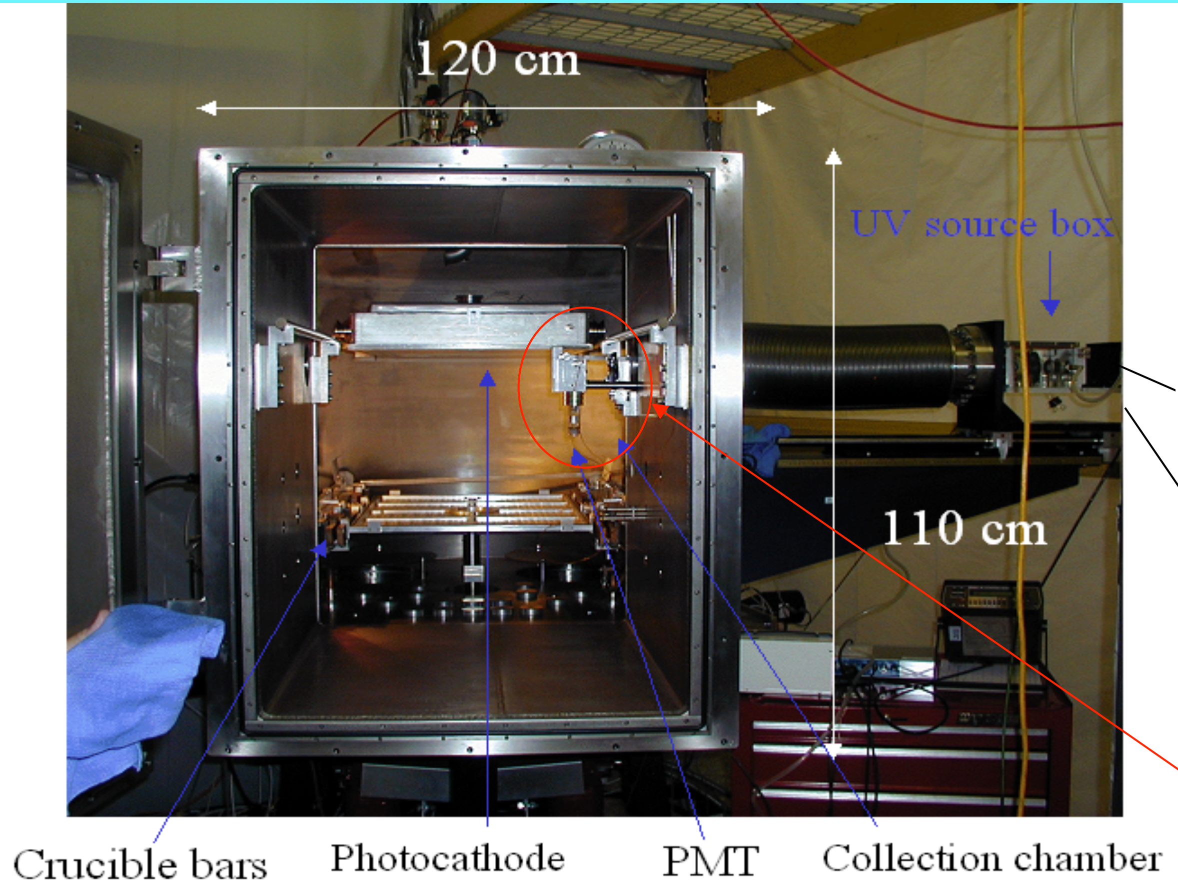

UV source and optical system

Quantum Efficiency measurement system

2–axes movement system
3 band filters (160, 185, 220 nm)

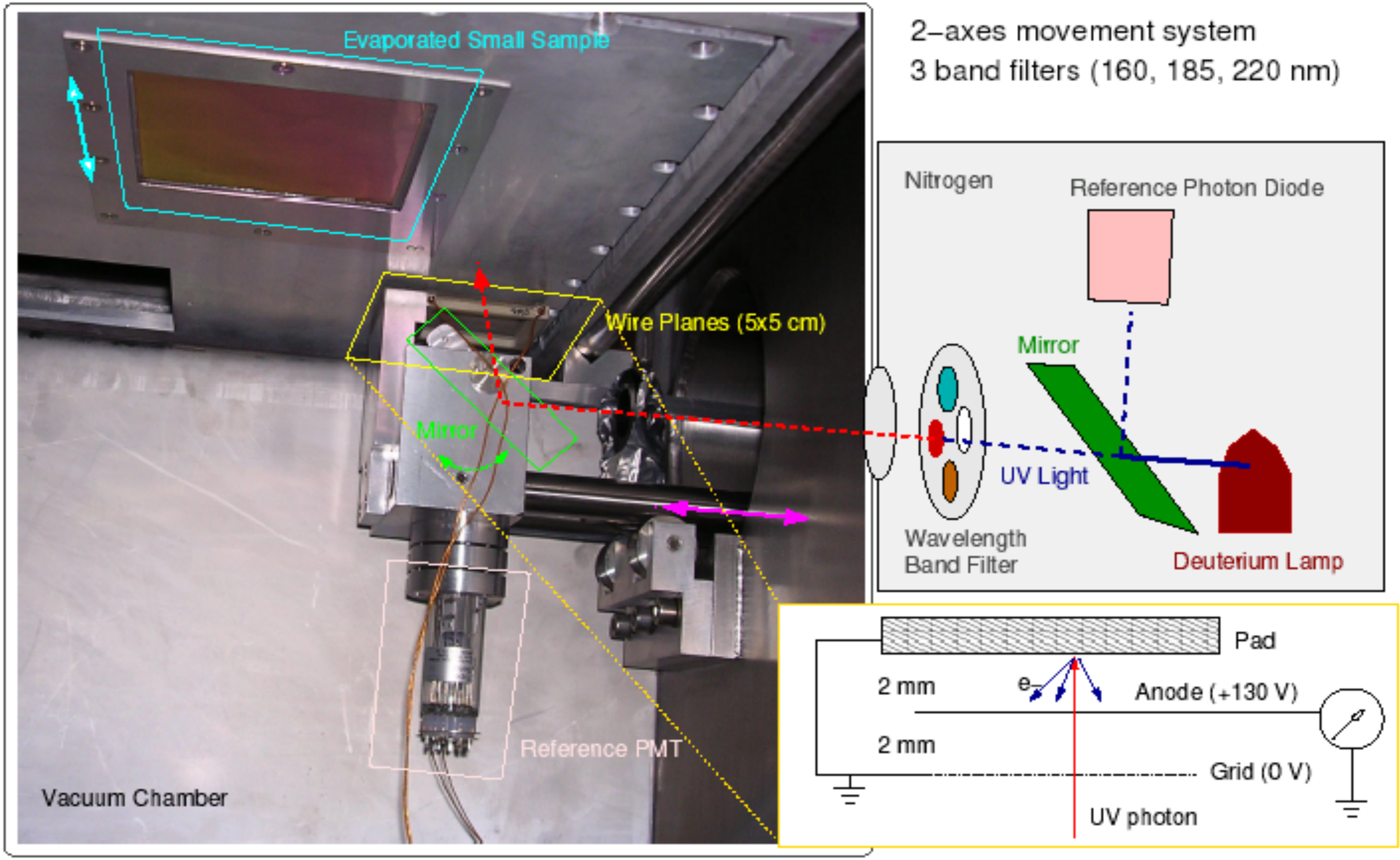

$$QE = \frac{I_{chamber}}{I_{PMT}} \cdot QE_{PMT}$$

Forward angle Septum magnets

No degradation in HRS perf.

General purpose device

Two independent arms

p GeV/c	Θ deg	B deg	R cm	∫B. dl T .m	B0 T
2	6	6.5	740.8	0.76	0.9

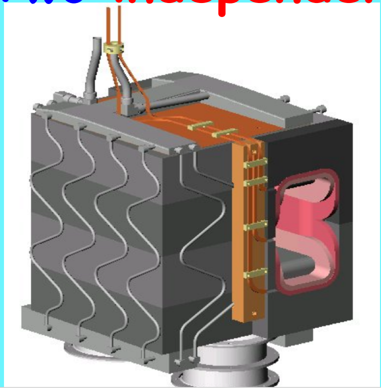

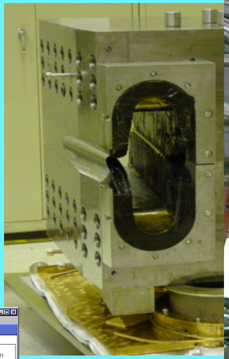

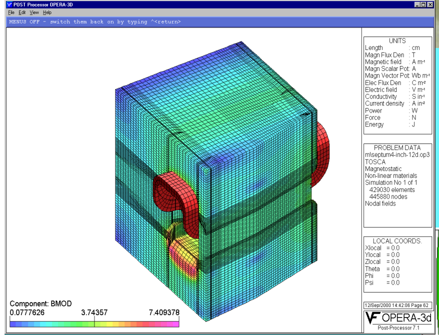

UNITS
Length : cm
Magn Flux Den : T
Magnetic field : A m-1
Magn Scalar Pot: A
Magn Vector Pot: Wb m-1
Elec Flux Den : C m-2
Electric field : V m-1
Conductivity : S in-1
Current density : A in-2
Power : W
Force : N
Energy : J

PROBLEM DATA
m\septum4-inch-12d.op3
TOSCA
Magnetostatic
Non-linear materials
Simulation No 1 of 1
429030 elements
445880 nodes
Nodal fields

LOCAL COORDS.
Xlocal = 0.0
Ylocal = 0.0
Zlocal = 0.0
Theta = 0.0
Phi = 0.0
Psi = 0.0

12/Sep/2000 14:42:06 Page 62

Back side view of septum showing the field within iron and the cutout of iron near the front that allows for small angle.

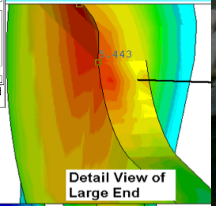

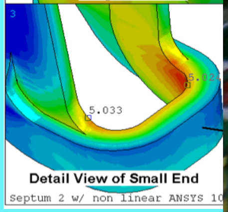

Coil Magnetic Flux Density

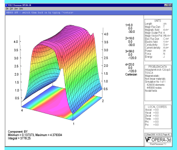

Midplane Histrogram of By at 12.0° setting. Current density of 24,000 Amp/cm^2

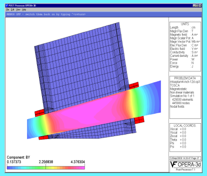

Midplane map of B_y at 12° configuration.

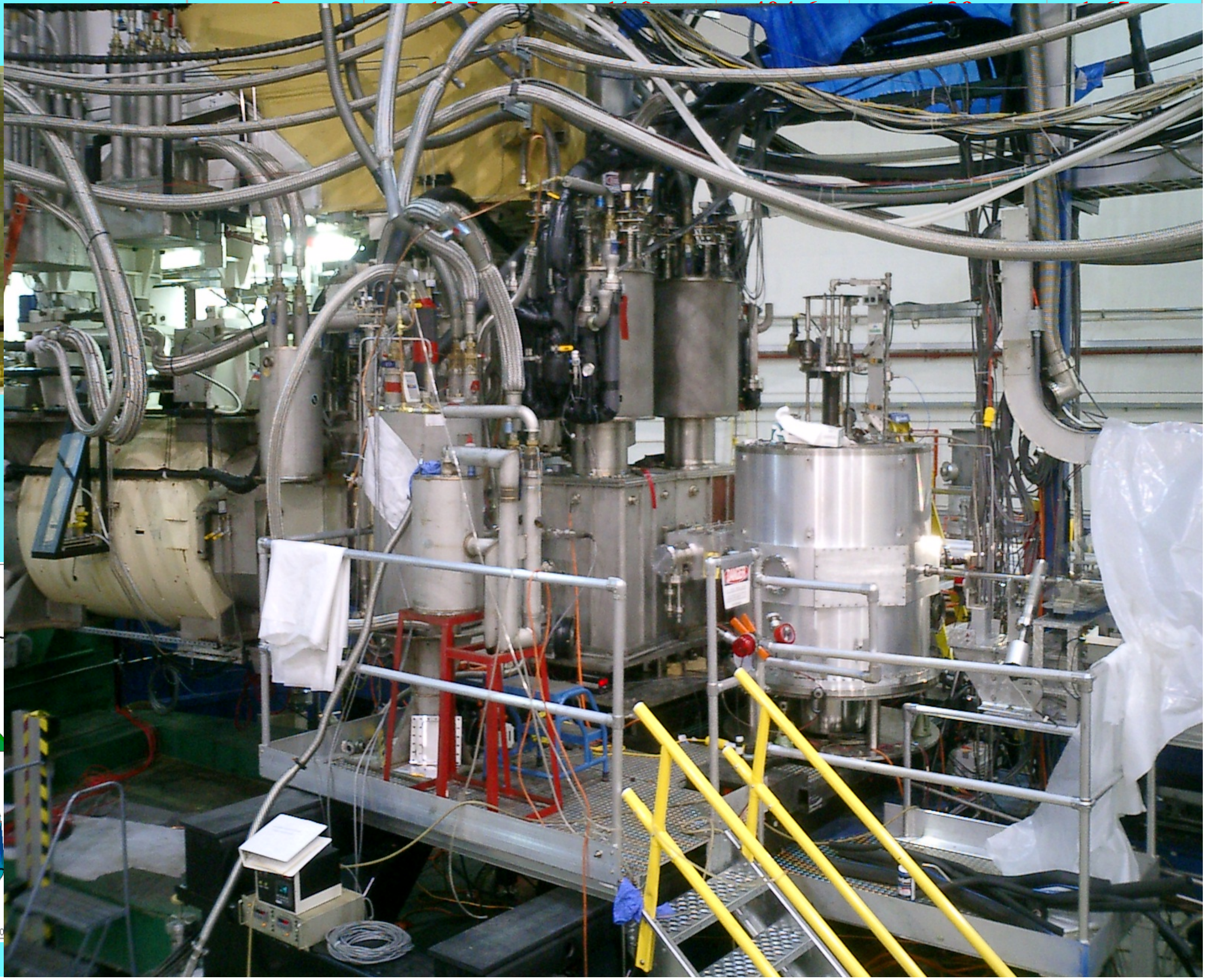

Beam and Optics (3)

- Four Optical Elements (QQDQ)
- Design Resolution 1.0E-4 FWHM momentum resolution
- NIM Paper Shows 2.5E-4 FWHM momentum resolution
- Multiple Coulomb Scattering Is The Reason For The Difference

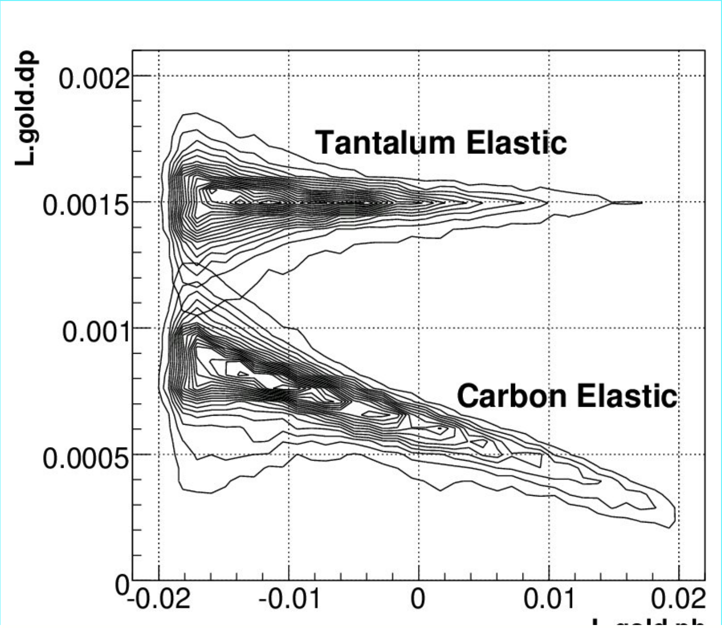

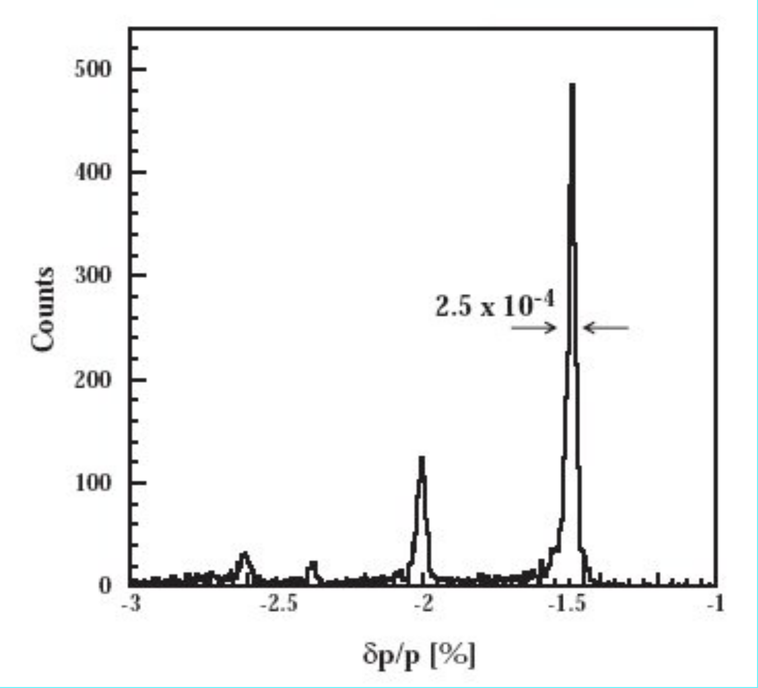

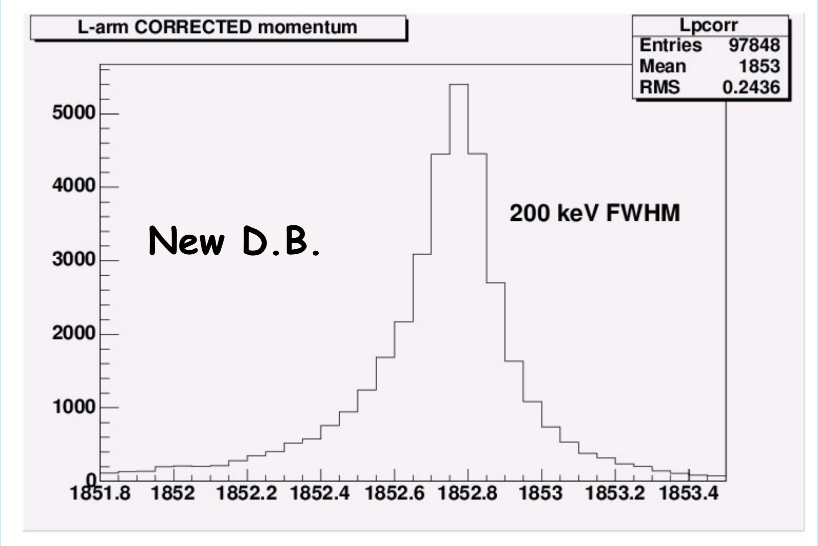

- Both Spectrometers Have Demonstrated ~ 1E-4 FWHM δ Resolution

Mass dependence of B_Λ

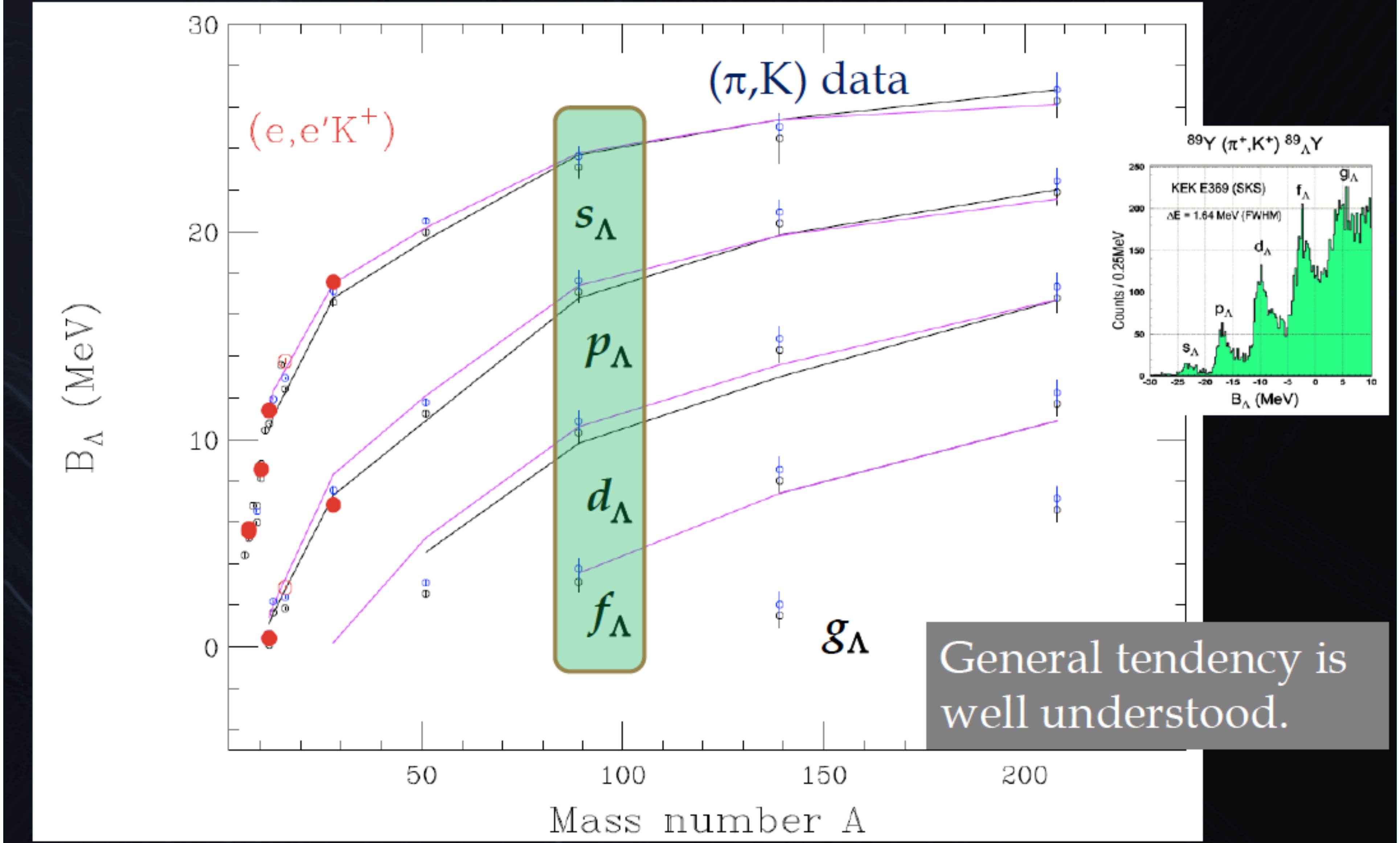

General tendency is well understood.

Lines: Calc. by Yamamoto & Rijken

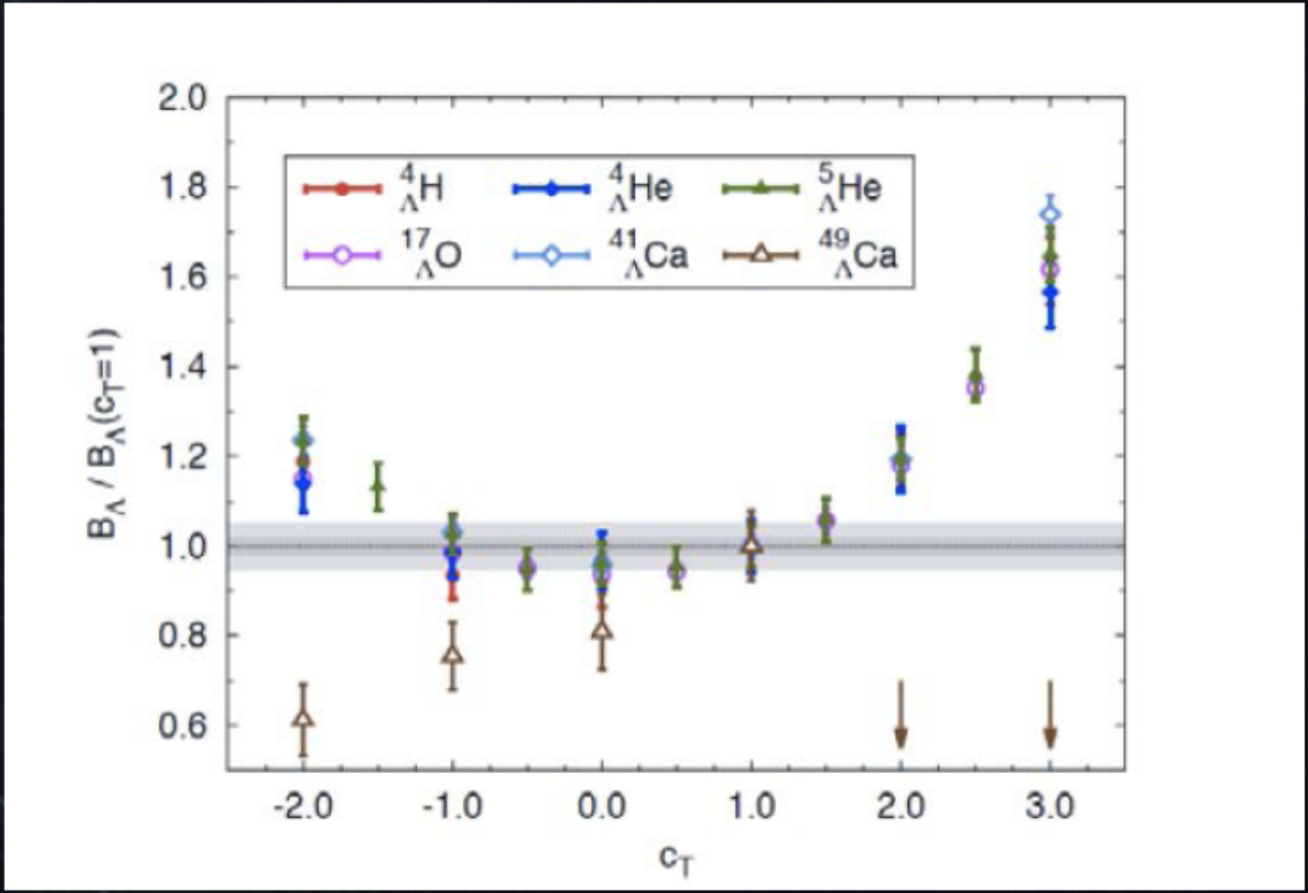

Figure 2-10: Λ separation energies normalized with respect to the $C_T = 1$ case as a function of C_T. Grey bands represent the 2% and 5% variations of the ratio B_Λ/B_Λ ($C_T = 1$). Brown vertical arrows indicate the results for ^{49}Ca in the case of $C_T = 2$ and $C_T = 3$, outside the scale of the plot.

NS EOS with hyperon and 3BRF

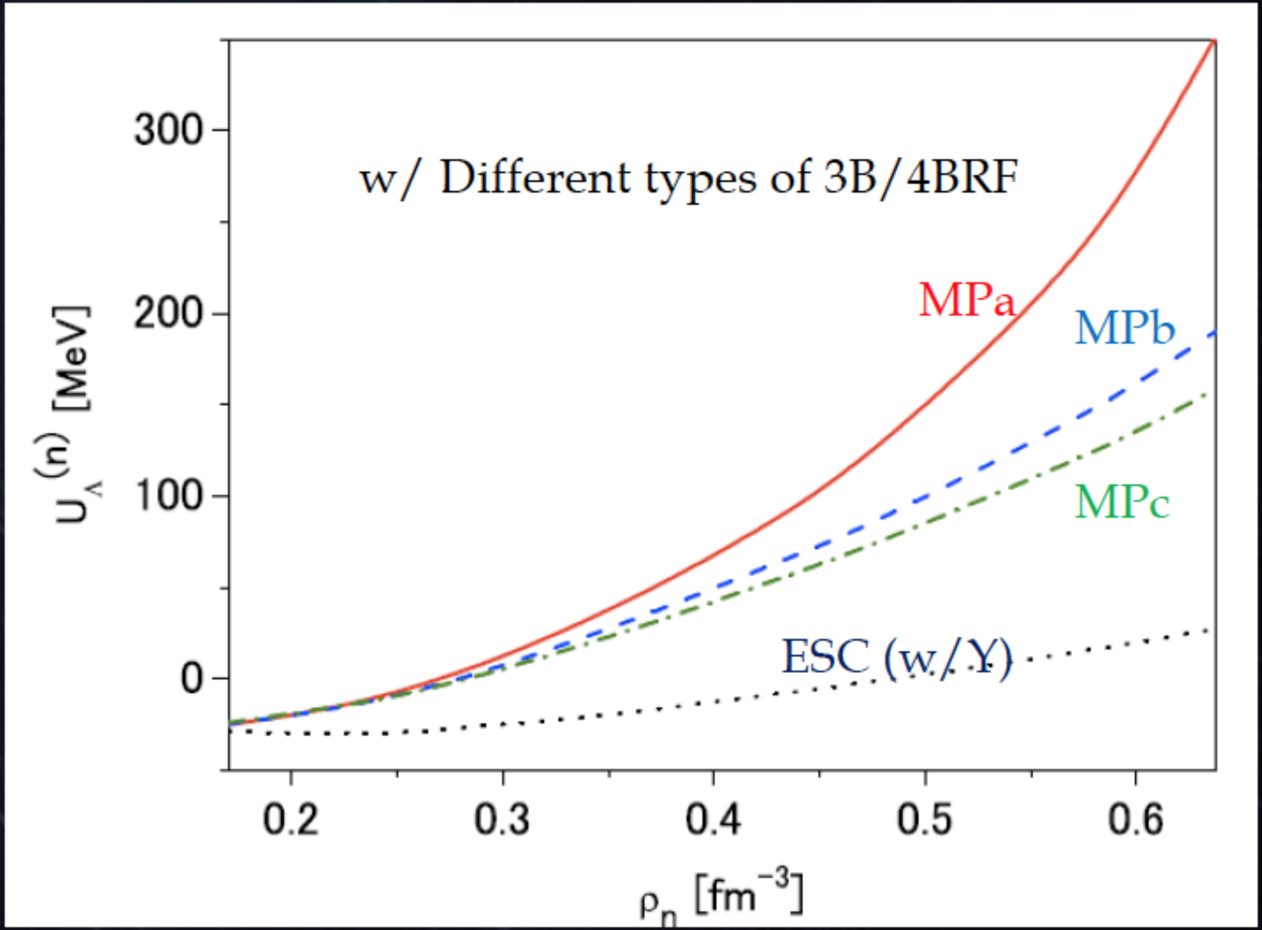

With 3BRF recover hardness

With Hyperon too Soft

Yamamoto et al., Brueckner theory + G-matrix YN

Λ N vs Σ N

H. J Schulze and T Rjiken, Phys Rev C84, 035801 (2011)

New potential (ESC08) and TBF stiffen the EOS, allowing for higher maximum masses of hyperon stars.

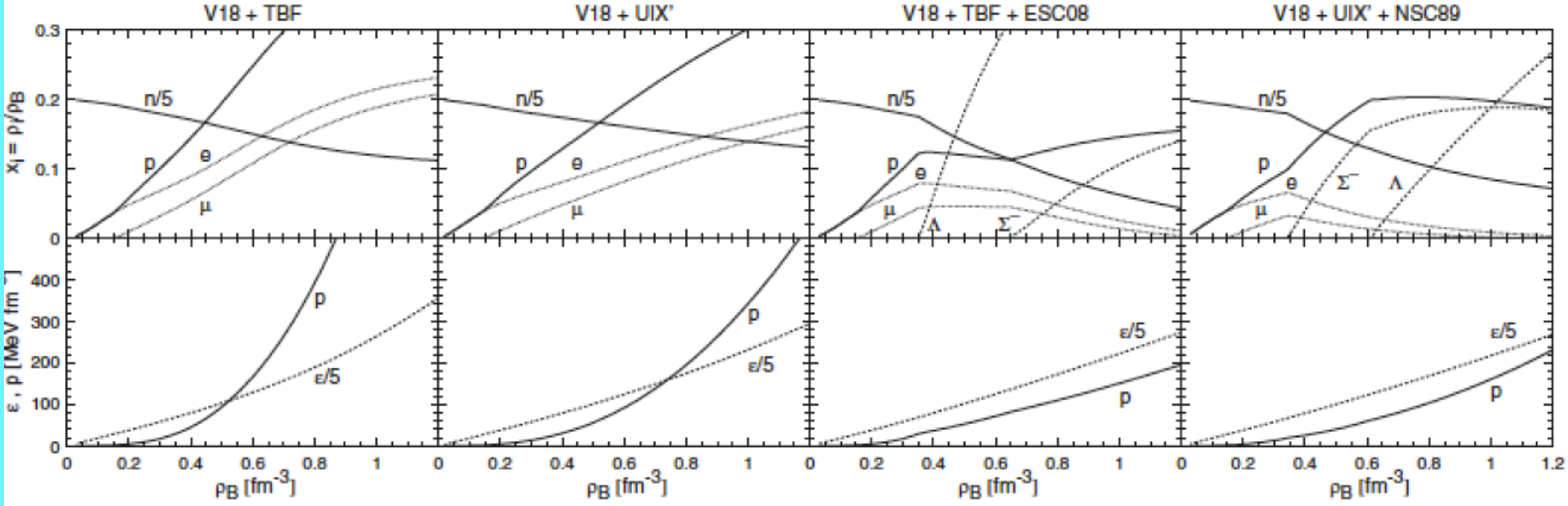

FIG. 2. Composition of β-stable matter (upper panels) and equation of state (lower panels) for different models.

massive neutron stars have to be hybrid stars containing a core of nonbaryonic ("quark") matter, since the possibility of them being nucleonic stars is ruled out by the early appearance of hyperons

Λ appears earlier than Σ

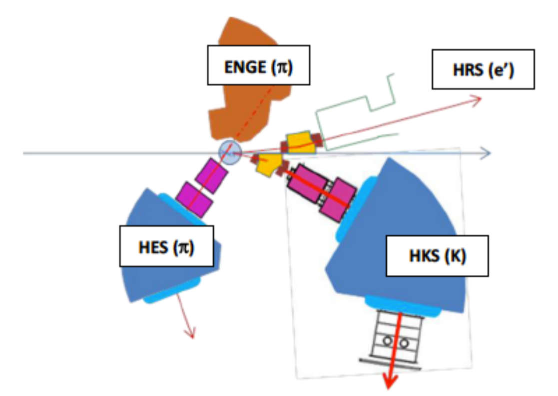

HKS PID

3 TOF, 2 water Cherenkiv, three aerogel Cerenkov
Power rejection capability is:
- In the beam p:K:p 10000:1:2000
- in the on-line trigger 90:1:90
- after analysis it is 0.01:1:0.02
- so for π the rejection power is 10^6
- and for p 10^5

HKS PID

(gas Cherenkof + shower counter)
e,π rejection
10^5

RICH Detector

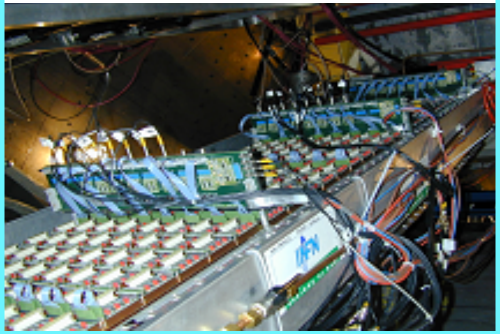

PID $\pi/K \sim 10^{12}$ (threshold + RICH)

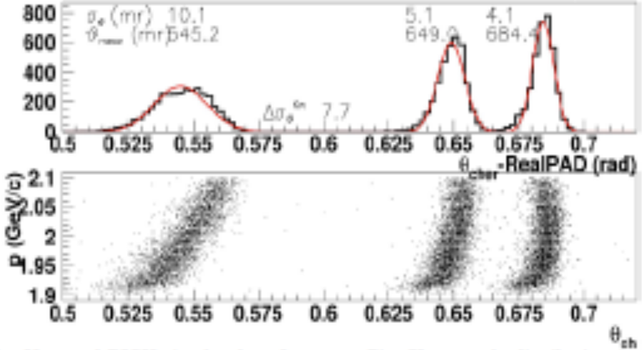

Targets
standard solid + waterfall + solid cryocooled for Pb

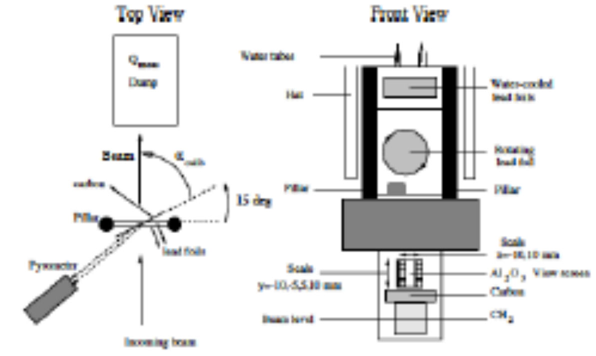

Fig. 7 The NIKHEF ^{208}Pb target layout

<i> = 25 μA – 100 mg/cm cryocooling

Elastic scattering measurement off Pb-208 to know the actual thickness of the target then monitor continuously by measuring the electron scattering rate as a function of two-dimensional positions by using raster information.

HYPERNUCLEI and ASTROPHYSICS

There is growing evidence that hyperons appears the first of the strange hadrons in neutron stars at around twice normal density…. The onset of the hyperon formation is controlled by the attactive hyperon-nucleon interaction wich can be extracted from hypernucleon scattering data and hypernuclear data (J. Shaffner-Bielich et al: Hyperstars: Phase Transition to (meta)-Stable Hyperonic matter in neutron Stars, arXiv: astroph/0005490

Impact of hyperons on the maximum mass of neutron stars

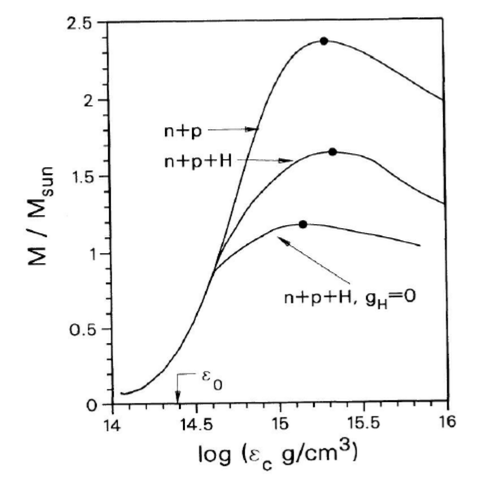

- neutron star with nucleons and leptons only: $M \approx 2.3 M_\odot$
- substantial decrease of the maximum mass due to hyperons!
- maximum mass for “giant hypernuclei”: $M \approx 1.7 M_\odot$
- noninteracting hyperons result in a too low mass: $M < 1.4 M_\odot$!

- Strange baryons may appear in neutral b-stable matter through process like:

$$n + e^- \rightarrow \Sigma^- + \nu_e$$

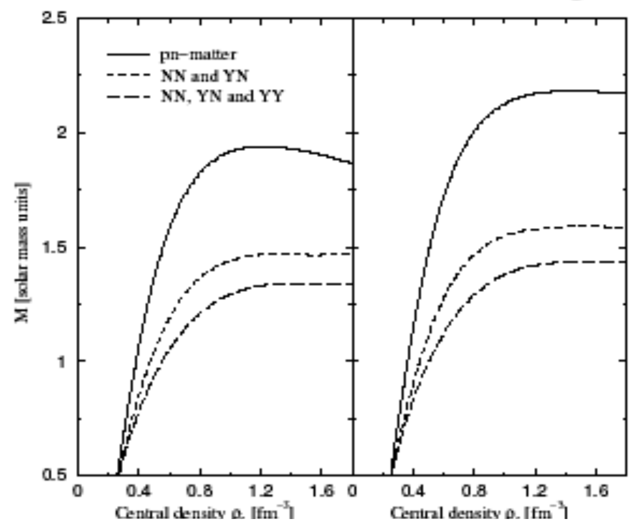

- The presence of strange baryons in neutron stars strongly affect their properties. Example: mass-central density relation for a non-rotating (left) and a rotating (right) star

- The effect strongly depends upon the poorly known interactions of strange baryons

More data needed to constrain theoretical models.

HYPERNUCLEI and ASTROPHYSICS

There is growing evidence that hyperons appears the first of the strange hadrons in neutron stars at around twice normal density….The onset of the hyperon formation is controlled by the attactive hyperon-nucleon interaction wich can be extracted from hypernucleon scattering data and hypernuclear data (J. Shaffner-Bielich et al: Hyperstars: Phase Transition to (meta)-Stable Hyperonic matter in neutron Stars, arXiv: astroph/0005490

Additional experimental data from hypernuclei will be useful in establishing the foundations of high density matter models. This is especially relevant for the hyperon-nucleon interactions, for which relevant systems are more likely to be produced in current accelerators than for hyperon-hyperon interactions" , in S. Balberg et al: Roles of hyperons in Neutron Stars, arXiv: astro-ph/9810361

- Strange baryons may appear in neutral b-stable matter through process like:

$$n + e^{-} \rightarrow \Sigma^{-} + \nu_{e}$$

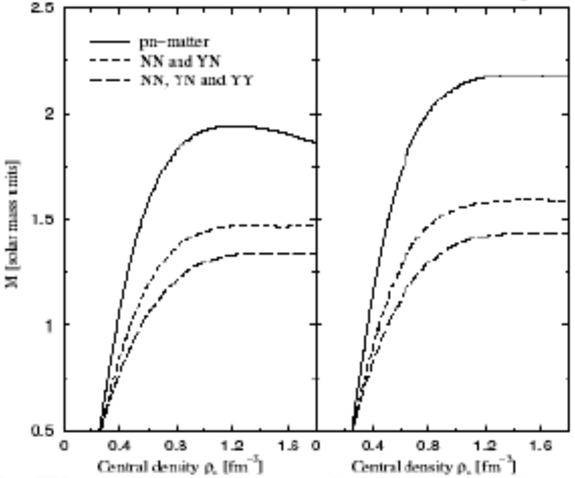

- The presence of strange baryons in neutron stars strongly affect their properties. Example: mass-central density relation for a non-rotating (left) and a rotating (right) star
- The effect strongly depends upon the poorly known interactions of strange baryons

More data needed to constrain theoretical models.

H.-J. Schulze, T. Rijken PHYSICAL REVIEW C 84, 035801 (2011)

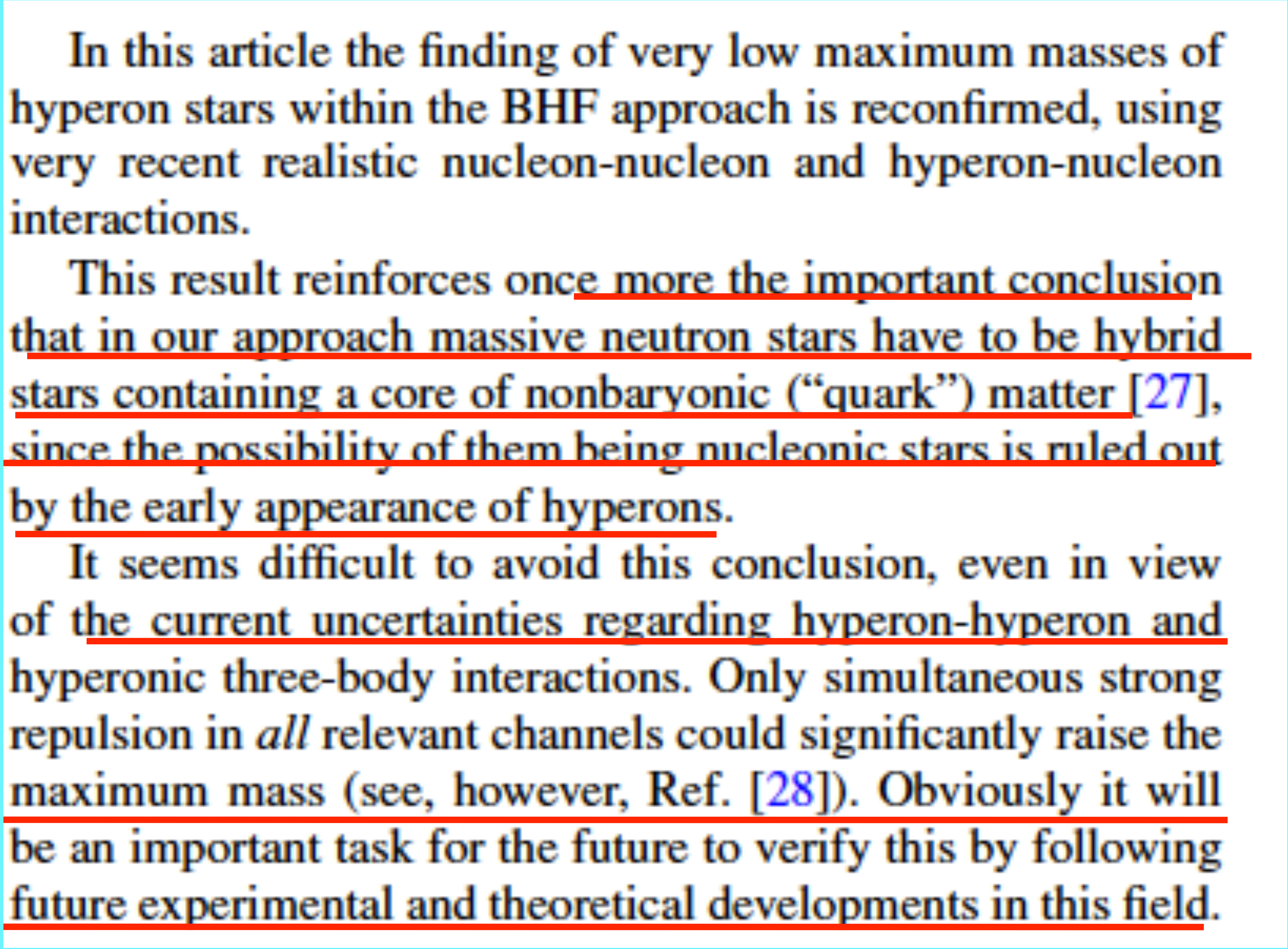

In this article the finding of very low maximum masses of hyperon stars within the BHF approach is reconfirmed, using very recent realistic nucleon-nucleon and hyperon-nucleon interactions.

This result reinforces once more the important conclusion that in our approach massive neutron stars have to be hybrid stars containing a core of nonbaryonic ("quark") matter [27], since the possibility of them being nucleonic stars is ruled out by the early appearance of hyperons.

It seems difficult to avoid this conclusion, even in view of the current uncertainties regarding hyperon-hyperon and hyperonic three-body interactions. Only simultaneous strong repulsion in *all* relevant channels could significantly raise the maximum mass (see, however, Ref. [28]). Obviously it will be an important task for the future to verify this by following future experimental and theoretical developments in this field.

Λ separation energy of the hypernucleus $^9{}_\Lambda Li$

A separation energy B_Λ of 8.36 ± 0.08 (stat) ± 0.08 (sys) was measured, quite in agreement with the value of 8.50 ± 0.12 MeV from emulsion data

The separation energy B_Λ was determined after a careful calibration of the missing-mass scale, needed because of uncertainties in the kinematical variables such as the primary electron energy and the central momenta and the central scattering angles of the scattered electrons and the produced kaons. Because the experiment $^9Be(e,e'K^+)$ $^9{}_\Lambda Li$ was performed after and with the same kinematical setting of the experiment $^{12}C(e,e'K^+)^{12}{}_\Lambda B$, the kinematical variables were determined reproducing the binding energy of the hypernucleus $^{12}{}_\Lambda B$ ground state at the known position of 11.37 ± 0.06 MeV.